THIS NUMBER COMPLETES VOLUME I

# EXPERIMENTAL CELL RESEARCH

UNIVERSITY OF HAWAII LIBRARY
FEB 13 '51

*Published under the auspices of*

THE INTERNATIONAL SOCIETY FOR CELL BIOLOGY

EDITORS:

TORBJÖRN CASPERSSON · HONOR B. FELL · JOHN RUNNSTRÖM

FRANCIS O. SCHMITT · PAUL WEISS · RALPH W. G. WYCKOFF

VOLUME I · NOVEMBER 1950 · NUMBER 4

ACADEMIC PRESS INC., PUBLISHERS, NEW YORK, N.Y.

# EXPERIMENTAL CELL RESEARCH


EDITORS:

T. Caspersson, Department of Cell Research, Karolinska Inst., Stockholm 60, Sweden
Honor B. Fell, Strangeways Laboratory, Cambridge, England
J. Runnström, The Wenner-Gren Institute for Experimental Biology, Stockholm, Sweden
Francis O. Schmitt, Massachusetts Institute of Technology, Cambridge 39, Massachusetts
Paul Weiss, University of Chicago, Chicago 37, Illinois
Ralph W. G. Wyckoff, Laboratory of Physical Biology, National Institute of Health, Bethesda, Maryland.

EXECUTIVE COMMITTEE:

T. Caspersson, Honor B. Fell, J. Runnström and J. F. Danielli, King's College, London, W. C. 2, England.

ADVISORY BOARD:

H. Bauer (Wilhelmshafen), W. Bloom (Chicago), J. Brachet (Bruxelles), F. Buchthal (Copenhagen), A. Buzzati-Traverso (Verbania Pallanza), R. Chambers (New York), E. Chargaff (New York), J. F. Danielli (London), C. D. Darlington (London), J. N. Davidson (Glasgow), M. Demerec (Cold Spring Harbour, N. Y.), J. Engelbreth-Holm (Copenhagen), E. Fauré-Frémiet (Paris), A. Fischer (Copenhagen), A. Frey-Wyssling (Zürich), N. Fries (Uppsala), R. J. Gautheret (Paris), L. Geitler (Wien), G. Gomori (Chicago), A. Haddow (London), E. Hammarsten (Stockholm), B. Hanström (Lund), E. Newton Harvey (Princeton, N. J.), L. V. Heilbrunn (Philadelphia, Pa), G. C. Heringa (Amsterdam), A. Hollaender (Oak Ridge, Tenn.), H. Holmgren (Stockholm), H. Holter (Copenhagen), J. Holtfreter (Rochester, N. Y.), P. Koller (London), F. Lehmann (Bern), P. L'Héritier (Paris), G. Levi (Torino), P. E. Lindahl (Uppsala), G. Lindeberg (Uppsala), C. C. Lindegren (Carbondale, Ill.), R. J. Ludford (London), S. E. Luria (Bloomington, Ind.), A. Lwoff (Paris), A. Mirsky (New York), G. Montalenti (Naples), H. Okkels (Copenhagen), O. Olivo (Bologna), A. W. Pollister (New York), J. Randall (London), W. J. Schmidt (Giessen), F. Schrader (New York), W. Seifriz (Philadelphia, Pa), T. M. Sonneborn (Bloomington, Ind.), J. M. Sosa (Montevideo), J. Spek (Rostock), W. M. Stanley (Berkeley, Calif.), E. Suomalainen (Helsingfors), E. L. Tatum (Stanford University, Calif.), T. Teorell (Uppsala), A. Tyler (Pasadena, Calif.), W. Wilbrandt (Bern).


---


*Subscriptions*

**EXPERIMENTAL CELL RESEARCH**

will be published in four issues annually at $12.00 per volume. The price of one issue is $3.50. Please send your subscription orders to Academic Press Inc., 125 East 23 St., New York 10, N.Y.


---

# AMINO ACID CONSTITUENTS OF CHROMATIN THREADS FROM ERYTHROCYTE NUCLEI

G. YASUZUMI and G. MIYAO

*Genetic Laboratory and the Anatomical Institute of Medical School, University of Osaka, Osaka, Japan*

Received January 23, 1950

## INTRODUCTION

In order to make clear the structure of the gene, it is necessary to analyze the chemical constitution of the chromosome. Researches on these lines have been carried on by many scholars since the end of the last century. Recently, the salivary gland chromosomes of Diptera have proved to be excellent material for this purpose; they have been investigated by polarizing microscopy (10), ultra-violet spectroscopy (Caspersson and others (2, 3, 4)), micro-incineration (1, 16) and cytochemistry (8, 12, 13, 15).

Consden, Gordon and Martin (5) introduced paper chromatography, a comparatively simple technique for detecting amino acids in very small samples of material. Kirby (6) used this technique for studies on the amino acid content of various tissues of Drosophila virilis. The development of paper chromatography has made it possible to analyze the amino acids of chromatin threads isolated from carp erythrocytes.

Mirsky and Ris's technique (9) for isolating chromatin threads from carp erythrocytes has been used in these experiments. A sample of 0.01 g was obtained from about one hundred carp of 20 cm in length and 100–120 gram in weight. The whole procedure was carried out in a room attached to the enzyme laboratory of the physiological institute in Osaka University. The temperature of the room was kept at 1° C. Morphological researches on the isolated chromatin threads have been made by W. G. P. Lamb (7) and G. Yasuzumi and Y. Mizuta (12) by means of the electron microscope.

The tissues were hydrolyzed in 6 N HCl for 20 hours at 120° C. We prepared two-dimensional paper (Toyo filter-paper No. 2) chromatograms. The solutions of n-butanol (four parts) and acetic acid (one part), to which water was added to 95 per cent saturation, was used as the first solvent. The phenol solution, in which 100 grams crystalline phenol was dissolved in 20 cc. distilled water was used as the

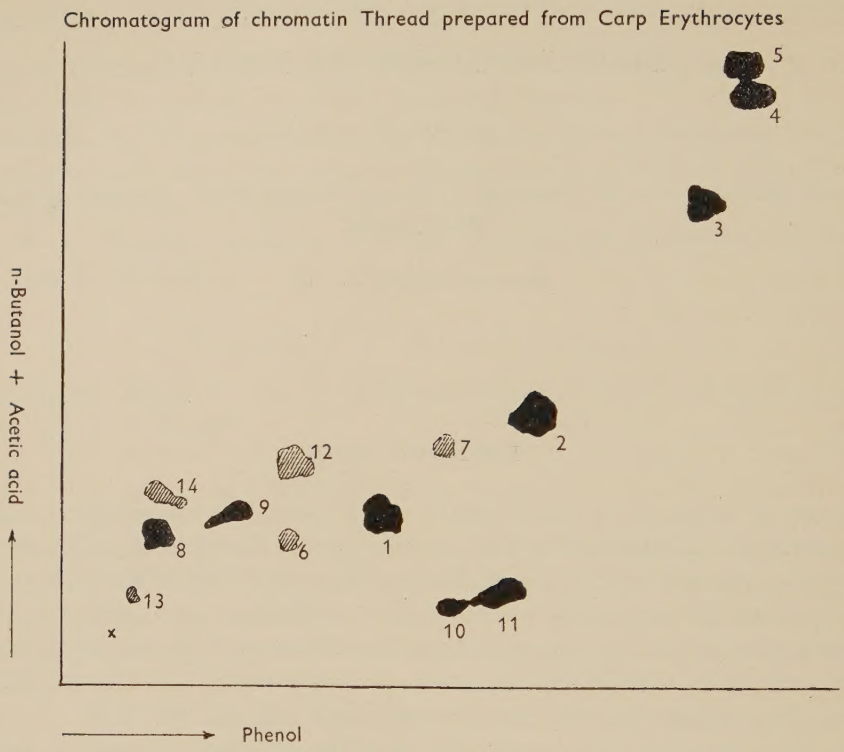


Fig. 1. Tracing of a two-dimensional paper chromatogram of a 20 hours' hydrochloric acid hydrolyzate of chromatin threads from carp erythrocyte nuclei. Black spots show strong ninhydrin reactions. Spots marked with oblique lines show faint ninhydrin reactions. Cross shows point where the sample was placed. 1:glycine, 2:alanine, 3:valine, 4:leucine, 5:phenylalanine, 6:serine, 7:threonine, 8:aspartic acid, 9:glutamic acid, 10:lysine, 11:arginine, 12:$X_1$ (taurine ?), 13:$X_2$, 14:$X_3$.

second solvent. During the course of the research on free amino acids in the chromatin threads, an analysis of both free and combined amino acids was made. Tryptophane is destroyed during acid hydrolysis, so the sample was also hydrolyzed in 6 N NaOH. The rest of the manipulation was the same as described above. Tryptophane was not recognized in the sample which had been hydrolyzed with NaOH. In the sample which was dissolved in distilled water but not hydrolyzed in NaOH or HCl, no amino acid was detectable.

Figure 1 is a tracing of a chromatogram showing the amino acids which were present in the chromatin threads of carp erythrocytes. The amino acids glycine, alanine, valine, leucine, phenylalanine, serine, threonine, aspartic acid, glutamic acid, lysine, arginine have been identified in the chromatogram. The spot 12, may possibly correspond to taurine, whereas two fur-

ther spots, 13 and 14, remained unidentified. Lysine and arginine were clearly demonstrated, although the sensitivity of these amino acids to ninhydrine is believed to be very low. This fact shows the existence of these basic amino acids in a considerable quantity.

## DISCUSSION

In this work glycine, alanine, leucine, phenylalanine, valine, serine, threonine, aspartic acid, glutamic acid, lysine, arginine, $X_1$ (taurine?), $X_2$ and $X_3$ have been demonstrated in the hydrolyzate of chromatin threads isolated from carp erythrocytes by using a paper chromatogram. By the same method, B. Kirby (6) has demonstrated the amino acids of the salivary gland chromosomes of Drosophila virilis, but phenylalanine, serine, threonine, arginine, and lysine were not identified. It is of interest that leucine, valine, alanine, glycine, aspartic acid and glutamic acid have been demonstrated in salivary gland chromosomes of Drosophila virilis and chromatin threads of carp erythrocytes.

By combined cytochemical and electron microscopic studies Yasuzumi and Hasegawa (13) revealed the intimate connection between desoxyribonucleic acid and the formation and division of the chromosome. It remains, however, to elucidate whether the amino acids demonstrated in the chromatin threads are derived from the thread-like structure of the chromosome or are gene constituents.

## SUMMARY

The chemical components of chromatin threads isolated from carp erythrocytes have been analyzed by means of a paper chromatogram with the following results:

1. The amino acids were not found in the free state (naturally).
2. Amino acids such as glycine, alanine, valine, leucine, phenylalanine, serine, threonine, aspartic acid, glutamic acid, lysine, arginine, and taurine (?) were demonstrated in the hydrolyzate in HCl or NaOH.
3. The presence of tryptophane was not demonstrated.

## ACKNOWLEDGMENTS

This work was supported in part by a grant from the Scientific Research Council of Japan.

## REFERENCES


1. Barigozzi, C., *Z. f. Zellforsch. u. mikroskop. Anat.*, **26**, 462 (1937).
2. Caspersson, T., *Skand. Arch. Phys.*, **73**, Suppl. 8 (1936).
3. Caspersson, T., and Schultz, J., *Nature*, **142**, 294 (1938).
4. Caspersson, T., Nyström, C., and Santesson, L., *Naturw.*, **29**, 33 (1941).
5. Consden, R., Gordon, A. H., and Martin, A. J. P., *Biochem. J.*, **38**, 224 (1944).
6. Kirby, B., *Proc. Natl. Acad. Sci.*, **34**, 561 (1948).
7. Lamb, W. G. P., *Nature*, **164**, 109 (1949).
8. Mazia, D., and Jaeger, L., *Proc. Natl. Acad. Sci.*, **25**, 456 (1939).
9. Mirsky, A. E., and Ris, H., *J. of general Phys.*, **31**, 7 (1947).
10. Schmidt, W. J., *Verh. Deutsch. Zool. Ges.*, **41**, 253 (1939).
11. Yasuzumi, G., *Symposia on nucleic acid*, Tokyo (1949).
12. Yasuzumi, G., and Mizuta, Y., *54th Japanese Anatomical Congress* (1949).
13. Yasuzumi, G., and Hasegawa, Y., *21st Japanese Genetical Congress* (1949).
14. Yasuzumi G., Mori, T., Matsukura, A., and Minamino, R., *Cytologia* **14** (1950) (in print).
15. Yasuzumi, G., Mori, T., Sumida, Y., and Minamino, R., *Man and Heredity*, **1** (1947).
16. Yasuzumi, G., and Sawada, A., *Cytologia* **14** (1950) (in print).

# THE PHYSICAL PROPERTIES OF CYTOPLASM. A STUDY BY MEANS OF THE MAGNETIC PARTICLE METHOD. PART II. THEORETICAL TREATMENT

F. H. C. CRICK

*Strangeways Research Laboratory, Cambridge*

Received February 9, 1950

## A. INTRODUCTION

In Part I (1) a method was described for measuring some of the physical properties of the cytoplasm of chick cells in tissue culture by means of magnetic particles. The cells were allowed to phagocytose these particles, which were then acted on by magnetic fields, their movements being observed simultaneously under high magnification.

In this paper the theoretical basis for the experimental methods used has been set out. The results are mainly standard pieces of magnetism and hydrodynamics, but as they are scattered about in the literature it was thought worth while to bring them all together in one place.

The paper has been written for workers who may wish to use the method themselves, or who wish to examine its foundations critically. For those only interested in the results an extended summary of the theoretical conclusions has already been given in Part I. An elementary knowledge of magnetism and hydrodynamics is therefore assumed. There are occasional remarks from a more advanced standpoint, but they are not crucial to the main results.

The experimental methods have been set out in part I. It will suffice here to state the general theoretical problems for which we require solutions. There are three main cases. They are

(1) Twisting: the permanent magnet case.

In this case the magnetic particle is turned into a little permanent magnet by applying a large magnetic field momentarily. It is subsequently twisted by a much smaller field applied in a direction roughly perpendicular to its permanent magnetic moment.

(2) Twisting: the soft iron case.

In this case the material is considered to have no hysteresis. A magnetic field is applied at a small angle to the length of the particle, which is thus twisted.

(3) Dragging.

In this case a large field, with a large field gradient is applied. The magnetic particle is magnetically saturated, and after being twisted into line, is dragged by the field gradient.

We wish to calculate the velocity (or the angular velocity) of the particle in terms of its size, shape, and magnetic properties, and the physical properties and boundaries of the medium in which the particle is embedded.

We tackle the problems in the following order. We first show that we can neglect the effects of inertia, and by elementary arguments find how the forces vary with scale. We then consider the behaviour of the medium, discussing the effects of the shape of the particle, of boundaries, and of non-newtonian and elastic behaviour. Next we give the formulae for the magnetic forces on the particle, and then in section F we show how all the factors can be combined to evaluate the velocity (or angular velocity) of the particle for the three main cases.

Finally we give some brief theoretical notes on the production of large field gradients and a note on some comparative numerical values for the stress.

## B. GENERAL CONSIDERATIONS

### *1. Inertia*

Inertia will delay the approach to the steady state and will alter the final velocity distribution. We shall show that both of these effects can be neglected in our experiments mainly because the particles are so small.

There are two problems that can be considered separately. Firstly, the inertia of the fluid, secondly the inertia of the particle.

For the inertia of the fluid the relevant characteristic of the motion is the ratio of the inertia forces to the viscous forces (Reynold's number). It is given by

$$\frac{\sigma \varrho a^2}{\eta}$$

where $\sigma$ = reciprocal of a characteristic time
$\varrho$ = density of the fluid
$\eta$ = viscosity of the fluid
$a$ = a characteristic length

(see for example the case of an oscillating sphere, (7), paragraph 354). This formula applies strictly only to short particles.

If the above parameter is $\ll 1$, the inertia of the liquid is negligible. Another use of the parameter is that the value of $\left(\frac{1}{\sigma}\right)$ defined by putting $\frac{\sigma \varrho a^2}{\eta}$ equal to unity, gives the *order* of the time required to approach the steady state.

We shall not be considering particles bigger than 10 $\mu$ in diameter, so we

may put $a = 5 \times 10^{-4}$ cm. If we take as a lower bound for $\eta$ the value for water (0.01 poise), since biological fluids can scarcely be less viscous, and put $\varrho = 1$, we obtain for the upper bound of $\left(\frac{1}{\sigma}\right)$ the value $\frac{1}{40}$ milliseconds. This is naturally very much smaller than anything we have measured. We should note in passing that if the margin were not so great a more exact treatment would be advisable. Our formula gives the time for the particle to reach a good fraction of its final velocity, but in certain cases the later stages of the asymptotic approach to the final velocity may take much longer than the earlier stages.

These results only apply strictly to the case of an infinite fluid. We can give an argument which suggests that the effect of adding fixed boundaries will usually be to decrease the time to approach the steady state. Consider two cases: firstly a particle in an infinite fluid, secondly the same particle with fixed boundaries added to the fluid. Let the forces applied to the particles be such that the same steady velocity is attained in the two cases. We will assume that as a rough measure of the time to approach equilibrium we may take the ratio of the kinetic energy of the fluid to the rate of dissipation of energy, both *for the steady state.* The effect of fixed boundaries is to increase the resistance and therefore the rate of dissipation of energy. The boundaries also reduce the amount of fluid in motion and over most of the volume[1] decrease the fluid's velocity. The total kinetic energy is thus likely to be reduced. Therefore the ratio referred to above will be decreased.

To estimate the effect of the inertia of the particle we consider the case of the dragging of an iron sphere. The ratio of the inertia to the viscous forces is

$$\frac{\frac{4\pi}{3} a^3 \varrho' \frac{dv}{dt}}{6\pi\eta a v}$$

where $v$ = velocity
$\varrho'$ = density of sphere

If we define the characteristic time $\frac{1}{\sigma}$ by the equation

$$\frac{dv}{dt} \equiv \frac{v}{\left(\frac{1}{\sigma}\right)}$$

[1] This assumes that the boundaries do not force the flow into a very restricted channel, in which case the velocity would be increased considerably.

this ratio becomes

$$\frac{2}{9}\frac{\sigma \varrho' a^2}{\eta}$$

which apart from the numerical factor is the same form as before, except that $\varrho'$ is now the density of the iron. It can easily be shown that exactly the same type of parameter is involved in the case of rotation. Thus the effects of the inertia of the particle are negligible.

The case for non-newtonian fluids, whose "viscosity" varies with shear is not quite so clear cut. However the margin in our experiments is so big that we can simply consider the extreme case where the inner parts of the liquid move effectively as a solid, and the outer parts as a newtonian liquid. This is clearly similar to the movements of a body of increased radius in water. In our experiments the radius of the body is bounded by the size of the cell, so that we again get a very small value for the time to reach equilibrium.

The case for the visco-elastic medium is given on page 519.

The conclusion is the same. Thus for all possible cases in our experiments the steady state is reached in a time very much smaller than anything we can measure.

*2. Scale*

We shall next show, by simple dimensional arguments, how the forces involved in dragging and twisting change with scale. We only consider a range of scale over which the magnetic factors $\left(\text{e.g. } \frac{dH}{dx}\right)$ can be considered constant.

(a) Dragging

As before let $a$ = characteristic length of particle
$v$ = characteristic velocity of particle
$\eta$ = viscosity of (newtonian) liquid
$\varrho$ = density of fluid

The density of the particle is clearly not involved in the steady state condition. We restrict ourselves to a range of scale over which the density of the fluid can also be ignored, for the reasons given above.

The magnetic field will produce a force per unit volume given by

$$I\frac{dH}{dx}$$

where $I$ = magnetic induction of the particle

$\frac{dH}{dx}$ = magnetic field gradient producing the force.

A force per unit volume has the dimensions $M\,L^{-2}\,T^{-2}$. The only combination of $a$, $v$ and $\eta$ which will give this is $\left(\frac{\eta v}{a^2}\right)$.

Whence we obtain

$$v \sim \frac{a^2}{\eta} \cdot I\left(\frac{dH}{dx}\right).$$

Thus, as the scale is reduced, the velocity decreases as the square of the characteristic length. The time for the body to traverse its own length increases linearly with the reciprocal of the characteristic length.

(b) Twisting

Here the magnetic couple per unit volume depends on

$$(I\,H)\,f(\theta)$$

where $\theta$ is an angle.

This has the dimensions $M\,L^{-1}\,T^{-2}$ and from $\omega$ (the typical angular velocity), $\eta$ and $a$ we can only form the combination $\eta\,\omega$.

Thus

$$\omega \sim \frac{I\,H}{\eta} \cdot f(\theta).$$

Therefore the angular velocity does not vary with scale.

Note that if the liquid has boundaries they, too, must be scaled for the above results to apply.

If the liquid is non-newtonian comparisons can only be made between conditions under which the shear is the same. For dragging this occurs when the time for the particles to go their own lengths is the same; for twisting, when the angular velocities are the same. The interesting result for twisting, that the angular velocity is independent of scale is therefore also true for the non-newtonian case.

Finally note that the magnetic conditions have *not* been scaled. Scaling the magnets producing the field makes no difference to the value of the field, but does alter the field gradient. This reservation is therefore important in dragging but not in twisting. It is easy to see that if we *do* scale the magnets for the dragging case the time for a particle to be dragged its own length is independent of scale for both the newtonian and the non-newtonian cases.

## C. THE FORCES ON A BODY IN A VISCOUS FLUID

### *1. Variation with shape*

The variation with shape is naturally more complicated than the variation with scale, and has only been worked out for special cases, usually in an infinite fluid. It is possible to obtain the result for the general ellipsoid, but we shall only quote those for ovary ellipsoids of revolution, as we require them merely to give some idea of the general behaviour. We consider in this section the formulae for a body immersed in an infinite newtonian liquid, leaving to the two following sections the consideration of boundaries and of non-newtonian behaviour.

We shall use the following notation for the ovary ellipsoid:

major axis $= a$
minor axes $= b = c$
eccentricity, $e$, given by $1 - e^2 = \dfrac{b^2}{a^2}$

We denote

$$\frac{2(1-e^2)}{e^3}\left(\tfrac{1}{2}\log\frac{1+e}{1-e} - e\right) \text{ by } \alpha_0.$$

$$-\left(\frac{(1-e^2)}{2e^3}\log\frac{1+e}{1-e} - \frac{1}{e^2}\right) \text{ by } \beta_0.$$

and

$$\frac{b^2}{e}\log\frac{1+e}{1-e} \text{ by } \chi_0.$$

(All logs are natural logs).

(a) *Twisting*

For a sphere: couple $= 8\pi\eta a^3\omega$
where $\omega$ = angular velocity
(7, para 334)

For an ovary ellipsoid of revolution:

We shall only consider the case of rotation about a minor axis. This has been solved by Edwards (2), but owing to an algebraical slip towards the end he omits the factor 2/3. The correct result, *in his notation*, is, for the general ellipsoid,

$$\text{couple} = \frac{32\mu\pi\omega}{5}\left(\frac{b^2 + \frac{2}{3}c^2}{b^2 B + c^2 C}\right).$$

This being adapted to our notation, and restricted to the case of the ovary ellipsoid, becomes

$$\text{couple} = \frac{32\,\eta\,\pi\,\omega}{5}\left(\frac{a^2 + \frac{2\,b^2}{3}}{a^2\,\alpha_0 + b^2\,\beta_0}\right) a\,b^2.$$

We express this as couple $= k \cdot 8\,\pi\,\eta\,\omega\,a^2\,b$ and evaluate $k$ numerically for different values of $a/b$.

Some values are given in Table I.

Table I

| $\frac{a}{b}$ | 1.0 | 2.0 | 3.0 | 4.0 | 5.0 | 10.0 | 20.0 |
|---|---|---|---|---|---|---|---|
| $k$ | 1.0 | 0.84 | 0.91 | 1.00 | 1.10 | 1.60 | 2.50 |

In the limit $(a/b) \to \infty$, $k \to \frac{2}{5}\left(\frac{a}{b}\right)\frac{1}{\left(\log\frac{2\,a}{b} - 1\right)}$.

(b) *Dragging*

For a sphere:

the force is $6\,\pi\,\eta\,a\,v$ with the usual notation

(7, para 337)

For an ovary ellipsoid of revolution

(i) in the direction of its major axis, $a$

we have $\quad \text{force} \equiv 6\,\pi\,\eta\,R\,v$

where $\quad R = \frac{8}{3}\cdot\frac{a\,b^2}{\chi_0 + \alpha_0\,a^2}$

(7, paras 339 and 114)

This reduces to

$$R = \frac{8}{3}\cdot\frac{a\,e}{\left(1 + \frac{1}{e^2}\right)\log\frac{1+e}{1-e} - \frac{2}{e}}.$$

For the special case where the ellipsoid is very long, so that $a \gg b$

$$R \to \frac{4}{3}\cdot\frac{a}{\left(2\,\log\frac{2\,a}{b} - 1\right)}.$$

Numerical values are given in Table II below.

(ii) in the direction of its minor axis, $b$

we have $$R = \frac{8}{3} \cdot \frac{a\,b^2}{\chi_0 + \beta_0\,b^2}$$

(7, paras 339 and 114)

whence we obtain

$$R = \frac{16}{3} \cdot \frac{a\,e}{\left(3 - \frac{1}{e^2}\right)\left(\log \frac{1+e}{1-e}\right) + \frac{2}{e}}$$

and when $a \gg b$

$$R \to \frac{8}{3} \cdot \frac{a}{\left(2 \log \frac{2a}{b} + 1\right)}.$$

Numerical values are given in Table II.

TABLE II

Values of $a/R$ for the dragging of an ovary ellipsoid.

| $b/a$ | 0.0 | 0.1 | 0.2 | 0.3 | 0.4 | 0.5 | 0.6 | 0.7 | 0.8 | 0.9 | 1.0 |
|---|---|---|---|---|---|---|---|---|---|---|---|
| $a/R$ (along major axis) | $\infty$ | 3.764 | 2.799 | 2.267 | 1.914 | 1.662 | 1.467 | 1.314 | 1.191 | 1.091 | 1.000 |
| $a/R$ (along minor axis) | $\infty$ | 2.617 | 2.108 | 1.815 | 1.606 | 1.451 | 1.326 | 1.224 | 1.138 | 1.063 | 1.000 |

The numerical values are taken from Gans (4), where the numerical results for a planetary ellipsoid are also given.

2. *The effect of boundaries*

(a) Boundaries are, in general, more important in dragging than in twisting. This is not surprising when we remember that the viscosity of a viscous fluid through which a sphere is *dragged* falls off as $\frac{1}{r}$ a long way from the sphere (in contrast to the case where the inertia is important and viscosity negligible), while the angular velocity in the fluid round a *rotating* sphere falls off as $\frac{1}{r^3}$.

The following examples illustrate this point. In all cases $a$ is the inner radius, $b$ the outer radius.

(i) translation of a sphere in a fixed cylindrical tube

$$\text{force} = 6\pi\eta a v\left(1 + 2.104\frac{a}{b} + \cdots\right)$$

(ii) rotation of a sphere in a fixed spherical shell

$$\text{couple} = 8\pi\eta a^3\omega\left(\frac{1}{1 - a^3/b^3}\right)$$

(iii) translation of a cylinder in a fixed cylinder

$$\text{Force per unit length} = 2\pi\eta v\left(\frac{1}{\log a - \log b}\right)$$

(iv) rotation of a cylinder in a fixed cylinder

$$\text{couple per unit length} = 4\pi\eta a^2\omega\left(\frac{1}{1 - a^2/b^2}\right).$$

(b) *Dragging*

For the translation of a sphere along the axis of a fixed cylindrical tube the solution with the higher terms included is

$$\text{force} = \frac{6\pi\eta a v}{1 - 2.104\left(\frac{a}{b}\right) + 2.09\left(\frac{a}{b}\right)^3 - 0.95\left(\frac{a}{b}\right)^5 \cdots}$$

where $a$ = radius of sphere
$b$ = radius of tube.

This formula is for the case when Reynold's number is infinitesimal. (3.)

Thus when $b = 3a$ the formula gives a resistance of $2 \cdot 7$ times that for an infinite fluid, and for $b = 4a$, a factor of about $2 \cdot 0$, so that increases of this sort are very probable in a small cell. Neighbouring inclusions may well have quite a large effect.

For bodies of a shape not greatly different from a sphere, a good approximation is to use the above formula taking for "$a$" the value for the "equivalent sphere" in the infinite fluid case. This approximation can only be very rough for the case of a very elongated body, or of a wall very close to a body.

(c) *Twisting*

The effect of boundaries on the couple exerted on a compact body of revolution rotating about its axis of symmetry is fairly easily grasped, and is small unless the boundaries are near the equatorial belt of the body.

The effect of the boundaries on less restricted bodies (including our particles) has not been worked out, but below we try to give a rough bound.

(i) Bodies of revolution.

These have been treated by Jeffery (6). He gives a general treatment which can be described as follows: for *any* body of revolution rotating in an infinite fluid about its axis of symmetry we can find a family of surfaces each of which rotates with constant angular velocity. We can then always obtain the solution for the body rotating within one of these surfaces, regarded as a fixed wall, by superimposing a uniform counter-rotation on the whole system to bring the "wall" to rest. This explains the form and intimate relationship between the fall-off of angular velocity and the increase of couple due to a boundary in the two simple cases of rotation quoted above.

Jeffery gives the formulae for the case of an ellipsoid of revolution. A typical result, for a planetary ellipsoid with an axial ratio of 2.24, surrounded by a confocal planetary ellipsoidal shell such that the spacing at the equator is 20 per cent of the body's equatorial radius, shows that the shell increases the viscous couple by a factor of 1.9.

Jeffery has also solved another illuminating case; that of a sphere rotating close to a fixed plane perpendicular to the axis of rotation. The results show that the plane has to be extremely close to the pole to have any considerable effect e.g. at a distance of 2 per cent of the radius it increases the resistance by only 17 per cent. This is because the major part of the viscous couple comes from the equatorial belt, where both the arm of the couple and the velocity are big.

We may thus conclude that unless the boundary approaches close to the body at points far from the axis of rotation, the increase in couple is unlikely to be big.

(ii) Other bodies.

In general our particles are not bodies of revolution, and even if they were we could not easily distinguish their different angular positions under the microscope. Apparently no case has been solved which helps us here.

We propose to estimate the couple on an ovary ellipsoid of revolution rotating inside a fixed spherical shell, radius $d$ ($d$ not too close to $a$) as follows: we suspect that such a shell would not increase the couple on the el-

lipsoid by more than it would increase that of a sphere of radius $a$. This implies that the couple would be increased by no more than

$$8\pi\eta a^3 \omega \left(\frac{a^3}{d^3}\right)$$

neglecting terms higher than $\left(\frac{a^3}{d^3}\right)$

Now we have shown (page 511) that the couple on the ellipsoid in an infinite fluid is approximately given by

$$8\pi\eta a^2 b \omega$$

so that the total couple could be written as

$$8\pi\eta a^2 b \omega \left(1 + p \cdot \frac{a^3}{d^3}\right)$$

where $p$ is probably between $(a/b)$ and 1. However this estimate is little more than a guess.

For a comparatively short particle the boundaries are not likely to cause a large variation in the couple e.g. for $d$ one half greater than $a$, and for a particle of axial ratio 2 : 1, the couple is probably not more than doubled.

Finally we consider how a fixed obstruction at one end of the particle affects its behaviour. A rough estimate can be made by comparing this case with that of a particle of twice the length, and acted upon by double the magnetic couple, with obstructions near its middle. It is clear that in this second case the motion would hardly be altered at all by the obstructions, as they are so near the axis of rotation. The viscous couple on the second particle in a newtonian fluid is very roughly 4 times that of the first (see page 512). Therefore the angular velocity will be halved.

Thus in an infinite newtonian liquid an obstruction at one end increases the resistance so that about twice the couple needs to be applied to give the same angular velocity. It also, of course, produces a small translation of the particle.

Stated in this way it seems probable that the result would also apply to most non-newtonian liquids.

Note that it is not essential for the obstruction to *touch* the particle, as a very close approach may produce sufficient resistance to reduce the angular velocity appreciably.

*3. Non-newtonian behaviour*

So far we have only considered newtonian liquids. This is sufficient for calibration liquids, but may not be for the cytoplasm.

Consider first the behaviour of a liquid, whose "viscosity" varies with shear, in a concentric cylinder viscometer (neglecting end effects). It can be shown that what we measure is the average value of the *fluidity* $\left(\frac{1}{\eta}\right)$. In symbols

$$\eta_e = \frac{\int_{s_a}^{s_b} ds}{\int_{s_a}^{s_b} \frac{ds}{\eta}}$$

where $\eta_e$ = experimental value of the viscosity
$s$ = shearing stress
$s_a$ = shearing stress at inner cylinder
$s_b$ = shearing stress at outer cylinder

That is, if we substitute the experimental values of angular velocity, etc in the usual formula for the viscosity, we obtain the above value of $\eta_e$. It is assumed that the "viscosity" is a function of the instantaneous value of the shear only.

This solution is possible because the surfaces in the fluid which retain their shape (i.e. move as if solid) are surfaces of constant stress, and one can therefore give the stress distribution across the annulus irrespective of the curve of $\left(\frac{1}{\eta}\right)$ against $s$. This condition also applies to the only other case which has been worked out, namely that of the flow through a capillary, although the actual formula given above does not.

We thus see, as is intuitively obvious, that the effect is to slur over the detailed variations in the curve of $\left(\frac{1}{\eta}\right)$ against $s$, and to give an average value. The details are usually got by making $b$ only slightly greater than $a$, so that the average is taken over only a very small portion of the curve on each occasion, and by repeating at different rates of shear to cover a wide range.

We are clearly unable to do anything of this sort in our experiments. Even for a sphere in a non-newtonian liquid the problem is of a different order of

difficulty and does not appear to have been solved. The shear stress varies with latitude from zero to a maximum and it is not at all clear how it distributes itself in the non-newtonian case. The problem of the ellipsoid is even more hopeless.

However it appears extremely plausible that if we substitute the experimental values in the formula, the value of $\eta$ derived will correspond to some average value; that is, to some point on the curve of $\eta$ against $s$ between the maximum value of $s$ and some minimum, probably zero. Moreover it seems very likely that the apparent change of $\eta$ with shear will be less than the maximum change anywhere within this region. Since we cannot rely on our experimental arrangements to measure small differences accurately, we conclude that this method will only show up large changes of "viscosity" with shear, and may conceal small changes.

We note at this point a feature which may be expected in the behaviour of a non-spherical particle in a non-newtonian fluid of the type which becomes very viscous at low shearing stresses. Since the shear near the axis is much less than that near the ends of the particle, the fluid may behave almost as a solid at points near the axis, and also at points far from the particle, so that the flow may take place over a rather restricted region.

*D. The forces on a body in a jelly*

We can apply almost all the previous formulae to the case of a particle in an isotropic elastic medium. Since we are only dealing with feeble jellies we may take Poisson's ratio equal to $\frac{1}{2}$. For *small* strains all the algebraical results for *velocity* in a viscous newtonian fluid apply to the *deflection* in a hookian elastic medium, providing we substitute $n$, the rigidity modulus, for $\eta$ the viscosity.

For example, the couple on a sphere rotating in a viscous liquid, which is

$$8\pi\eta a^3\omega$$

$\eta$ = viscosity
$\omega$ = angular velocity
$a$ = radius of sphere

enables us to write down the couple on a sphere embedded in an elastic medium as (for small angles)

$$8\pi n a^3\theta$$

$n$ = rigidity modulus
$\theta$ = angular deflection

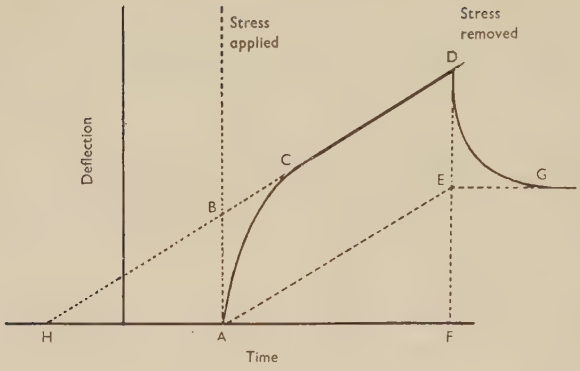


Fig. 1.

To clarify our terms consider next a simple visco-elastic medium, which behaves as shown in figure 1 when a constant stress is suddenly applied and later suddenly removed. In this figure the elastic properties are represented by *AB* and *DE*, the viscous damping by the exponential rise *AC* and fall *DG*, and the pseudo-viscous yield occurring along *CD*, by *EF*. The relaxation time is *HA*.

If we have a particle embedded in a simple visco-elastic medium whose relaxation time is constant with stress, we can obtain the relaxation time experimentally without knowing any of the details of the particle, boundaries, etc. by simply dividing the elastic deflection (for small strains) by the corresponding pseudo-viscous yield rate for any given applied couple. This follows from the similarity in form of the viscous and elastic coefficients mentioned above. If the relaxation time is a function of the stress, there is no simple solution for the general case.

We have so far neglected inertia. We now take it into account and show that the period of free oscillation is very short, and the damping high, again mainly because the particles are so small.

We first consider a particle in a simple elastic medium without viscosity. Due to the inertia it will be capable of free oscillations of both translation and rotation. It can easily be shown that, neglecting for simplicity the inertia of the medium, the dimensionless parameter for both cases is of the form

$$\frac{\sigma^2 \varrho' a^2}{n}$$

where $\frac{1}{\sigma}$ is the order of the period of free oscillation, and $\varrho'$ is the density of the particle.

Putting $\frac{1}{\sigma} = 1$ millisecond, $a = 5\ \mu$, and $\varrho' = 4$, we see that for the parameter to equal unity, $n$ must be 1 dyne/cm$^2$. This is extremely feeble (for a normal gelatin gel $n = 10^3$ to $10^5$ dynes/cm$^2$). For a stiffer medium the time is of course shorter.

It is clear that for a substance as feeble as this the viscous damping would in practice be important. We will therefore consider a particle in a medium with both viscous and elastic properties, and find the condition for critical damping. We assume that the times involved are so short that we can neglect any pseudo-viscous yield.

If we work through a particular case, such as a sphere undergoing rotary oscillations about its axis, and neglect for simplicity the inertia of the medium, we obtain the condition for critical damping as

$$n \backsimeq \frac{4\eta^2}{\varrho' a^2}$$

$\varrho' =$ density of sphere.

We could have derived this, without the constant, in a rough and ready manner by equating the values of $\sigma^2$ which make the two previous dimensionless parameters (page 506 and page 518) equal to unity.

Putting a $= 3\ \mu$, $\eta = 0 \cdot 01$ poise, and $\varrho' = 4$, we obtain $n = 1{,}100$ dynes/cm$^2$. This is not high, but it is rather higher than our estimates. Moreover as already observed it is highly unlikely that the "viscosity" coefficient in biological materials is as low as that of water.

As regards the effects of boundaries, a closer examination shows that since the ratio of the viscous to elastic forces is independent of them, the condition for the damping remaining critical or greater when boundaries are added, reduces to the condition that the ratio of the damping forces to the inertia forces shall not decrease, which we have already shown (page 507) to be probable in most cases.

We thus conclude that the time-period of free oscillation of our particles is less than a milli-second (probably much less) and that the damping is critical or greater unless the rigidity modulus is high and the viscosity low, which is not the case in our experiments.

We have only considered the case of small strains. Large strains may well increase the apparent value of the rigidity modulus, calculated using the simple theory. It is unlikely however in our cases to increase it sufficiently to alter our general conclusions.

We have dealt with this point about critical damping because it is sometimes suggested that a resonance method should be used. Apart from the experimental difficulties due to the very short time periods, it is clear that the extremely low "Q" of the system would make this unprofitable.

It has also been suggested that the restoring force on a particle could be increased by magnetic means, though this would mask any elastic effect due to the medium. The simple theory shows that in the case of a sphere this is equivalent to the medium having a rigidity modulus of

$$\frac{B\,H}{24\,\pi} \text{ dynes/cm}^2.$$

A more exact treatment would be required if the method were seriously contemplated. It is thus not impossible that oscillations could be produced. The envelope of these oscillations is determined by the ratio of the viscous to the inertia forces, and this could be used to measure the former. As has been shown this involves making measurements in a time probably of the order of microseconds. This is not impossible, but it is certainly not easy. The only advantage of such a method is that it is not necessary to know the magnetic forces accurately, although it is essential to know the exact formulae for the viscous and the inertia forces. These could if necessary be checked by calibration experiments in a known liquid. We have not pursued this approach further.

## E. THE FORCES ON A BODY IN A MAGNETIC FIELD

### *1. Twisting: the permanent magnet case*

Assuming that the particle is magnetically homogeneous we note that the magnetic condition is independent of scale, and therefore the forces per unit volume are also independent of scale, over a range where $H$ and $\frac{d\,H}{d\,x}$ can be considered constant.

The variation with shape is more complex. The ellipsoid is the only body for which the magnetic conditions are constant throughout the volume for a uniform applied field. As in the hydrodynamic cases, we will consider only ellipsoids of revolution.

We proceed as follows: we first calculate a factor depending on the shape of the ellipsoid. Using this we find from the $B/H$ curve of the material the relevant value of $B$ for an ellipsoid permanently magnetised along its ma-

jor axis. From this we easily obtain the magnetic moment ($M$) of the ellipsoid. The couple due to a small applied field, $h$, perpendicular to the length of the ellipsoid, is then $Mh$.

The factors which are calculated for ellipsoids are "demagnetising factors." These express the amount by which the magnetisation of the ellipsoid produces a reversed magnetic field acting upon itself, and thus tending to demagnetise itself, and are defined by the equation

$$H' \equiv D\,I$$

where $H'$ = the demagnetising field produced
$I$ = the intensity of magnetisation
$D$ = demagnetisation co-efficient.

$D$ will in general depend upon direction, and will have three different values corresponding to the three axes of the general ellipsoid. The behaviour for other directions can be found by compounding $I$ and $H$ vectorially.

We shall, as usual, only quote the formulae for an ovary ellipsoid of revolution. They are

$$D_1 = 4\pi\left(\frac{1}{e^2} - 1\right)\left(\frac{1}{2e}\log\frac{1+e}{1-e} - 1\right) \quad \text{for the major axis.}$$

$$D_2 = 2\pi\left(\frac{1}{e^2} - \frac{1-e^2}{2e^3}\log\frac{1+e}{1-e}\right) \quad \text{for the minor axes.}$$

(The logs are natural logs)

where $a$ = major axis, $b = c$ = minor axes and $1-e^2 = \frac{b^2}{a^2}$. When $a \gg b$, these formulae become

$$D_1 \doteq 4\pi\frac{b^2}{a^2}\left(\log\frac{2b}{a} - 1\right). \qquad D_2 \doteq 2\pi$$

For the particular case of a sphere $D_1 = D_2 = \frac{4\pi}{3}$

$$\text{that is} \quad \frac{4\pi}{D_1} = \frac{4\pi}{D_2} = 3$$

((8). The notation has been altered.)

Thus if we consider the case of $b$ fixed and $a$ increasing, we see that $\left(\frac{4\pi}{D_1}\right)$

increases rapidly, while $\left(\frac{4\pi}{D_2}\right)$ tends to the value 2. We give a few values in Table III.

Table III

| $\frac{a}{b}$ | 1.0 | 2.0 | 3.0 | 4.0 | 5.0 | 10.0 | 20.0 |
|---|---|---|---|---|---|---|---|
| $\frac{4\pi}{D_1}$ | 3.00 | 5.71 | 9.17 | 13.2 | 17.9 | 49.3 | 148 |
| $\frac{4\pi}{D_2}$ | 3.00 | 2.42 | 2.24 | 2.16 | 2.12 | 2.04 | 2.02 |

As is well known there is a simple graphical construction to find the working point on the $B/H$ curve for a body with a given $D$ in a (parallel) external field $H_1$. The curve of $(B–H)$ against $H$ is plotted, and a line is drawn from the point $H_1$ on the $H$ axis with slope $-\left(\frac{4\pi}{D}\right)$. The working point is the point where this line cuts the curve. This construction applies for any value of the applied field $H_1$. For a permanent magnet we usually have $H_1 = 0$; in this case we are working in the top left-hand quadrant of the $(B–H)$ against $H$ curve.

Once we have found the working value of $(B–H)$ the magnetic moment $(M)$ of the ellipsoid is simply

$$M = \frac{(B - H)}{4\pi} \cdot V$$

where $V$ = volume of the ellipsoid.

*2. Twisting: the soft iron case*

We consider the case of an ellipsoid of soft iron in a magnetic field inclined at a small angle to its major axis. By soft iron we mean here a material with no hysteresis. We do not restrict ourselves to the case of constant permeability, and will in fact consider a material which becomes magnetically saturated.

We calculate the case of an ovary ellipsoid of revolution (major axis = $a$, minor axes = $b = c$) where the applied field, $H$, makes and angle $\theta$ with the major axis, and the intensity of magnetisation, $I$, makes an angle $\alpha$ with the major axis. In general $\alpha \neq \theta$. I is constant throughout the body

both in magnitude and direction. We solve by splitting into components We obtain

$$I \cos \alpha = \frac{\mu - 1}{4\pi}(H \cos \theta - D_1 I \cos \alpha) \quad \text{along the major axis}$$

$$I \sin \alpha = \frac{\mu - 1}{4\pi}(H \sin \theta - D_2 I \sin \alpha) \quad \text{along a minor axis.}$$

We shall only consider the cases where the angles are small. We therefore put sin $\theta = \theta$ and cos $\theta = 1$, etc, and eliminating $I$ we obtain

$$\alpha = \theta \left[ \frac{\frac{1}{(\mu - 1)} + \frac{1}{\left(\frac{4\pi}{D_1}\right)}}{\frac{1}{(\mu - 1)} + \frac{1}{\left(\frac{4\pi}{D_2}\right)}} \right].$$

Now to this approximation the couple ($C$) experienced by the particle is

$$C = I\ V\ H\ (\theta - \alpha)$$

where $V$ = volume of particle.
That is

$$C = I\ V\ H\ \theta \left(1 - \frac{\alpha}{\theta}\right)$$

which we can write

$$C = I\ V\ H\ \theta \left[ \frac{\frac{1}{\left(\frac{4\pi}{D_2}\right)} - \frac{1}{\left(\frac{4\pi}{D_1}\right)}}{\frac{1}{(\mu - 1)} + \frac{1}{\left(\frac{4\pi}{D_2}\right)}} \right].$$

This is the expression we require.
It follows that

(i) if $(\mu - 1) \geqslant \left(\frac{4\pi}{D_2}\right)$ (the suffix 2 referring to the broadways-on case) the term in the bracket is effectively constant as $H$ varies, and

$$C \text{ varies as } I\ H$$

as we should expect.

(ii) if we have a material of low permeability, or one which is saturated so that $(\mu-1)$ has become low, we may have $(\mu-1) < \left(\frac{4\pi}{D_2}\right)$. This latter factor varies from 3 for a sphere to 2 for a long ellipsoid (page 522). Writing the expression for the couple as

$$C = I\,V\,H(\mu-1)\,\theta\left[\frac{\frac{1}{\left(\frac{4\pi}{D_2}\right)} - \frac{1}{\left(\frac{4\pi}{D_1}\right)}}{1 + \frac{(\mu-1)}{\left(\frac{4\pi}{D_2}\right)}}\right]$$

we see that $C$ varies as $I\,H\,(\mu-1)$ approximately
that is $C$ varies as $I^2$ approximately.

Thus if the material is saturated the couple does not increase with the field indefinitely, but tends to a limit.

(iii) for short ellipsoids the couple is less than might be expected on simple theory by the factor

$$\frac{\left(1 - \frac{D_1}{D_2}\right)}{\left(1 + \frac{\left(\frac{4\pi}{D_2}\right)}{(\mu-1)}\right)}$$

which is always less than 1, and moreover becomes zero for a sphere, for which $D_1 = D_2$.

A moment's thought shows that this latter point is obvious. If a *soft* iron sphere is subjected to a slowly rotating magnetic field, the *magnetism* rotates, not the sphere. This is in fact the clue to all the effects. As the magnetic material saturates with increasing field, for example, it becomes easier for the magnetism to rotate. For magnetite, where $(\mu-1)$ can be small these effects may be quite important.

### *3. Dragging*

As we are concerned with obtaining the maximum drag, we will only give the case where the particle is in a magnetic field large enough to saturate it. The magnetic moment $(M)$ will normally be in the direction of the applied field. The force on the particle *in the x direction*, $F_x$, is given by

$$F_x = M_x \frac{\partial H_x}{\partial x} + M_y \frac{\partial H_x}{\partial y} + M_z \frac{\partial H_x}{\partial z}$$

where $M_x$, $M_y$, $M_z$ are the vectorial components of $M$ and $H_x$ is the $x$ component of the applied field $H$. There are similar expression for $F_y$ and $F_z$.

The force thus depends on terms of the form $\left(\frac{\partial H_x}{\partial x}\right)$ rather than of the form $\left(H_x \frac{\partial H_x}{\partial x}\right)$ which occur in certain other cases.

The force on the particle is not necessarily along its length. For example, if the particle is in a magnetic field which lies in the $y$ direction ($H_x = H_z = 0$), so that it, too, points in the y direction ($M_x = M_z = 0$), there will nevertheless be a force on the particle in the $x$ direction if $\left(\frac{\partial H_x}{\partial y}\right)$ is not zero.

## F. THE VARIATION IN RATE OF MOVEMENT WITH SHAPE

We can now combine the results of the previous sections.

### *1. Twisting: the permanent magnet case*

We assume that an ovary ellipsoid is magnetised parallel to its major axis so that it becomes a permanent magnet, of magnetic moment $M$, and that it is then acted on by a small magnetic field ($h$) perpendicular to its length. This will produce a couple $Mh$ and if the ellipsoid is immersed in a newtonian liquid it will rotate with an angular velocity $\omega$. The problem we wish to solve is, how big is $\omega$ and how does it vary with shape?

To obtain the value of $\omega$ for any particular case we merely have to work out the magnetic and the viscous couples from the formulae given in the previous sections and equate them. However it is useful to get a qualitative idea of how $\omega$ changes with shape (we know that it is independent of scale) so we shall suppose that $b$ is kept constant and $a$ allowed to increase. The nature of the variation depends on the nature of the magnetic material.

We take the extreme case first. If the ellipsoid is long, so that the slope of the $(B–H)$ against $H$ curve is much less than $\left(\frac{4\pi}{D_1}\right)$, then $(B–H)$ will effectively be constant, and $M$ will only increase due to the increase in volume, that is proportional to $ab^2$. The viscous couple, however, increases at a rate be-

tween $a^2b$ and $a^3$. Thus in this range the angular velocity decreases rather faster than $\left(\frac{1}{(a/b)}\right)$.

On the other hand, if the ellipsoid is short, and the magnetic material such that the slope of the $(B–H)$ against $H$ curve is much greater than $\left(\frac{4\pi}{D_1}\right)$, then the angular velocity varies as

$$\frac{a\,b^2\left(\frac{4\pi}{D_1}\right)}{k\,a^2\,b}$$

where $k$ is tabulated on page 511.

We thus evaluate $\left(\frac{1}{3}\cdot\frac{4\pi}{D_1}\cdot\frac{1}{k}\cdot\frac{b}{a}\right)$ for various values of $a/b$.

Table IV

| $\left(\frac{a}{b}\right)$ | 1.0 | 2.0 | 3.0 | 4.0 | 5.0 |
|---|---|---|---|---|---|
| $\left(\frac{1}{3}\cdot\frac{4\pi}{D_1}\cdot\frac{1}{k}\cdot\frac{b}{a}\right)$ | 1.00 | 1.13 | 1.12 | 1.10 | 1.09 |

It can be seen that the variation with shape is not very great. Eventually the angular velocity will fall off, but by this time the approximation used is unlikely to be still valid. Thus for a real $(B–H)$ against $H$ curve the angular velocity will eventually decrease with increasing $(a/b)$. It may be roughly constant over a range for $(a/b)$ small, but this depends on the shape of the curve. The exact values can be calculated for any given curve from the formulae given.

The above results apply strictly to the special ellipsoids chosen. It seems reasonable to assume that in the region where the shape of the ellipsoid is making a large difference the approximation for a body of arbitrary shape will not be as good as for ranges where the ellipsoid's shape is having little effect on the angular velocity. However it is not easy to put a figure to the usefulness of the approximation.

We have not pursued this further, as the problem is complicated and we have in any case in our actual experiments taken an average value. If greater accuracy is required the solutions for the viscous forces and the demagnetising co-efficients for the general ellipsoid are available, and might give a better idea of the effects of irregular shape.

*2. Twisting: the soft iron case*

The qualitative results for the corresponding problem in the soft iron case can easily be seen. For very long ovary ellipsoids the angular velocity will fall off rather faster than $\left(\frac{1}{(a/b)}\right)$ as in the previous case. For almost spherical ones it will again be small. Somewhere in between there will be a maximum, depending on the properties of the material and the size of the applied field. The exact values can be calculated for particular cases from the formulae given.

It seems probable that for actual particles of irregular shape we shall get similar effects to those calculated for the ellipsoid. That is, for very short particles we shall get smaller couples than might be expected on the simple theory, and for larger applied fields the couple tending to a maximum instead of increasing indefinitely. In the case of any particular material the evaluation of a few cases for the ellipsoid should give a good idea of the general behaviour, though the reduction in couple due to shortness is likely to be less important for irregular bodies.

The treatment will not apply to materials which show hysteresis.

*3. Dragging*

We will only consider the cases of an ovary ellipsoid of revolution being moved either parallel or perpendicular to its length. Other directions can be solved by compounding vectorially. We consider the relevant field gradient as fixed, and investigate how the velocity of movement depends on the dimensions. For our case the magnetic force, for a given value of $(B–H)$ at saturation, depends only on the volume, not on the shape. We have already shown (page 509) that the effect of size is to make the velocity vary as the square of the characteristic length, so that it only remains to investigate shape variations. As before the formulae will give an exact solution for any chosen case.

(a) dragging parallel to the major axis.

The formula for the viscous resistance and a selection of values are given on page 512. These show that for a fixed $b$, the drag increases with $a$, initially rather slowly, say as $\sqrt[4]{a}$, and gradually increases to rather slower than $a$. Taking $\sqrt[3]{a}$ as a typical value, the velocity of the particle will roughly be proportional to

$$\frac{b^2\, a}{\sqrt[3]{a}\, b^2}.$$

(b) dragging parallel to a minor axis.

The formula and a selection of the values are given on page 512. These show that if $b$ is fixed and $a$ increased, the drag increases initially a little faster than the previous case, so that we may take $\sqrt{a}$ as typical, giving

$$\text{velocity} \sim \frac{b^2 a}{\sqrt{a b}}.$$

What is wanted in fact in both cases is a good estimate of the volume of the particle, plus an approximate estimate of $a$ and $b$. This conclusion is likely to stand for particles having irregular shapes.

## G. PRODUCING FIELD GRADIENTS

We first note that since

$$\frac{\partial H_x}{\partial x} + \frac{\partial H_y}{\partial y} + \frac{\partial H_z}{\partial z} = 0$$

we cannot get a large value of $\frac{\partial H_x}{\partial x}$ without either one or both of the other two being large, and of opposite sign. This implies that the lines of force cannot be parallel in such a region. They must either diverge or be bent.

It can be shown that a magnetically saturated particle can never be in true stable equilibrium under the influences of magnetic forces *alone*. This follows simply by regarding the particle as having a (fixed) surface distribution of magnetic poles, and applying the appropriate analogue of Earnshaw's Theorem (5, 374 and 167). The particle will in fact be either in unstable equilibrium or be moving towards one of the magnets producing the field.

We next wish to show, quite generally, that a very large field gradient can only be produced (leaving aside electric currents for the moment) by having ferromagnetic material *near* the particle. This is perhaps obvious on dimensional grounds. A magnet of a given *shape* and of a given material will produce the same field at corresponding points, irrespective of scale. Thus, clearly, the smaller the magnet, the greater the field gradient. As there is an upper limit to the size of ($B$–$H$) for magnetic materials, there must come a time when the gradient can only be increased by making everything smaller.

We can illustrate this by calculating the result for an ideal polepiece in

the shape of a truncated cone, semi-angle $\alpha$, with the particle at the apex of the cone, which we will take as the origin. We will assume that the direction of magnetisation is everywhere parallel to the axis of the cone. The solution of this problem, which is quite straightforward, gives the field gradient at the origin as

$$\left(\frac{\partial H}{\partial x}\right)_{x=0} = \frac{6\pi I}{x_0} \sin^2\alpha \cos^3\alpha$$

where $I$ = intensity of magnetisation of the pole-piece, which is assumed to be uniform.

$x_0$ = distance of pole-piece from the particle at the origin.

There are three points to notice about this answer. Firstly that the expression has a maximum with respect to $\alpha$ at $\cos\alpha = \frac{3}{\sqrt{15}}$. Secondly that we can write this maximum (putting $4\pi I = B{-}H$) as

$$\frac{(B-H)}{x_0}\frac{18\sqrt{3}}{50\sqrt{5}} \quad (B, H \text{ refer to the polepiece})$$

so that the field gradient at the origin is of the form

$$p\frac{(B-H)}{x_0}$$

where $p$ is a constant a bit less than 1. This form of result is very general.

Thirdly we note that if we had not continued the pole to infinity, but stopped it at the point $x_1$, we should have obtained

$$p(B-H)\left(\frac{1}{x_0}-\frac{1}{x_1}\right)$$

which shows that as long as $x_1$ is several times $x_0$, the result is not sensitive to its exact value. This obviously follows from the fact that we are integrating an expression of the form $\left(\frac{B-H}{r^4}\right)$ through a volume. Thus distant contributions have hardly any effect, because of the upper limit to $(B{-}H)$.

It is not necessary, however, to produce the magnetic gradient *directly* with the primary magnet. We can produce a large uniform field, and consider the gradient near a small body of soft iron placed in this field. For simplicity we will consider the case where this body is a sphere. This is

extremely easy, as for points outside it behaves exactly as a doublet of strength

$$\frac{B-H}{4\pi} \cdot \frac{4\pi}{3} a^3$$

located at its center ($a$ = radius of sphere). Let the particle be a distance $r$ from the centre of the sphere ($r > a$).

If we consider the case where the applied field is parallel to the line joining the particle and the sphere, the force is an *attraction* given by

$$|F| = \frac{B-H}{r}\left(\frac{a}{r}\right)^3 2M$$

($M$ refers to the particle, $B$ and $H$ to the soft iron sphere.)

For the case where the field is perpendicular to the joining line, we have a *repulsion* of

$$|F| = \frac{B-H}{r}\left(\frac{a}{r}\right)^3 3\,\mathrm{M}$$

It is thus possible to control the direction of the force to some extent by altering the direction of the applied field. It should be noted that the force falls off as $\frac{1}{r^4}$, so that it will vary rapidly with the position of the particle.

To sum up, the maximum gradient will usually be of the form

$$p\frac{(B-H)}{x_0}$$

where ($B$–$H$) is the value for the iron in the immediate vicinity, $x_0$ is the distance of the nearest iron from the particle, and $p$ is a constant depending in a complicated way on the configuration, but approaching a value of the order of 1 in well-designed cases. The more distant parts of the magnetic circuit do not affect the gradient directly, but only in so far as they determine ($B$–$H$) in the iron near the particle.

We must consider briefly the possibility of producing high field gradients by electric currents in air-cored coils. We first observe that we require a *sustained* force for our purposes; a short pulse is in general not sufficient. The limitation is therefore the steady heating effect: either the small rise in temperature which the culture will tolerate, which would be important for coils close to, or the rise in temperature of the coil itself for larger, more

distant coils. We will not give a general treatment, but will give one simple example. Consider the conical polepiece of page 529. Instead of a cone of magnetic material, imagine that this cone is a former upon which a coil is wound. What is the current through such a coil which would produce the same field-gradient as the magnet did? By considering the equivalent magnetic shell we arrive at the simple answer that

$$n\,i = I \text{ where } \begin{aligned} n &= \text{number of turns per cm} \\ i &= \text{current in coil (e.m.u.)} \\ I &= \text{magnetic intensity of the iron.} \end{aligned}$$

Now we can easily make $I = 10^3$, so that if we had 1 turn per mm ($n = 10$) i must be $10^2$, or $10^2$ amps. This will clearly give an enormous amount of heat. The margin in the calculation is so big that more precise considerations would not be appropriate. Briefly we note that the heating effect allows $(n\,i)$ to increase as $1^{3/2}$, where 1 is a characteristic length, so that air-core coils can only compete with magnets if they are both very large, which, as we have shown is the case which produces low field gradients. Thus, in general, magnets are much better than air-cored coils for our purpose.

## H. SOME NUMERICAL VALUES FOR THE STRESS

Although we have argued that the method is a very poor one for finding how the "viscosity" of a non-newtonian liquid varies with stress, it is clear that if the range of stresses is very wide indeed we may expect quite considerable differences in behaviour. It is therefore useful to compare the maximum values of the stresses due to twisting and dragging magnetically, and due to gravity. To simplify matters, since we are only concerned with orders of magnitude, we will consider the case of a sphere, taking its radius ($r$) as 1 $\mu$.

1. twisting of a sphere magnetically.
   The maximum stress in this case is

$$\frac{B\,H}{4\,\pi} \text{ dynes/cm}^2.$$

For $B = 225$ and $H = 45$ oersteds we get

$$\sim 400 \text{ dynes/cm}^2.$$

2. dragging a sphere magnetically.
The maximum stress is

$$\frac{B}{12\pi} \cdot r \left(\frac{dH}{dx}\right) \text{ dynes/cm}^2$$

$$\text{for B} = 1500 \text{ and } \frac{dH}{dx} = 10^4 \text{ oersteds/cm (say)}$$

$$\text{and } r = 10^{-4} \text{ cm}$$

we get

$$\sim 40 \text{ dynes/cm}^2.$$

3. dragging a sphere due to gravity.
For the general case (as in a centrifuge) where the centrifugal acceleration is $ng$ we have the maximum stress equal to

$$(\varrho - \varrho_0)\frac{ng}{3} \cdot r$$

where $\varrho$ = density of particle
$\varrho_0$ = density of liquid.

There are two cases of interest.
(a) for magnetic particles under gravity.

$$\text{Taking } \varrho = 4 \quad \varrho_0 = 1 \quad n = 1 \quad r = 10^{-4} \text{ cm}$$

we get

$$= \frac{1}{10} \text{ dynes/cm}^2.$$

(b) for natural inclusions of the cell, in a centrifuge.

Take, arbitrarily, $(\varrho - \varrho_0) = 0 \cdot 1$.

We obtain for the maximum stress

$$\frac{n}{300} \text{ dynes/cm}^2$$

for an acceleration of $ng$.

The point we wish to bring out is not merely that the stresses produced during magnetic twisting are rather bigger than in magnetic dragging, but that both are enormously bigger than the effect of gravity. Moreover, these

stresses are only equaled when centrifuging natural inclusions of the same size by centrifugal fields of the order of $10^5$ times gravity.

Finally we must emphasize that these results only apply for particles of the chosen size, as can be seen from the factor $r$ in the later expressions.

## SUMMARY[1]

1. The paper gives the theory of the magnetic particle method, in which some of the mechanical properties of a fluid are estimated by observing the movements of magnetic particles in it due to applied fields.

2. For the very small particles likely to be used in biological systems the inertia can be neglected.

3. The effect of scale is derived for particles of irregular shape in a newtonian liquid.

4. Exact formulae are quoted, for the three cases most often encountered, for an ovary ellipsoid of revolution in an infinite newtonian liquid. References to the general ellipsoid are given.

5. The effects of the irregular shape of a particle, of boundaries, and of non-newtonian and elastic behaviour of the fluid are discussed qualitatively.

6. Some theoretical notes are given on producing large gradients of magnetic field.

7. Some comparative numerical values of the stresses in certain biological applications are evaluated.

## ACKNOWLEDGEMENTS

The author wishes to thank Dr. Honor B. Fell for the hospitality of the Strangeways Research Laboratory, the Medical Research Council for a Studentship, and Mr. G. Kreisel for many helpful and characteristic suggestions on presentation.

## REFERENCES

1. Crick, F. H. C., and Hughes, A. F. W., *Exp. Cell Res.* **1**, 37 (1950).
2. Edwards, *Quart. J. Maths.* **XXVI**, 70 (1893).
3. Faxén, O., quoted in C. W. Oseen's Hydrodynamik, p. 198, Leipzig, 1927.
4. Gans, *Sitzungsb. K. B. Acad.*, München, **191** (1911).
5. Jeans, J., Electricity and Magnetism. 5th Ed. Camb. Univ. Press, 1925.
6. Jeffery, G. B., *Proc. London Math. Soc.* (2) **XIV**, 327 (1915).
7. Lamb, H., Hydrodynamics, 6th Ed. Camb. Univ. Press, 1932.
8. Maxwell, J. C., A treatise on Electricity and Magnetism, 3rd Ed. Vol II, Oxford Univ. Press, 1892.

[1] A more extended summary has been given in Part I (1, p. 79).

# THE UNUSUAL MEIOTIC BEHAVIOR OF ELYMUS WIEGANDII

HILDA VILKOMERSON

*Department of Botany, Brown University, Providence, Rhode Island*

Received Febr. 15, 1950

*Elymus Wiegandii* is a robust grass of normal vigor and fertility. A well-defined species of shaded alluvial banks in northern New England and in adjacent Canada, it is characterized by a rare, and in some respects unparalleled, meiotic behavior. Therefore it is singularly suited to a study of chromosome structure and mechanics.

## MATERIALS AND METHODS

Spikes excised from flowering culms were fixed in acetic acid-alcohol (1 : 3) and transferred to 70 per cent alcohol. Anthers from florets of this material provided the sporocytes studied, which were squash-smeared in aceto-orcein.[1]

## OBSERVATIONS

At the onset of meiotic prophase, the meiocytes present a bizarre appearance (Figs. 1–4). In ordinary meiosis the loosely reticulate fabric of the resting nucleus appears to ravel out into chromosome threads. Here, however, all the deeply staining part of the reticulum appears to gather, to be stripped from the threads, to coalesce into a number of dark round masses, large and small, and finally to be ejected from the nucleus into the cytoplasm. Sometimes at the ends of fine, tenuous, pale threads, sometimes wholly separated from the nucleus, these pycnotic masses—a few large or several small ones for each nucleus—lie scattered in the cytoplasm, usually peripherally, and often touching the cell wall and deforming it by their pressure. Usually undifferentiated, these chromatic masses sometimes appear

[1] For all the material used in this investigation, as well as for the identification of the species, I am deeply indebted to Professor George L. Church of Brown University.

as dark circles surrounding a light central disc, as though each enclosed an individual little nucleolus. The eventual fate of these masses is obscure, but their material seems to be redistributed on the chromosomes by the time the cells are in diakinesis. As the chromatic network, variously distorted, moves off the nuclear surface, a large, colorless nucleolus appears. It remains faintly discernible through pachytene as a clear area delimited by chromosomes but through which no chromosomes pass.

Zygotene, pachytene, and diplotene stages are uneventful, as is also diakinesis, except that a noteworthy feature here is the presence on one chromosome pair of an appendage—an "extra" piece of deep-staining chromatin attached to the main body by a fine thread, quite unlike an ordinary satellite.

Congression on the spindle proceeds as usual, but orientation at the metaphase plate does not. For now there appear, at or near the ends of the chromosome arms, those secondary kinetic (spindle-fiber-forming) regions which Rhoades (6) so aptly terms neo-centromeres. Their arms precociously drawn poleward by the neo-centromeres, and with their sub-median centromeres still paired on the plate, the metaphase chromosomes form a ragged double line of inverted V's (Fig. 5). Variously stretched, uncoiled (Fig. 7), and sometimes fantastically elongated (Figs. 6 and 9), the chromosomes show here again a separation of their component substances. During the poleward stretching, the thin inner thread outstrips the thicker surrounding (matrix?) material, which seems to be carried along passively and irregularly, often resulting in a lumpy, thick-and-thin appearance of the chromosomes (Fig. 6). Incidentally, all these phenomena vary widely in the intensity of their expression. That is, in some plants only one or two pairs of chromosomes are affected, in others half a dozen, in still others more. (There are fourteen pairs in all.)

First anaphase presents a striking appearance, with a great variety of configurations (Figs. 8–10). Chromosomes with neo-centromeres on both arms back into the poles; others with but one arm stretched describe a lazy S or move poleward as straight rods, parallel with the spindle fibers; still other pairs, with one arm still fixed to the plate and the other outstretched, span the cell from pole to pole like great bridges (Fig. 10). Laggards are frequent, as are also precociously separating pairs. But disjunction, when at last it is accomplished, is regular. Telophase and interphase are undistinguished.

Second prophase shows the usual cruciform dyad, held together only by the sub-median centromere, but somewhat less contracted than is usual at

this stage, and occasionally showing small, translucent, centromere-like regions near the ends of the arms. These ends appear to be non-specifically sticky.

Metaphase II resembles MI, with some dyads oriented as usual, others with arms turned poleward and elongated (Fig. 11); but here the single chromatids, however much attenuated, never show that lumpy, irregular outline so frequently seen at MI. Instead there often appears on the spindle at MII and AII, around and between the chromosomes, an irregularly distributed, amorphous, sticky material (shadows in Fig. 12).

Anaphase II, though not so arresting as AI, is similar to it. The most frequent picture presented is that of chromosomes moving rod-like to the poles, with the arm which is provided with a neo-centromere in the lead. Normal and inverted V's are also seen (Figs. 12–14), and occasionally one that is moving poleward parallel with the metaphase plate, as diffuse-centromere chromosomes do. Lagging is frequent and pronounced; thus, at telophase II, in some plants, it is not uncommon to see a pair or a single chromosome or a fragment lying stranded between the separating cells (Figs. 15 and 16).

Quartets of microspores, and the pollen grains into which they develop, appear to be fully formed and normal. A curious circumstance, however, is the appearance, in about 20 per cent of the microspores, of small, sharply defined ring chromosomes outside the nucleus, in the cytoplasm (Figs. 17 and 18). The rings described and figured here are not formed by a pair of chromosomes or more, but by one chromosome or a fragment thereof. A ring may occur in one cell of a quartet, most frequently in two cells, rarely in more. Sometimes two rings are formed in a single cell, mostly widely separated but occasionally very close together. Most rings are of uniform size, but a few cells show two rings of different size in a single cell. The rings persist and are plainly visible even after the thick pollen grain wall is formed,

---

(All photographs ×1,900 except Figs. 5 and 8, which are ×880.)

Fig. 1–4. Meiocytes in early prophase, showing various stages in, and degrees of, the coalescence of pycnotic material and its expulsion from the nucleus.
Fig. 5. Early metaphase cells, showing their characteristic ragged appearance. (Only a part of the stretched chromosome arms are in focus.)
Fig. 6. A metaphase I cell showing precocious and irregular poleward movement of some chromosome arms. One pair, not stretched, has disjoined already.
Fig. 7. A stretched metaphase chromosome, showing uncoiling.
Fig. 8. A variety of anaphase configurations.
Fig. 9. Early anaphase, with a few chromosomes still anchored on the plate.
Fig. 10. A similar cell, with one pair, much attenuated, stretched from pole to pole.

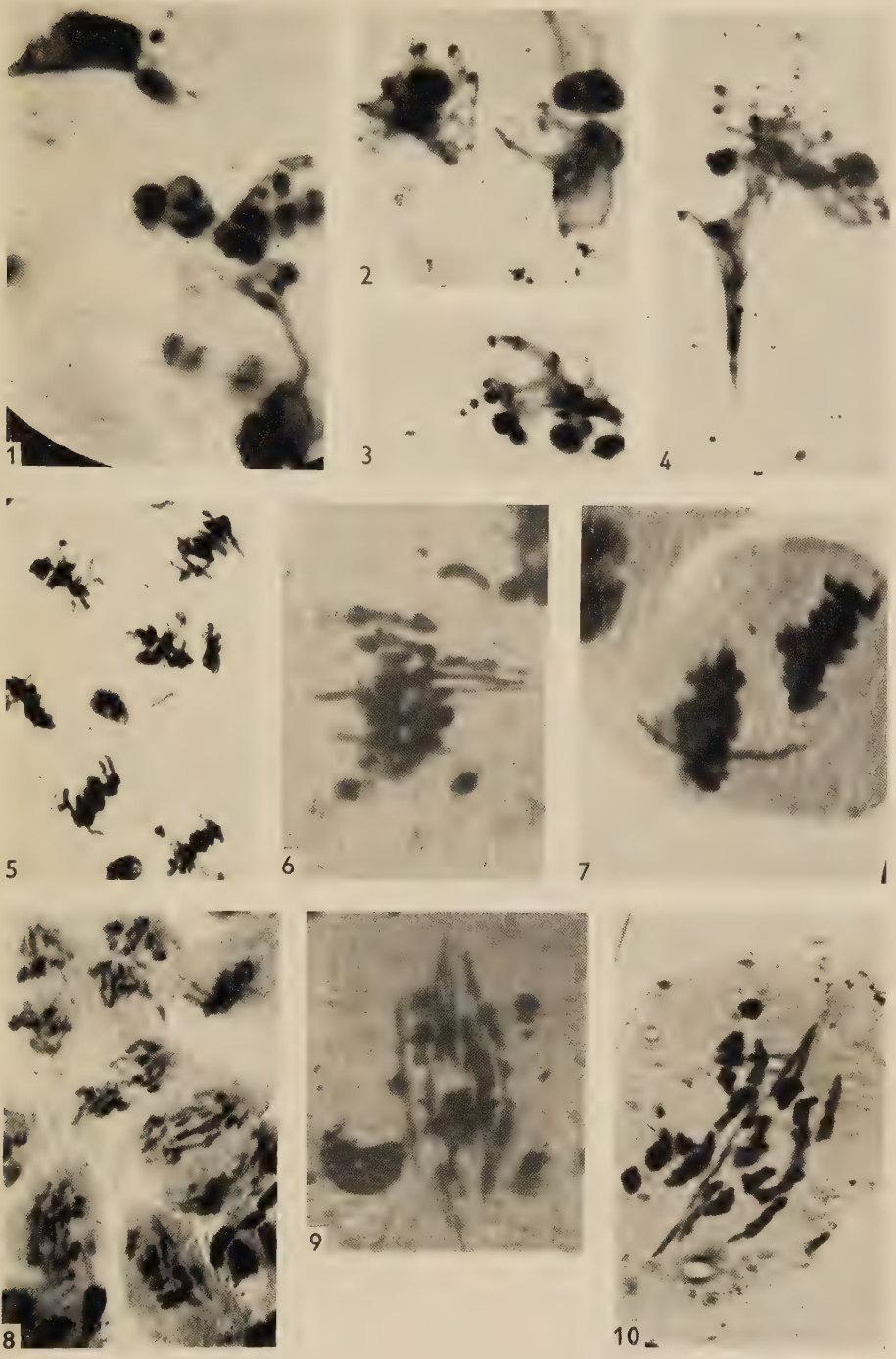
1
2
3
4
5
6
7
8
9
10

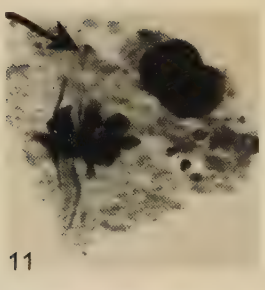
11

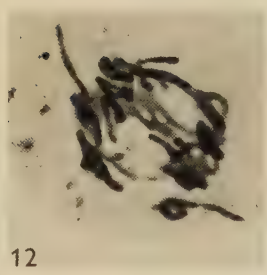
12

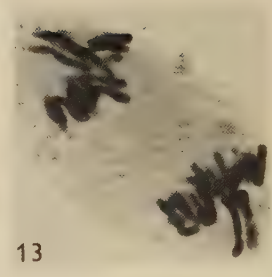
13

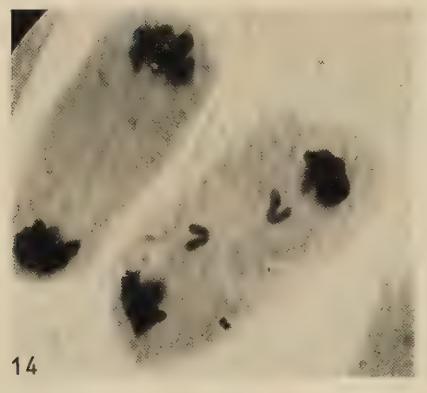
14

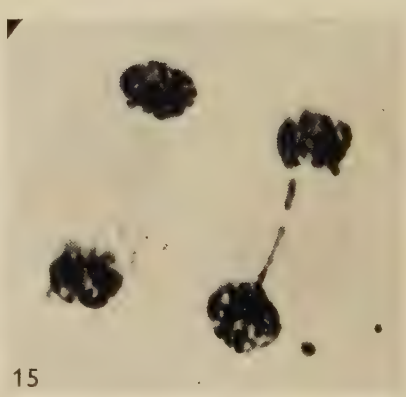
15

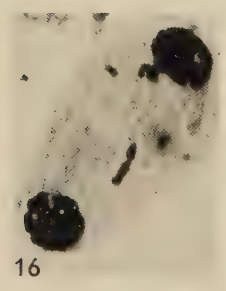
16

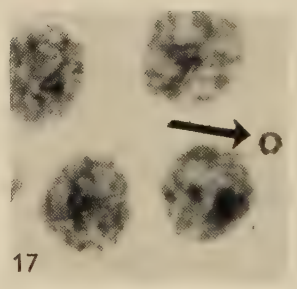
17

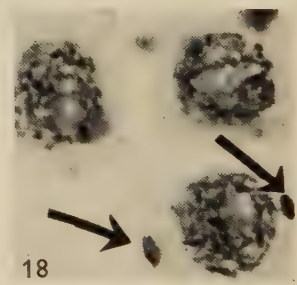
18

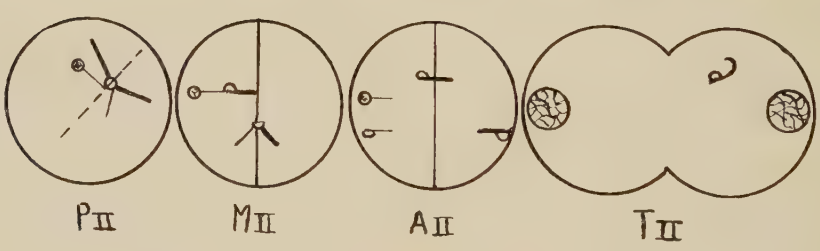

19

though occasionally they collapse, or grow diffuse like any micronucleus. Unlike ordinary laggards lost on the spindle, these rings do not become pycnotic nor do they degenerate subsequently. Rather, at the beginning of the first microspore division, when the nuclear membrane disintegrates, they simply rejoin the chromosome complement from which they had been separated since the previous TII.

Neither megasporogenesis nor somatic mitosis in this material has been investigated as yet. Cytochemical tests for the nucleic acid cycle are in progress. Cytogenetic tests await the new growing season.

## DISCUSSION

The formation of terminal secondary-centric regions on meiotic chromosome arms, with the consequent stretching, backing into the poles, etc., is not unique. Identical behavior has been reported in a strain of *Zea Mays* carrying an abnormal tenth chromosome (7). Also, the drawings in the report of a like occurrence in *Secale cereale* (3), as well as those of another description of the same phenomenon (5), are all strikingly similar to some of our photographs of *Elymus Wiegandii*. Kattermann, Müntzing, Östergren, & Prakken (3, 4, 5) call these "T-ends" or "T-chromosomes." (Incidentally, both Secale and Elymus are members of the grass tribe HORDEAE.)

The early prophase expulsion of pycnotic masses, the appearance at metaphase and anaphase of the as yet unidentified sticky substance, and the formation in the microspores of ring chromosomes, are not reported for maize or rye. In the former, however, the effect of the "sticky" gene (1) in maintaining the "synizetic knot" suggests the first observable meiotic activity of our Elymus cells—a massing and coalescence of chromatic material. In the latter there is described (5) a breaking away of "blobs of chromatin" from the stretched ends of the metaphase and anaphase chromosomes, but

---

Fig. 11. Metaphase II, showing extreme stretching of a few chromosomes, one bent back at the tip (arrow).
Fig. 12. Anaphase II, showing the shadowy, sticky substance that often invests the chromosomes and covers the spindle.
Fig. 13. Anaphase II, with chromosomes moving poleward as elongated rods and as normal V's.
Fig. 14. Telophase II, showing a pair of laggards moving poleward as inverted V's.
Figs. 15.–16. Telophase II showing lagging chromosomes, such as those from which rings are derived.
Fig. 17. A quartet of microspores with a ring chromosome (arrow).
Fig. 18. Three microspores, one of which has two rings seen in side view (arrows).
Fig. 19. Formation of ring-fragment-chromosomes by mis-division of the centromere in a cross-over/non-crossover chromosome carrying a neo-centromere on one chromatid.

no mention is made of the fate of these blobs. Some very similar "blobs" in our material appeared in cells in which a neo-centromere was sub-terminal, and the tip of the chromosome beyond it was bent back on itself, giving the appearance of a small lump, connected by so fine a thread as to seem quite separate (Fig. 11). The detached blobs figured and described in rye are slightly reminiscent, however, of the pycnotic masses seen at early prophase in *Elymus Wiegandii.*

The whole complex of special meiotic behavior in *Elymus Wiegandii* tends to indicate a derangement, or at least a variation from the usual, of the nucleic acid cycle, associated with an unusual distribution of heterochromatin. The gathering and expulsion of pycnotic masses, the lumpy distribution on the stretched chromosomes of the matrix-like material, the formation of neo-centromeres, and the presence among the anaphase chromosomes of the shadowy, gluey substance, all could be accounted for by a variation in timing and in extent of nucleic acid formation.

In connection with the formation of neo-centromeres, other relationships are of interest. The "extra" piece of chromatin on one pair at DK appears in plants of this species from widely scattered collections (New Hampshire, Vermont, Massachusetts, in the U. S. and in Ontario, Canada), but not at all in the closely related species *E. canadensis* and *E. riparius*, which are meiotically undistinguished. In maize, neo-centromeres are formed only in the presence of the abnormal tenth chromosome, which carries extra chromatin (7). Also, they develop only on knobbed chromatids (6). Further, in rye, they appear only on the short, heterochromatic arm of the chromosome involved (4). The formation of neo-centromeres, then, appears to be closely associated with heterochromatin, and presumably with its products.

The origin of the little ring chromosomes, set in the cytoplasm of the microspores like micronuclei, is not clearly established. They derive, apparently, from lagging parts of chromosomes which are stranded in the cytoplasm when the newly formed cells separate at the end of TII (Figs. 15, 16). Figure 19 (diagram) gives a tentative account of their formation. When anaphase disjunction is normal, micronuclei are formed rarely if at all, even where there is considerable lagging, as the new nuclear membrane is not usually completed until the full complement of chromosomes is included. But a chromosome fragment, even though possessed of part of a centromere, if sufficiently retarded, may be excluded from the nucleus and remain in the cytoplasm as a micronucleus. Such a fragment, consisting of one arm of a daughter-chromosome at AII, may be formed whenever, in consequence

of a crossover in first division, a chromosome enters second division with chromatids heterozygous for a neo centromere. The precocious poleward movement of the neo-centromere sets up an unbalanced tension resulting in mis-division of the regular centromere, with poleward movement of two sister-half-chromatids prior to normal disjunction. Now when disjunction occurs, one half-daughter-chromosome must traverse, in order to reach its proper pole, almost the whole length of the spindle from pole to pole. When it arrives too late for inclusion in the telophase nucleus, its broken centromere, following the tendency of broken ends to unite with other ends, joins the only available one, its own, and forms a ring. Thus, each one of the resulting quartet of microspores contains its full complement of chromosomal material, properly distributed to each, but carried (where rings are formed) in two nuclei instead of one. Hence the normal, functional pollen. Even if the rings were lost in the cytoplasm, or if their formation involved a duplication-and-deficiency in chromatin distribution, the viability of the pollen grains need not necessarily be impaired. For *E. Wiegandii* is considered to be, at least phylogenetically, a tetraploid species, and in tetraploids even a considerable loss may be covered by duplicate genes. However, there seems to be no such loss of chromatin in this species.

It is altogether possible, too, that the ring-chromosome formation is wholly independent of the neo-centromere phenomenon. It could be a distinct, gene-controlled behavior pattern, rather than a mechanical consequence of precocious poleward chromosome movement. We have no data, as yet, to decide this issue, but the possibility may be inferred from the fact that these rings persist through microspore division. In this respect *E. Wiegandii* resembles the "divergent spindle" condition in maize (2), in which microspores containing a full set of chromosomes function normally, regardless of whether the chromatin is carried in a single nucleus in the orthodox way, or in several separate nuclei. Unlike comparable conditions in maize and rye, however, the meiotic phenomena described here are not restricted to special genetic strains, nor to irradiated or otherwise treated material, but they characterize, insofar as we can learn, the whole of this wild species.

## SUMMARY AND CONCLUSION

The anomalous meiotic behavior of *Elymus Wiegandii*, a species of wild rye grass, is described. This includes the early prophase separation from the nucleus of pycnotic chromatin material; the formation, at metaphase, of terminal or sub-terminal neo-centromeres on some of the chromosome

arms; extreme stretching of these chromosomes with consequent unusual anaphase configurations; the irregular distribution of certain sticky chromosome substances; and the formation of ring-shaped fragment micronuclei in part of the microspores. Tentative interpretations are suggested, which could account for this behavior.

## REFERENCES

1. Beadle, G. W., *Zeitschr. f. indukt. Abst. u. Vererb.*, **63**, 195 (1932).
2. Clark, F. J., *Amer. Jour. Bot.*, **27**, 547 (1940).
3. Kattermann, G., *Chromosoma*, **I**, 284 (1939).
4. Östergren, G., and Prakken, R., *Hereditas*, **XXXII**, 473 (1946).
5. Prakken, R., and Müntzing, A., *Hereditas*, **XXVIII**, 441 (1942).
6. Rhoades, M. M., 1950. (In press.)
7. Rhoades, M. M., and Vilkomerson, H., *Proc. Nat. Acad. Sci.*, **28**, 433 (1942).

# THE NUCLEIC ACID CONTENT OF MOUSE ASCITES TUMOR CELLS

LEONARD GOLDBERG, EVA KLEIN and GEORGE KLEIN

*Pharmacological Department and Department for Cell Research, Karolinska Institutet, Stockholm*

Received March 25, 1950

In a previous work (18) the desoxypentose and pentose nucleic acid (DNA and PNA) content of mouse ascites tumor was determined in fresh state and after storage at +4° C. By referring the content of nucleic acids to the number of cells in the sample the average amount of nucleic acids in one cell was calculated. A parallel between the virulence of the tumor and the content of PNA in the cells was observed, both diminishing during storage while DNA remained unchanged. No chemical examinations of the nucleic acid content of ascites tumor have previously been carried out.

Solid tumors were used for nucleic acid determinations by previous authors but the lack of homogeneity of the analyzed samples (stroma, necrotic tissue, high variation in PNA content of single cells) made it difficult to compare the data and results obtained for tumor tissues with corresponding normal tissues (for references see Discussion). These difficulties seemed not to be present in ascites tumor.

The aim of the present investigation was to establish the content of nucleic acids in mouse ascites tumor under varying conditions. The following problems were approached:

a. the error of the methods involved,

b. the average PNA and DNA content of mouse ascites tumor cells on a large material under normal conditions and during starvation,

c. the variability of the survival time and nucleic acid content in different animals inoculated with various amounts of tumor cells,

d. a comparison between the values for tumor cells and those obtained in exudate cells from experimentally produced sterile peritonitis,

e. a comparison between the content of nucleic acids of whole cells and of isolated nuclei.

## A. METHODS AND PROCEDURE

### I. *Material*

#### a. ASCITES TUMOR

The ascites tumor was obtained by intraperitoneal inoculation of a suspension of Ehrlich carcinoma cells into white mice of 20–25 gram weight (21, 23). The tumor strain was maintained by intraperitoneal transfer of 0.2 ml amounts of the developed ascites. If an adequate number of cells was inoculated (over $0.4 \times 10^6$) ascites developed in all animals; the inoculum being under $0.4 \times 10^6$ cells, ascites developed only in a certain percentage (see table V), a solid tumor of the abdominal wall developing in the rest of the animals.

In the present experiments white mice were inoculated with counted numbers of cells ($0.8 \times 10^6$–$39 \times 10^6$). The animals were killed with ether on the median survival time ($LD_{50}$) $\pm 2$ days, and the available 1–8 ml ascites fluid was collected. The ascites varied in character from chylous to grossly bloody. Potassium oxalate was added to prevent coagulation (1 drop of 20 per cent solution per 5 ml of fluid), the fluid otherwise clotting readily. 0.5–1 ml was pipetted into calibrated centrifuge tubes for the total nucleic acid (NA) and pentose nucleic acid (PNA) determination in duplicate, another sample was diluted and used for cell counting in a Buerker haemocytometer.

#### b. EXUDATE FROM STERILE PERITONITIS

0.5 ml Omnadin (Bayer) was injected intraperitoneally in white mice, the abdominal cavity being rinsed with physiological saline after 24 hours. In this way exudate cells were obtained from 15 animals. The cells were then centrifuged and resuspended in a small amount of saline. One sample was used for determination of NA and PNA, another for cell counting.

### II. *Cell counting*

The part of the ascitic fluid intended for cell counting was generally diluted 1 : 100 or 1 : 200 with physiological saline without staining, and the number of cells was counted in a checked Buerker haemocytometer, counting 4 squares of each chamber (each square containing 0.1 $mm^3$) and two chambers for each dilution. The final value used was the mean of two diluted portions.

### III. *Determination of NA, PNA and DNA phosphorus*

a. *Total fluid:* The contents of NA and PNA phosphorus were established on 0.5–1.0 ml fluid by the method of Schmidt and Thannhauser (26) with a slight modification of the extraction procedure (11). Phosphorus determinations were performed according to Fiske and Subbarow (16) with the modification of Teorell (30).

DNA phosphorus was calculated as the difference between NA and PNA phosphorus.

Duplicates were run in all the determinations using two portions of the same fluid.

The content of NA, PNA and DNA phosphorus was calculated per ml and also per cell as the ratio between total content and number of cells in one ml of fluid.

b. *Isolated nuclei:* In a number of experiments one part of ascitic fluid, pooled from 2–4 animals, was treated with 1 per cent citric acid in a Waring blendor for 2 minutes and a microscopically checked pure suspension of isolated nuclei was obtained after 3 subsequent centrifugations. NA and PNA phosphorus were then determined as above, and the number of nuclei counted in the same way as the number of cells.

A second part of the fluid was used for cell count and a third part for determination of NA and PNA phosphorus on whole cells.

## IV. *U. V. examinations*

Solid subcutaneous tumors (produced by subcutaneous injection of ascitic fluid) and ascites fluids were fixed in 10 per cent formalin, paraffin-embedded and cut in sections of 5 μ thickness. Two adjacent sections were stained with haematoxylin-eosin respectively transferred to quartz slides for U. V.-microscopy. A general orientation was first performed in the Köhler ultraviolet microscope at 257 mμ, and then serial photographic plates were taken from representative areas. Objectives with numerical aperture 0.35 and 0.85 were used. The photographic plates (Ilford Ordinary Plates) were exposed, developed and printed under strictly identical conditions.

## V. *Statistical methods*

1. *Errors of Means, Sums and Differences.*

a. The standard error ($\varepsilon_M$) of a *mean* ($M$), of $n$ values, with the standard deviation $\sigma_x$, is

$$\varepsilon_M = \frac{1}{\sqrt{n}} \cdot \sigma_x \qquad [1]$$

where $\sigma_x$ = standard deviation of $x = \sqrt{\frac{s(x - \bar{x})^2}{n - 1}}$.

b. The error of a *sum* or *difference* of two means $A$ and $B$ with the same number of values is:

$$\varepsilon_{A \pm B} = \sqrt{\varepsilon_A^2 + \varepsilon_B^2} \qquad [2]$$

where $\varepsilon_A$ = standard error of mean $A$; $\varepsilon_A = \frac{\sigma_A}{\sqrt{n_A}}$; $\varepsilon_B = \frac{\sigma_B}{\sqrt{n_B}}$

$n$ = number of values in $A$ or $B$ resp.

*2. Calculation of experimental error from duplicates.*

The error involved in a single determination ($\sigma_x$) was determined from the stand. dev. of the difference ($\sigma_d$) between duplicates, provided that the mean difference ($D$) is not significant $\left(P > 0.05 \text{ for } t = \frac{D}{\varepsilon_D}\right)$ and that there is no correlation between the 1st and the 2nd determination (formula [3]):

$$\sigma_x = \frac{1}{\sqrt{2}} \cdot \sigma_d \qquad [3]$$

where $\sigma_x$ = error of single determination
$\sigma_d$ = standard deviation of differences.

*3. Time-mortality curves.*

In order to obtain time-mortality curves, allowing of establishing survival time and variability between animals, percentage mortality was transformed to probits (3) and plotted against log survival time, the time-mortality curve becoming a rectilinear line, which denotes log survival times to be normally distributed.
*a. Median survival time* ($LD_{50}$) was determined from the time-mortality curve by ordinary formulae (3).
*b. Variability between animals* (stand. dev.), $\sigma_a$, was calculated from the rectilinear probit-curve by formula [4]:

$$\sigma_a = \frac{1}{b} \qquad [4]$$

where $\sigma_a$ = variability between animals = stand. dev.
$b$ = regr. coeff. of probit line.

$\sigma_a$ will be expressed in log units, if probits are plotted against log survival time.

*4. Transformation of standard deviation* ($\sigma$) *in log units to percentage of mean:*

a. according to ordinary formulae, yielding a higher positive than negative deviation:

$+\sigma$ per cent = $100 \times$ antilog $[\sigma] - 100$ [5 a]
$-\sigma$ per cent = $100 - 100 \times$ antilog $(-[\sigma])$ [5 b]
where $[\sigma]$ = stand. dev. $\sigma$, in log units
$\sigma$ per cent = stand. dev. as percentage of mean.

b. according to Cochran (8), the resulting value being a good approximation for lower values of $\sigma$:

$\pm\sigma$ per cent = $230.26 \times [\sigma]$ [6]

5. Tests of significance, regression equations and correlation coefficients were computed according to ordinary formulae (15).

TABLE I

Errors in Counting Cells.

| Unit | | Number of Determ. | Mean | Errors of Single Unit ($\sigma_x$) | |
|---|---|---|---|---|---|
| | | | | $\sigma_x$ | Per Cent of Mean |
| 1 | | 2 | 3 | 4 | 5 |
| Chamber (Mean of 4 squares) | | | | | |
| Number of cells per chamber | 15—34 | 14 | 27.7 | 3.56 | 12.8 |
| | 35—49 | 26 | 43.6 | 6.84 | 15.8 |
| | 50—64 | 26 | 57.7 | 5.59 | 9.7 |
| | 65—79 | 15 | 70.4 | 8.50 | 12.1 |
| | 80—$\omega$ | 11 | 90.8 | 7.39 | 8.2 |
| | Average: | 92 | 55.3 | 6.44 | 11.6 |
| Diluted Portion (Mean of 2 chambers) | | | | | |
| Number of cells pr dilution ($\times 10^6$) | 60—119 | 21 | 100.3 | 9.0 | 9.0 |
| | 120—225 | 24 | 163.1 | 14.9 | 9.1 |
| | Average: | 45 | 133.8 | 12.8 | 9.6 |

Col. 4. Calculated from stand.dev. of diff. according to formula [3].
Col. 5. Calculated from cols. 3 and 4.
*Exp. Error* (mean of 2 diluted portions) $= \pm 9.1 \times 10^6$ cells $=$ *6.8 per cent.*

## B. ERROR OF METHODS

### CELL COUNTING

The errors involved in counting were established from duplicates by formula [3] (see Statistics) and are seen in table I. In all 46 fluids, 92 chambers and 368 squares were evaluated.

The absolute error increased (col. 4, table I), whereas the percentage error decreased somewhat (col. 5) with increasing number of cells counted. The best results, with the least work involved, will be to choose a dilution which corresponds to 40–60 cells per square, mixing the cells well so as to avoid aggregation. As each specimen was the mean of two diluted portions, *the error of counting cells in one specimen was* $\pm$ *6.8 per cent.*

DETERMINATION OF NA, PNA AND DNA PHOSPHORUS

The error of a single determination was established from 45 duplicates by formula [3] (see table II). Every final value was the mean of two determinations, and the resulting errors of the methods were:

Error of NA per ml = 16.1 μg P per ml fluid = 2.9 per cent
» » PNA » » = 23.3 μg P » » » = 6.6 » »
» » DNA » » = 26.2 μg P » » » = 13.3 » »

When the amount found per ml was referred to the number of cells in the fluid, the error of cell counting will be involved, and the percent error showed a slight increase. The resulting errors of determining the nucleic acid fractions per cell were:

Error of NA per cell = $0.30 \times 10^6$ μg P per cell = 7.4 per cent
» » PNA » » = $0.25 \times 10^6$ μg P » » = 9.5 » »
» » DNA » » = $0.22 \times 10^6$ μg P » » = 14.9 » »

The errors of NA and PNA are of the same order of magnitude and comparatively low. The higher value for the percentage error of DNA is due to DNA having a lower absolute value and being calculated as the difference NA–PNA.

ESTIMATION OF PNA/NA RATIO

The error of a single estimation was established from 45 duplicates (table II), the final value being the mean of two estimations.

Error of PNA/NA = 4.6 per cent, variation coeff. = 7.1 per cent.

This error ($\varepsilon_{P/N}$) can also be calculated from the errors of PNA ($\varepsilon_P$) and NA ($\varepsilon_N$) according to formula [2]:

$$\varepsilon_{P/N} = \sqrt{\varepsilon_P^2 + \varepsilon_N^2} = \sqrt{6.6^2 + 2.9^2} = 7{,}2 \text{ per cent.}$$

The agreement between the experimentally established (7.1 per cent) and the calculated error (7.2 per cent) is good.

ESTIMATION OF PNA/DNA RATIO

The error of the ratio ($\varepsilon_{P/D}$) was calculated according to formula [2] from the errors of PNA ($\varepsilon_P$) and DNA ($\varepsilon_D$) (table II):

$$\varepsilon_{P/D} = \sqrt{6.6^2 + 13.3^2} = 14.8 \text{ per cent.}$$

TABLE II

Error of Methods.
Established from Differences of Duplicates (formula [3]).

| Method | Number of Duplicates | Mean of All Samples | Stand. dev. ($\sigma_x$) of Single Determ. | Exp. Error of Method ($\varepsilon_{meth}$) Mean of Duplicates | |
|---|---|---|---|---|---|
| | | | | $\varepsilon_{meth}$ | Per Cent of Mean |
| 1 | 2 | 3 | 4 | 5 | 6 |
| Cells $\times 10^6$ per ml | 45 | 133.8 | 12.8 | 9.1 | 6.8 per cent |
| NA per ml | 45 | 546.5 | 22.7 | 16.1 | 2.9 per cent |
| NA µg P | | | | | |
| PNA per ml | 45 | 352.1 | 32.8 | 23.3 | 6.6 per cent |
| PNA µg P | | | | | |
| DNA per ml | 45 | 196.4 | 37.0 | 26.2 | 13.3 per cent |
| DNA µg P | | | | | |
| NA per cell $\times 10^{-6}$ µg P | 45 | 4.09 | 0.43[1] | 0.30[2] | 7.4[3] per cent |
| PNA per cell $\times 10^{-6}$ µg P | 45 | 2.64 | 0.35[1] | 0.25[2] | 9.5[3] per cent |
| DNA per cell $\times 10^{-6}$ µg P | 45 | 1.47 | 0.31[1] | 0.22[2] | 14.9[3] per cent |
| PNA/NA in per cent | 45 | 64.1 per cent | 6.5 | 4.6 | 7.1 per cent |
| PNA/DNA | 45 | 1.89 | | | 14.8[4] per cent |

Col. 3: The difference against col. 3 of table III is due to random variations.

[1] Calc. from col. $5 \times \sqrt{2}$.
[2] Calc. from col. $6 \times$ col. 3.
[3] Calc. from $\varepsilon_{meth}$ of NA etc. per ml and $\varepsilon_{meth}$ of Cell Count
Thus for NA per Cell $= \sqrt{2.9^2 + 6.8^2} = 7.4$ per cent etc.
[4] Calc. from $\varepsilon_{meth}$ of PNA and DNA $= \sqrt{6.6^2 + 13.3^2} = 14.8$ per cent.

## ADMIXTURE OF SMALL INFLAMMATORY CELLS

A special study was performed in order to investigate the role of an admixture of leucocytes and other small inflammatory cells to the ascitic fluid.

The relative number of these cells was determined on stained smears. In 23 fluids examined the admixture of leucocytes and other small inflammatory cells was 10.4 per cent on the average, ranging from 2 to 17 per cent. If we suppose that these cells contain the same amount of PNA and DNA as the cells from a sterile peritonitis, it can be calculated from the data in paragraph C that an admixture of as much as 10–15 per cent inflammatory cells would only constitute a maximal error of $\pm$ 2–3 per cent for the content of NA, PNA and DNA per cell, this error being a random variation. The influence of an admixture of leucocytes and other small inflammatory cells on the content of nucleic acids of the ascites tumor is thus negligible compared to the other errors involved.

## C. RESULTS

### NUMBER OF CELLS PER ML IN THE ASCITES FLUID

When the animals which had been inoculated with $0.8 \times 10^6 - 39 \times 10^6$ cells were sacrificed on the median survival time, the number of cells found in the ascites fluid varied between $61 \times 10^6$ and $207 \times 10^6$ cells per ml, the mean being $130.9 \times 10^6$ cells per ml ($n = 65$, $\sigma = 34.5 \times 10^6 = 26.4$ per cent, table III). The distribution of the values is seen in fig. 1 A and B, and conforms with the theoretically calculated range (see table III).

The error of counting (6.8 per cent) played a negligible role as compared to the total variation (26.4 per cent) which is seen in the following:

The variability between animals ($\sigma_a$) was calculated from the total variation ($\sigma_{tot}$) = 26.4 per cent and the error of the method ($\sigma_{meth}$) = 6.8 per cent:

$$\sigma_a = \sqrt{\sigma_{tot}^2 - \sigma_{meth}^2} = \sqrt{26.4^2 - 6.8^2} = 25.5 \text{ per cent.}$$

The correction for the error of the method thus only reduces the total variability from 26.4 per cent to 25.5 per cent.

### NA CONTENT

The content of NA in the ascitic fluid was established in 63 animals in all, and was found to be 525.5 $\mu$g P per ml fluid on an average ($n = 63$, $\sigma =$ 144 $\mu$g = 27.4 per cent) ranging from 244 $\mu$g to 923 $\mu$g. According to Tippett (31) the range of 63 values will approximate $M \pm 2.35\ \sigma$; the agreement between the range found and expectation was good (table III, cols. 6 and 7). This applies also to other data (table III, cols. 6 and 7) and will therefore not be mentioned in the following.

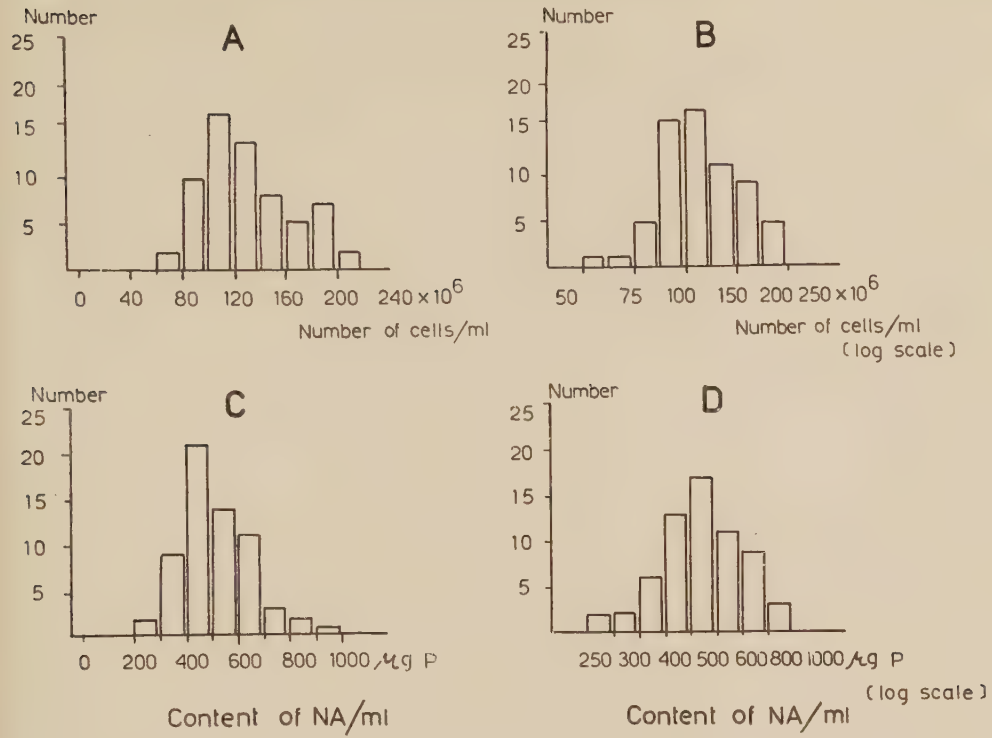


Fig. 1. Distribution of cells and of content of total nucleic acid (NA).
*Ordinates:* Number of animals.
*Abscissae:* A. Number of cells per ml,
B. Number of cells per ml, log scale,
C. Content of NA per ml,
D. Content of NA per ml, log scale.

This variation is rather large and may be due to a number of causes. As the cell-free ascitic fluid does not contain nucleic acids (18) the first cause of the large variation may be a varying number of cells in the fluid.

The content of NA was referred to the number of cells and a high correlation was found (corr. coeff. $+0.84 \pm 0.04$, $n = 65$, table IV). The relationship was approximately rectilinear between $61 \times 10^6$ and $207 \times 10^6$ cells in the fluid which also applies to PNA (see fig. 2) and to DNA. Regression equation, regression coefficient, correlation coefficient and errors are given in table IV.

The content of *NA per cell was* $4.09 \times 10^{-6}$ *µg P* ($n = 65$, $\sigma = 0.62 \times 10^{-6}$ = 15.2 per cent), ranging from 3.07 to $5.72 \times 10^{-6}$ µg P.

It is striking to see how the reference of the total content of NA to the num-

TABLE III

Data on Nucleic Acid Content of Mouse Ascites Tumor in 65 Animals.

| Factor | Numb. of Anim. | Mean (M) | | | Range | | Variability betw. Animals in Per Cent of Mean ($\sigma_a$) |
|---|---|---|---|---|---|---|---|
| | | $M \pm \varepsilon_M$ | Stand. dev. ($\sigma$) | | Found | Calculated ($M \pm 2.35\ \sigma$) | |
| | | | $\sigma_{tot}$ | Per Cent of Mean | | | |
| 1 | 2 | 3 | 4 | 5 | 6 | 7 | 8 |
| Cells per ml $\times 10^6$ | 65 | 130.9 ± 4.3 | 34.5 | 26.4 | 61—207 | 50—212 | 25.5 |
| NA per ml µg P | 63 | 525.5 ±18.1 | 144.0 | 27.4 | 244—923 | 187—837 | 27.3 |
| PNA per ml µg P | 63 | 342.1 ±11.4 | 90.8 | 26.5 | 162—546 | 111—537 | 27.5 |
| DNA per ml µg P | 63 | 184.6 ± 7.9 | 62.6 | 33.9 | 73—398 | 38—332 | 31.2 |
| NA per cell $\times 10^{-6}$ µg P | 65 | 4.09± 0.08 | 0.62 | 15.2 | 3.07— 5.72 | 2.63—5.55 | 13.3 |
| PNA per cell $\times 10^{-6}$ µg P | 65 | 2.68± 0.06 | 0.46 | 17.0 | 1.84— 4.22 | 1.60—3.76 | 14.1 |
| DNA per cell $\times 10^{-6}$ µg P | 65 | 1.42± 0.05 | 0.37 | 26.0 | 0.89— 2.51 | 0.55—2.29 | 21.3 |
| PNA/NA in % | 64 | 65.6 ± 0.9 | 7.05 | 10.7 | 50.1 —77.9 | 49—82 | 8.0 |
| PNA/DNA | 64 | 1.94± 0.07 | 0.59 | 30.5 | 1.01— 3.47 | 0.55—3.33 | 26.7 |

Col. 5: Calculated as col. 4 in percent of col. 3.
Col. 7: The range of 65 variates is theoretically $M \pm 2.35\ \sigma$ according to Tippett (1925).
Col. 8: Calculated from col. 5 of this table and col. 6 of table II = $\sqrt{\text{col. } 5^2 - \text{col. } 6^2}$.

ber of cells thus decreases the variability of NA by two thirds (69 per cent), from 27.4 to 15.2 per cent.

Only a slight part of this decreased variability is due to the error of the methods used to determine cell number and content of NA. If these errors (7.4 per cent) are subtracted, the variability left, thus between animals, is 13.3 per cent (table III, col. 8). The low variability indicates a high degree of uniformity of ascites tumor cells with regard to different animals.

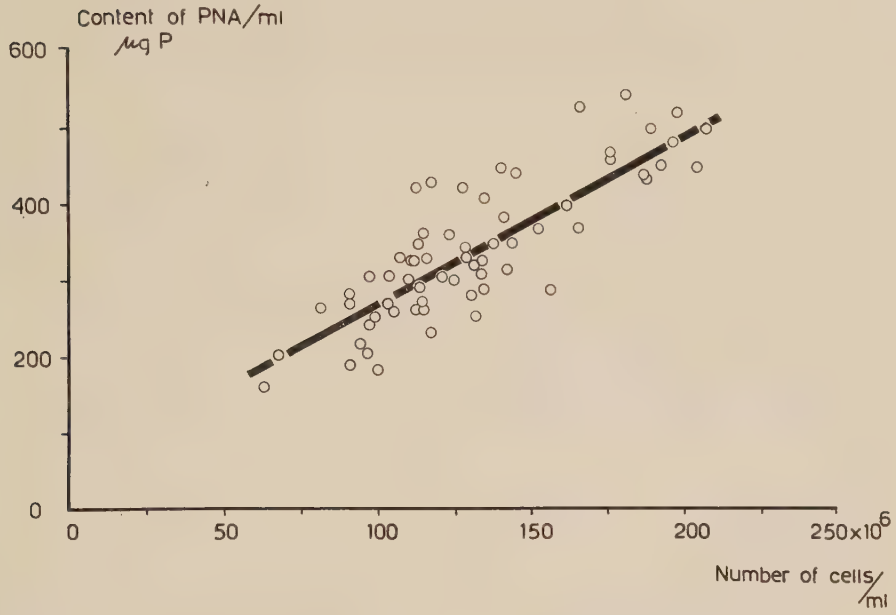


Fig. 2. Relation between the content of PNA and number of cells per ml fluid.

Another indication of the uniformity of ascites cells may be obtained in the following way: The error of a single determination of NA was 22.7 µg P = 4.15 per cent and was calculated from duplicates, i.e. two portions of the same fluid (table II, col. 4). The error thus calculated is composed partly of all errors involved in the chemical procedures of determining NA, partly of all the errors due to the variation in the composition of the cells contained in the specimen examined. The pure errors involved in the chemical procedure may be estimated to be 2–3 per cent, thus only 2–4 per cent is left for the errors due to variation in the average content of NA of the ascites tumor cells. This is an extremely low variation and thus an indication of the uniformity of the cells in one and the same animal.

### PNA CONTENT

The content of PNA in the ascitic fluid averaged 342.1 µg *P* per ml fluid with a range of 162–546 µg ($n = 63$, $\sigma = 90.8$ µg = 26.5 per cent). The variability was thus of the same order as that of NA (table III).

As there was a high correlation between PNA content and cell content in the fluid (illustrated in fig. 2),—correlation coeff. $0.83 \pm 0.04$ (table IV)—PNA

was referred to the number of cells and was found to be *2.68 $\times 10^{-6}$ µg P per cell* on an average, ranging from 1.84 to 4.22 $\times 10^{-6}$ µg P ($n = 65$, $\sigma =$ 0.46 µg = 17.0 per cent, table III), thus showing a striking decrease in variability.

Here, too, the errors of the methods involved were negligible in relation to the variability between animals, this being 14.1 per cent.

Furthermore, there was a high correlation between the content of PNA and NA—correlation coeff. $0.82 \pm 0.04$ ($n = 59$). It could thus be postulated that PNA as per cent of NA would be approximately constant. This was shown to be true, the percentage averaged 65.6 per cent, ranging from 50.1 to 77.9 per cent ($n = 64$, $\sigma = 7.05 = 10.7$ per cent).

If the errors of the methods involved are corrected for, the variation between single animals with respect to the ratio PNA/NA was extremely low, 8.0 per cent.

### DNA CONTENT

The content of DNA in the ascitic fluid was 184.6 µg per ml fluid, ranging from 73 to 398 µg P ($n = 63$, $\sigma = 62.6$ µg = 33.9 per cent, table III).

For DNA too, a correlation was found between content of DNA and number of cells per ml fluid (table IV). The lower correlation coefficient is due to the fact that the errors in determination of DNA are larger than those for NA and PNA respectively.

Calculating DNA per cell gave on the average *1.42 $\times 10^{-6}$ µg P*, ranging from 0.89 $\times 10^{-6}$ to 2.51 $\times 10^{-6}$ µg ($n = 65$, $\sigma = 0.37 \times 10^{-6} = 26.0$ per cent, table III), thus a definite decrease in variability. The variability between animals was 21.3 per cent.

There was no relation to be seen between PNA and DNA (corr. coeff. $0.24 \pm 0.14$, table IV). The average ratio PNA/DNA was 1.94, ranging from 1.01 to 3.47 ($n = 64$, $\sigma = 0.59 = 30.5$ per cent).

### INFLUENCE OF AMOUNT OF CELLS INOCULATED

*a. Survival time and growth rate of inoculated tumor.*

In an earlier work (18) some data were given concerning the influence of the number of cells inoculated on mortality and survival time. A group of 29 mice was inoculated with one and the same inoculum diluted to contain 0.2 $\times 10^6$–21 $\times 10^6$ cells.

The animals inoculated with 0.7 $\times 10^6$–21 $\times 10^6$ cells all subsequently

TABLE IV

Relation between NA, PNA and DNA resp. and Number of Cells.
Regression Equations and Correlation Coefficients.

| Relation | Numb. of Anim. | Means (μg P) | | | | Regression ($\times 10^{-6}$ μg P) | | | | | |
|---|---|---|---|---|---|---|---|---|---|---|---|
| | | $\bar{x} \pm \varepsilon_{\bar{x}}$ $\times 10^6$cells | $\bar{y} \pm \varepsilon_{\bar{y}}$ μg P | Stand. dev. ($\sigma_y$) | | Regression Equation | Regression Coeff. | Correlation Coeff. | Signi-ficance (P) | Departure from regr. line ($\sigma_{y-Y}$) | |
| | | | | $\sigma_{tot}$ | per cent of mean ($\bar{y}$) | | | | | | per cent of mean ($\bar{y}$) |
| 1 | 2 | 3 | 4 | 5 | 6 | 7 | 8 | 9 | 10 | 11 | 12 |
| NA/Cell | 64 | 129.9 ± 4.4 (cells) | 523.9 ± 17.9 (NA) | 143 | 27.3 per cent | y = 77.2 + 3.46 x | 3.46 ± 0.28 | 0.842 ± 0.037 | < 0.001 | 77.9 | 14.9 per cent |
| PNA/Cell | 64 | 129.9 ± 4.4 (cells) | 341.3 ± 16.9 (PNA) | 93.5 | 27.4 per cent | y = 52.2 + 2.23 x | 2.23 ± 0.19 | 0.827 ± 0.039 | < 0.001 | 53.0 | 15.6 per cent |
| DNA/Cell | 64 | 129.9 ± 4.4 (cells) | 184.0 ± 7.8 (DNA) | 62.3 | 33.9 per cent | y = 29.2 + 1.19 x | 1.19 ± 0.17 | 0.666 ± 0.070 | < 0.001 | 46.8 | 25.4 per cent |
| PNA/NA | 59 | 4.04 ± 0.08 (Na/cell) | 2.64 ± 0.06 (PNA/cell) | 0.45 | 17.0 per cent | y = 0.23 + 0.60 x | 0.60 ± 0.05 | 0.820 ± 0.043 | < 0.001 | 0.26 | 9.9 per cent |
| PNA/DNA | 45 | 2.61 ± 0.08 (PNA/cell) | 1.47 ± 0.06 (DNA/cell) | 0.39 | 26.7 per cent | y = 1.00 + 0.17 x | 0.17 ± 0.11 | 0.244 ± 0.140 | ~ 0.2 | 0.39 | 26.3 per cent |

Col. 10. Probability P; P < 0.001 = significant difference; P ~ 0.2 = no significance.

TABLE V

Relation between Survival Time, Mortality and Number of Cells Inoculated.

| Number of Cells Inoculated ($\times 10^6$) | Survival Time in Days | | | | | | | | | | | |
|---|---|---|---|---|---|---|---|---|---|---|---|---|
| | Mortality in Per Cent | | | | | | | | Median Survival Time ($LD_{50}$) | | | |
| | 20 | 25 | 40 | 50 | 60 | 75 | 80 | 100 | $LD_{50}$ (days) | Standard Deviation ($\sigma$) | | |
| | | | | | | | | | | Days | Log Units | Per Cent of Mean |
| 1 | 2 | 3 | 4 | 5 | 6 | 7 | 8 | 9 | 10 | 11 | 12 | 13 |
| 0.2 | | 15 | | 23 | | 42 | >50 | >50 | 25.7 | 19 | 0.32 | 74 per cent |
| 0.4 | 11 | | 22 | | 37 | >50 | >50 | >50 | 28.2 | >28 | 0.52 | 120 » » |
| 0.7 | | | 14 | | 17 | | 19 | 22 | 15.3 | 4.6 | 0.13 | 29 » » |
| 0.8 | 9 | | 10 | | 11 | | 15 | 18 | 11.0 | 3.5 | 0.14 | 32 » » |
| 2.0 | 7 | | 8 | | 10 | | 11 | 14 | 8.8 | 2.5 | 0.122 | 28 » » |
| 21.0 | 5 | | | | | | 7 | 9 | 5.9 | 1.1 | 0.084 | 19 » » |

Inoculates $0.2 \times 10^6$ and $0.4 \times 10^6$: The animals which developed ascites tumors, succumbed. The rest of the animals developed solid tumors and survived an observation time of 50 days.
Cols. 2—9: Observed lethal times in days.
Col. 10: Computed from probit curves (see Statistics).
Col. 11: Calc. as col. $13 \times$ col. 10.
Col. 12: Calc. from probit curves (see Statistics).
Col. 13: Approximate values (formula [6]); exact values see formula [5].

succumbed, the animals with the highest dose within 5–9 days, the animals with the lowest dose after 14–22 days. The inoculation of a smaller amount, $0.2 \times 10^6$–$0.4 \times 10^6$, produced ascites only in a certain percentage. A solid tumor of the abdominal wall developed in the rest of the animals, and these survived an observation time of at least 50 days (table V).

In order to establish quantitatively, for the present work, the median survival time and the standard deviation of the animals, the data were used in the following calculations:

The percentage mortality was transformed to probits and plotted against log survival time, $LD_{50}$ and standard deviation computed according to Bliss (3) (see Statistical Methods). The results are given in fig. 3.

The rectilinear time-mortality curves indicate log survival times to be normally distributed, and thus survival times to be skewly distributed. This is in accordance with the distribution of survival times after introduction of a large body of different agents (4).

A quantitative aspect of the variability between animals as one indication

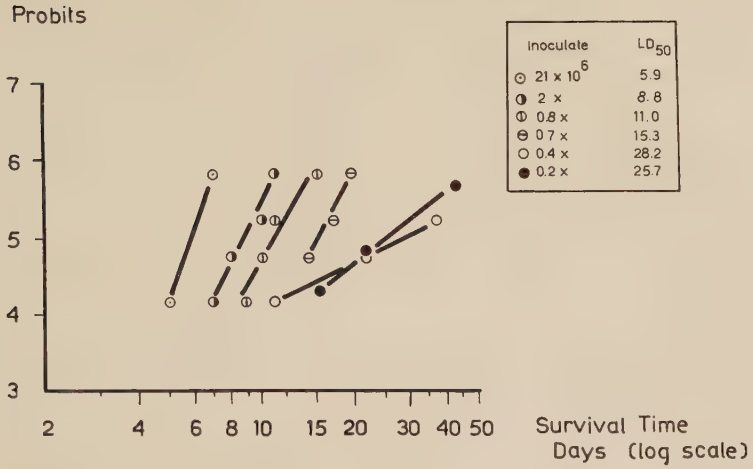


Fig. 3. Relation between mortality and survival time.
*Ordinate:* Mortality transferred to probits (0 and 100 per cent are not plotted and can be found in Table 5).
*Abscissa:* Log survival time in days.
Calculated $LD_{50}$ see text.

of the effect of inoculation may be obtained from the time-mortality curves (fig. 3). The curves present themselves in two groups. The first comprises 4 curves showing a parallel course with a rather steep inclination, with shorter survival times and larger amounts of cells inoculated. The second group includes 2 curves, with longer survival times after smaller amounts and with another inclination. As the inclination of a probit time-mortality curve is the inverse value of the standard deviation (formula [4], a parallel course of a group of curves indicates a uniformity of the standard deviation within each group.

This phenomenon was dealt with in table V.

It appears from the table that the standard deviation expressed in days (col. 11) decreases as the amount of cells inoculated increases.

If standard deviation, however, is calculated in log units (col. 12), or expressed as per cent of the median survival time (col. 13), it is obvious that the standard deviations of the different series gather themselves around two main values. In the series with $0.2 \times 10^6$ and $0.4 \times 10^6$ cells inoculated and ascites developing only in a certain percentage of the animals, this value was about 100 per cent, and only about 20–30 per cent in the series with an inoculum of $0.7 \times 10^6 - 21 \times 10^6$ cells, where ascites developed in all animals. This low variability in the ascites group is another expression of the uni-

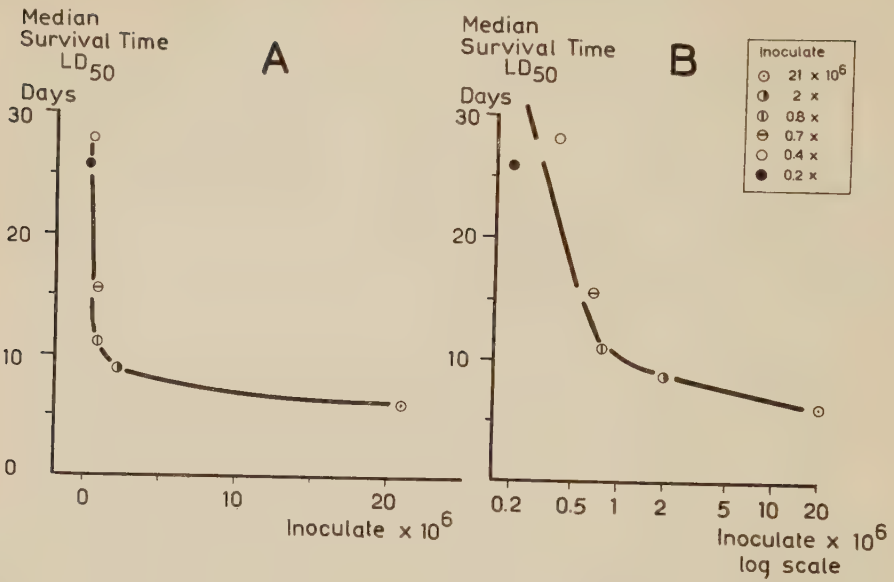


Fig. 4. Relation between survival time and number of cells inoculated.
*Ordinate:* Median survival time ($LD_{50}$).
*Abscissae:* A. Number of cells inoculated,
B. Number of cells inoculated (log scale).

formity in the growth rate of an ascites tumor, the variability increasing threefold when partly ascites and partly only solid tumors develop.

The median survival time ($LD_{50}$) was computed and plotted against the inoculated number of cells in fig. 4 A. It is striking to note how survival time falls abruptly with an increase in inoculated amount up to $0.7–0.8 \times 10^6$ cells, and then only slowly changes with even large amounts of cells inoculated. The exact values are given in table V col. 10. Plotting median survival time against log number of inoculated amount of cells, fig. 4 B, is a means of differentiating the effect of low numbers of cells inoculated.

*b. Content of NA, PNA and DNA.*

In order to study the influence on nucleic acid content of the time between inoculating and sacrificing the animals, 20 animals were inoculated with $1.3 \times 10^6$ cells, and 20 with $13 \times 10^6$ cells. The 40 animals were then killed after 7 to 11 days, thus $LD_{50} \pm 2$ days, about 8–10 animals each day, and the contents of nucleic acids were determined. No correlation whatever between time and the data found was seen within these time limits, neither with re-

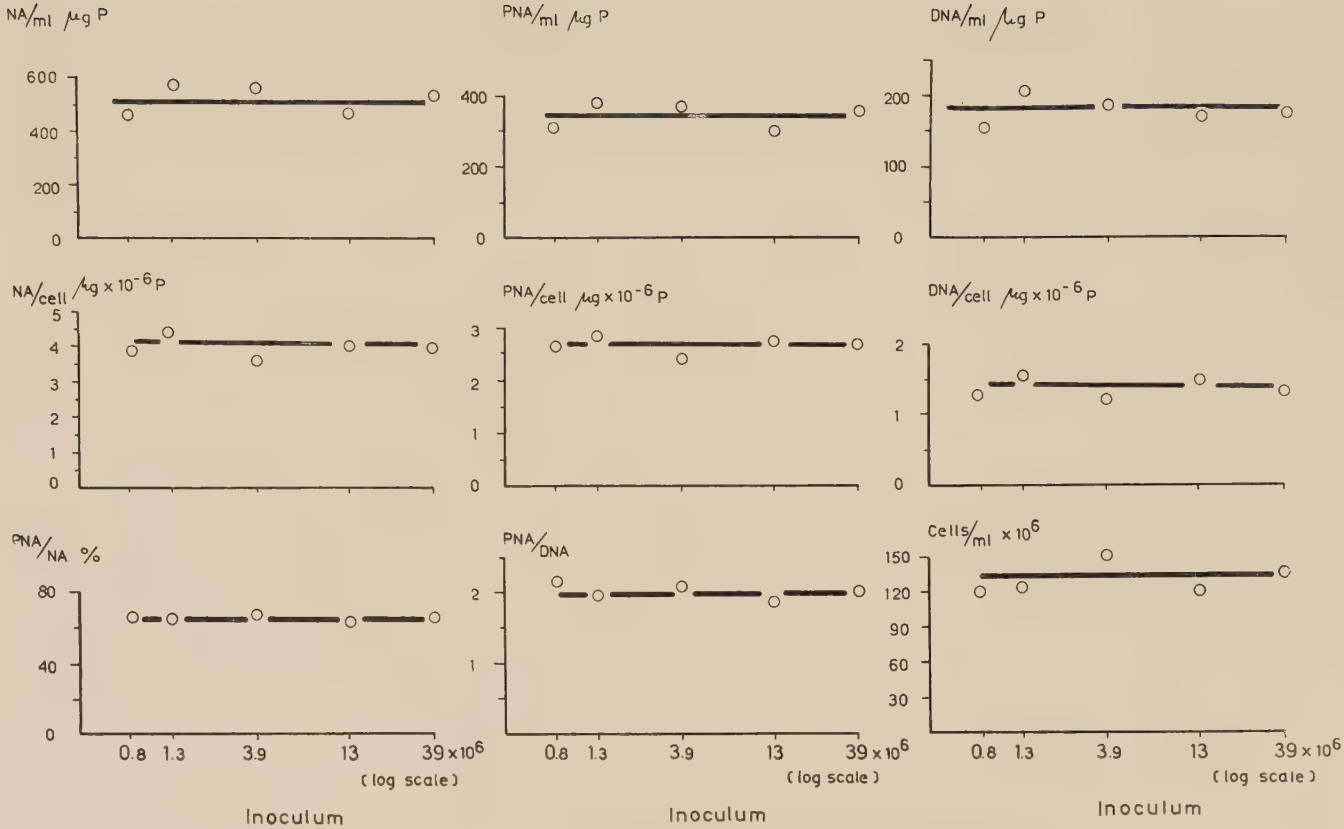


Fig. 5. Relation between content of nucleic acids in the ascitic fluid and number of cells inoculated. *Abscissae:* Log number of cells inoculated, the same scale for all curves.

gard to number of cells per ml, content of nucleic acids, nor to the ratios of PNA/NA and PNA/DNA.

In order to investigate the influence of survival time on the contents of nucleic acids, five groups of animals were inoculated with 0.8, 1.3, 3.9, 13 and $39 \times 10^6$ cells. These animals, 66 in all, were sacrificed around the median survival time $\pm 2$ days (cp. tab. V), and nucleic acid phosphorus was determined. The results are given in fig. 5.

The interesting fact is seen, that in spite of the number of cells inoculated playing a major role for the growth rate and survival time, yet no influence is seen on the content of nucleic acids as long as the animals are sacrificed after the median survival time $\pm 2$ days.

### STARVATION

A series of experiments were carried out in order to establish the possible influence of fasting on the content of nucleic acids in the tumor cells.

Seven animals, inoculated with about $10 \times 10^6$ cells, were starved for 48 hours, starting on the 6th day after inoculation, and were then killed. The content of nucleic acid of the ascitic fluid was determined.

The results are given in table VI and show a good agreement between the data of starved animals and of those not starved, the differences being due to random variations.

### ISOLATION OF NUCLEI

In order to determine whether the procedure of isolation of nuclei caused any loss in DNA content, 4 series of ascitic fluids were investigated. The fluids were pooled from 2–4 animals in each series and divided into two parts, one for isolation procedure and another, untreated, for nucleic acid determination on whole cells of the same fluid. The results are given in table VII.

The isolation procedure caused no loss of the DNA content of nuclei.

### NUCLEIC ACID CONTENT OF EXUDATE CELLS

In order to compare the nucleic acid content of tumor cells with that of non-tumorous cells, a sterile peritonitis was produced by injecting 0.5–1.0 ml Omnadin (Bayer) into a number of mice. The exudate cells found after 24 hrs were examined. Nucleic acid content was determined in pooled exudates from 15 animals (see Methods), with the following result:

TABLE VI

Nucleic Acid Content after Starvation for 48 Hours.

| Factor | Starvation | | Not Starved | | Difference | | |
|---|---|---|---|---|---|---|---|
| | n | $M \pm \varepsilon_M$ | n | $M + \varepsilon_M$ | $D \pm \varepsilon_D$ | t | Significance (P) |
| 1 | 2 | 3 | 4 | 5 | 6 | 7 | 8 |
| Cells $\times 10^6$ per ml | 7 | 135.6 ± 17.5 | 65 | 130.9 ± 4.3 | 5.7 ± 18.0 | 0.32 | 0.7 |
| NA per ml | 7 | 582.0 ± 78.9 | 63 | 525.5 ± 18.1 | 56.2 ± 81.0 | 0.69 | 0.5 |
| NA µg P | | | | | | | |
| PNA per ml | 7 | 373.4 ± 40.8 | 63 | 342.1 ± 11.4 | 31.3 ± 42.3 | 0.74 | 0.5 |
| PNA µg P | | | | | | | |
| DNA per ml | 7 | 208.3 ± 40.0 | 63 | 184.6 ± 7.9 | 23.7 ± 40.8 | 0.58 | 0.6 |
| DNA µg P | | | | | | | |
| NA per cell µg $\times 10^{-6}$ P | 7 | 4.28 ± 0.17 | 65 | 4.09 ± 0.08 | 0.19 ± 0.19 | 1.0 | 0.3 |
| PNA per cell µg $\times 10^{-6}$ P | 7 | 2.77 ± 0.14 | 65 | 2.68 ± 0.06 | 0.09 ± 0.15 | 0.60 | 0.6 |
| DNA per cell µg $\times 10^{-6}$ P | 7 | 1.50 ± 0.18 | 65 | 1.42 ± 0.05 | 0.09 ± 0.19 | 0.47 | 0.6 |
| PNA/Na in per cent | 7 | 65.1 ± 3.3 | 64 | 65.6 ± 0.9 | −0.5 ± 3.3 | 0.15 | 0.9 |
| PNA/DNA | 7 | 2.02 ± 0.28 | 64 | 1.94 ± 0.07 | 0.08 ± 0.29 | 0.27 | 0.8 |

Cols. 4 and 5: equal to cols. 2 and 3 of table III.
Col. 6: difference between col. 3 and col. 5 of this table.
Col. 7: $t = \frac{D}{\varepsilon D}$ (Fisher 1936); degrees of freedom $n_1 + n_2 - 2$.
Col. 8: Probability P; $P > 0.2$ denotes no significant difference.

Content of NA per cell = $1.21 \times 10^{-6}$ µg P per cell
» » PNA » » = $0.44 \times 10^{-6}$ µg P » »
» » DNA » » = $0.77 \times 10^{-6}$ µg P » »
PNA/NA in per cent = 36.3 per cent
PNA/DNA = 0.59

These values are decidedly lower than those found in ascites tumor cells (see e.g. table III). The implications will be discussed later.

TABLE VII

Nucleic Acid Content of Isolated Nuclei and of Simultaneously Determined Whole Cells of Same Fluid.

| Series | Number of Pooled Fluids | Content of Nucleic Acid ($\times 10^{-6}$ µg P) | | | | | | |
|---|---|---|---|---|---|---|---|---|
| | | Content per Cell | | | Content per Nucleus | | | Difference of DNA (Cell-Nucl.) |
| | | NA | PNA | DNA | NA | PNA | DNA | |
| 1 | 2 | 3 | 4 | 5 | 6 | 7 | 8 | 9 |
| I | 3 | 4.22 | 2.90 | 1.32 | 1.78 | 0.30 | 1.48 | —0.16 |
| II | 2 | 4.17 | 2.31 | 1.86 | 1.50 | 0.23 | 1.27 | +0.59 |
| III | 4 | 4.06 | 2.77 | 1.29 | 1.65 | 0.21 | 1.44 | —0.15 |
| IV | 3 | 3.81 | 2.18 | 1.63 | 1.95 | 0.34 | 1.61 | +0.02 |
| | | | | Mean: 1.53 | | | 1.45 | +0.08 |

Col. 9: Difference col. 5—col. 8.
*Mean Difference* +0.08: Not significant ($P \sim 0.2$).

## D. DISCUSSION

### NUMBER OF CELLS

If a number of animals be examined with regard to the total number of ascites tumor cells a certain time after inoculation, the number of tumor cells will vary from animal to animal, due to variations in growth rate, response etc. The number of cells after inoculation will multiply geometrically with increasing time. One consequence of this is that the varying numbers of cells found in the different animals will show a skew distribution, whereas the log numbers will be normally distributed.

We can assume, with a high degree of probability, that this not only applies to the total number of cells, but also to the number of cells per ml. This assumption is supported by our findings, the number of cells per ml being skewly distributed (fig. 1 A), and log number of cells per ml being approximately normally distributed (fig. 1 B).

As the content of nucleic acids was shown to be closely correlated to the number of cells (see fig. 2), the geometrical progression and skew distribution would also apply to the content of nucleic acids per ml. That this is the case is seen from fig. 1 C and D, showing the distribution of NA per ml

to be skew (fig. 1 C) and of log NA per ml to be approximately normal (fig. 1 D).

The number of cells per ml on a certain day after inoculation is most probably proportional to the number of cells inoculated and to the growth rate. According to Lettré (22) and to our own calculations one single cell will divide once in approximately 24 hours. Based on these assumptions, the cell number per ml during the median survival time ($LD_{50}$) can be calculated to be fairly constant, even after widely varying amounts of cells inoculated.

Thus, on the same basis of geometrical multiplication, the fact may be explained that the number of cells really found per ml varied by only 25.5 per cent round a common mean (Table III) between different animals, in spite of the animals being inoculated with a largely varying amount of cells ($0.8 \times 10^6$–$39 \times 10^6$) and the animals being sacrificed after varying times, from 5 to 11 days.

### PNA

Caspersson and Santesson (7) have shown by ultraviolet absorption studies that in the same tumor the cells have different cytoplasmic PNA concentration. The extreme types were called "A" and "B" cells. The authors stated that "the type of the individual cells seems to be determined to a considerable degree by the nutritional conditions." The A cells make up the zones bordering on neighbouring tissues, the parts right around the blood vessels, and cell complexes infiltrating loose connective tissue. "The extreme B type occurs in the inner parts of tumor complexes where the distance to the surface and to blood vessels is great." The A cells contain large amounts of cytoplasmic PNA compared to intermediate types and to extreme B cells.

Our plates of solid tumors, produced by subcutaneous inoculation of ascites tumor cells, show a very high variability in cellular U.V. absorption at 257 mμ (see figs. 6 and 7). This is in good agreement with the findings of Caspersson and Santesson.

In the ascites tumor, however, all the cells can be assumed to be under identical nutritional circumstances, as they are homogeneously distributed as a cell suspension. In agreement with this assumption, U.V. examination at 257 mμ shows a rather uniform picture (fig. 8). The magnitude of absorption at 257 mμ of the individual cells is of the same order as that of the A cells in the solid tumors of figs. 6 and 7. This might indicate that the ascites tumor cells are under rather favorable nutritional conditions and,

as judged from their absorption, have a high nucleic acid content. A comparatively high PNA content is also suggested by our chemical data, the PNA/DNA ratio found in ascites tumor being 1.94 on the average. Corresponding values obtained on different solid tumors, as far as they can be compared (see e.g. Schneider, 27), are in the order of 0.5–0.8. These lower values in solid tumors correspond to the cellular composition: solid tumors being constituted mainly of intermediate and B type of cells (7) and of only a small number of A cells with high PNA content.

A high cytoplasmic PNA is associated with a high growth rate (6). Thus the findings concerning the PNA content are in good agreement with the high growth rate of the ascites tumor. The reproducibility of the growth rate, reflected by the low variation in survival times (cp table V), corresponds to the low variability of the PNA content per cell.

Storage was shown to reduce the PNA content of the ascites cells, accompanied by a decrease in the growth rate (18).

Starvation is known to influence the content of nucleic acids of normal cells under certain circumstances. Thus for liver cells fasting is accompanied by a shrinkage in the volume of the cytoplasm and by decrease in NA content. This decrease is entirely due to a fall in PNA content, DNA remaining unchanged (10). Davidson found a 20 per cent decrease in PNA of rat liver cells after 48 hrs fasting, and a certain decrease in the thymus and the spleen (9).

We could establish no change, neither in the PNA content of ascites tumor cells nor in DNA after 48 hours starvation (table VI) in spite of the general condition of the starved animals being highly impaired.

The tentative comparison between the nucleic acid content of ascites tumor cells and that of non-tumorous peritoneal exudate cells shows clearly the PNA content of exudate cells to be only about 15 per cent of that of tumor cells, and the PNA/DNA ratio to be 0.59, thus about 30 per cent of that of the tumor. It may be worth mentioning in this connection that our value of the PNA/DNA ratio of exudate cells corresponds to the PNA/DNA ratios found in spleen and thymus, while in organs with active protein synthesis (e.g. liver, pancreas), this ratio is much higher (10).

---

Fig. 6. Solid tumor, developed after subcutaneous inoculation of 0.2 ml ascitic fluid. Picture taken at 257 mμ. Note high variation of absorption, presence of both "A" and "B" cells. Obj. ap. 0.35, cond. ap. 0.25.

Fig. 7. Solid tumor, produced as in Fig. 6. Optical conditions as in Fig. 6. Note "A" cells with high absorption around blood vessel.

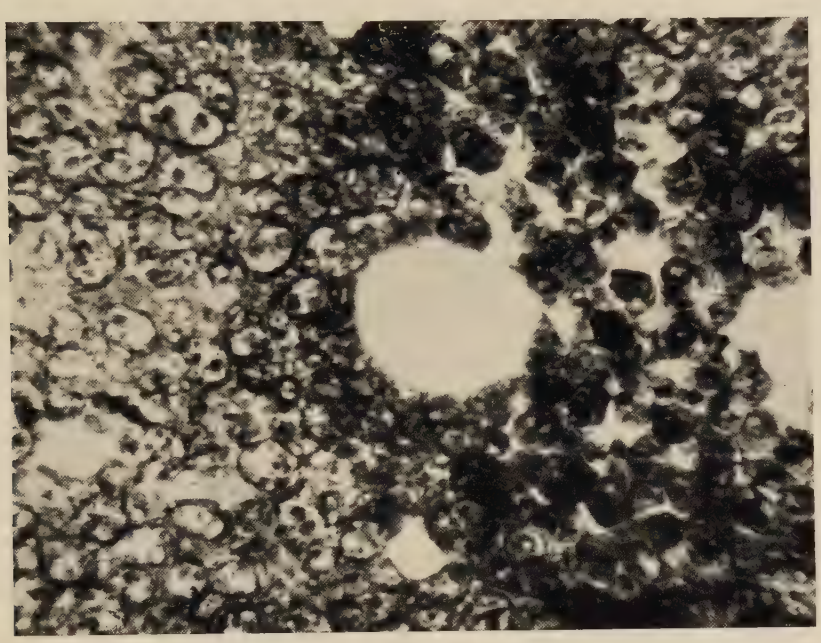

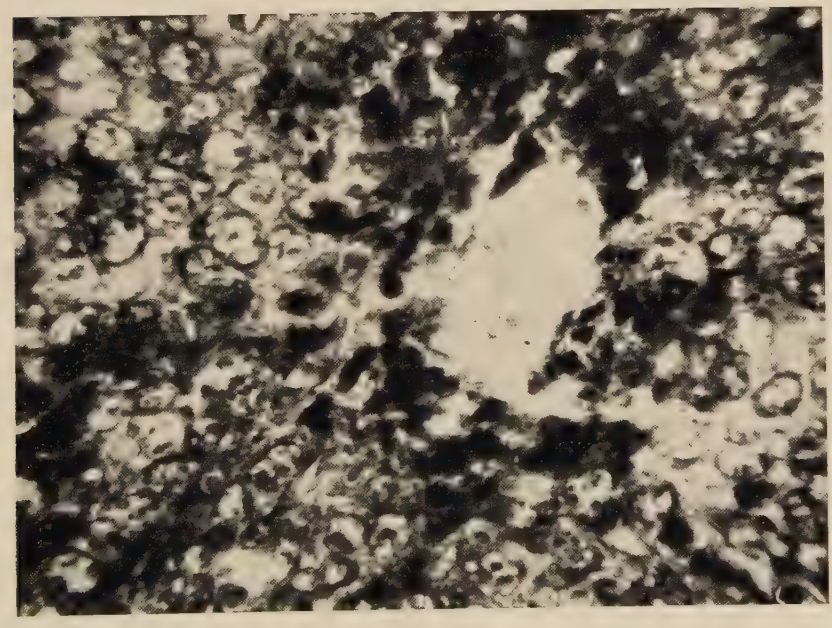

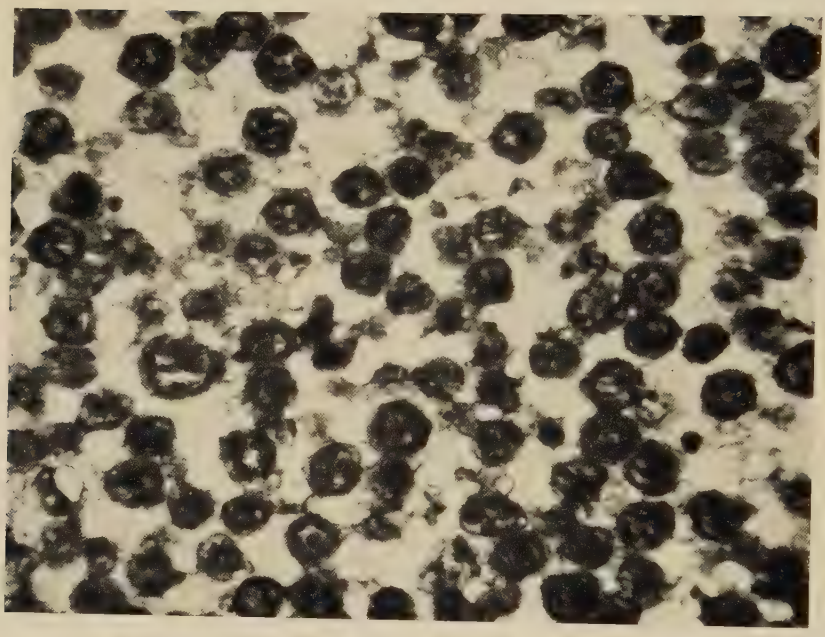

Fig. 8. Ascites tumor. Optical conditions as in Fig. 6. Note high and more uniform absorption of the cells, similar to that of "A" cells in the solid tumor.

**DNA**

The investigations concerning the role of DNA in normal and tumor cells were widely reviewed by Stowell (28, 29).

Studies on the nucleic acid content in neoplastic tissues compared to homologous normal tissues were carried out histochemically by Stowell (29). He showed a significantly increased amount of DNA per cell in 5 out of 11 specimens of epidermoid carcinoma, and in 7 out of 15 miscellanous tumors, when compared to corresponding normal tissues. No decrease could be found. Mark and Ris (24) however found no difference in the DNA content of normal liver, hepatoma and cholangioma nuclei while using only spherical nuclei of similar size for measurements.

Davidson and Waymouth (12) have found by chemical methods that the DNA content of "butter yellow" tumor is about 1.5 times that of normal liver. Schneider's value on mouse pulmonary tumor is about twice the value obtained for normal mouse lung and in rat hepatoma about 2.5 times as much as that of normal liver (27).

These authors expressed their values as a percentage of weight, which

makes comparison difficult. The samples may have a different cell number per unit weight, and a varying amount of stroma and necrotic tissue. Thus Schneider, after having disrupted rat liver tissue and rat liver tumor, found the isolated nuclear fractions to have almost the same DNA content, which, he claims, indicates a larger number of nuclei per volume of tissue in the tumor. Dounce (14) found that the nuclei of Walker rat carcinosarcoma 256 had about the same concentration of DNA as did normal liver nuclei, whereas the nuclei of hepatoma 31 had a much lower concentration. His values were referred to dry weight of nuclei.

Working with isolated nuclei from the spleen, and referring the results to the number of nuclei in the analyzed sample, Arnesen, Goldsmith and Dulaney (1) found no difference in the DNA content in normal and leucaemic mice.

According to Gopal-Ayengar (17) the average content of DNA in isolated chromosomes of normal epidermis of mice was 0.129 mg per mg dry weight, while the corresponding value in methylcholanthrene-produced squamous cell carcinoma was 0.208. The tumor chromosomes also stained more densely with the Feulgen stain than the normal ones.

Boivin, Vendrely and Vendrely (2) have suggested that the DNA content of normal somatic cells from different organs is constant within one species (it is double the value obtained in haploid or sperm nuclei). In the case of mouse Vendrely and Vendrely (32) found the diploid nucleus to contain $0.5 \times 10^{-5}$ μg DNA. Calculated from Arnesen, Goldsmith and Dulaney's data (1) on isolated spleen nuclei of the mouse, one nucleus contains $0.66 \times 10^{-5}$ μg DNA. According to Kurnick and Mirsky (20) the DNA content of liver nuclei in mice, rabbits and rats lies between $0.7 \times 10^{-5}$ and $0.9 \times 10^{-5}$ μg.

In our experiments the cells from an experimentally produced sterile peritonitis had a content of $0.77 \times 10^{-6}$ μg DNA phosphorus, corresponding to about ten times as much DNA, thus there is a fairly good agreement with the values obtained by the previous authors.

The cells of the ascites tumor were found to contain $1.42 \times 10^{-6}$ μg DNA phosphorus per cell, thus a value of about twice that found in non-tumorous exudate cells or in a number of normal somatic cells from different organs.

In trying to evaluate this high content of DNA in ascites tumor cells the following factors may be considered:

In Vendrely and Vendrely's (32) experiment the nuclei were isolated from tissues which are not actively growing, and were stated to contain very few cells which undergo mitosis. The active growth of tumor material as a possible source of the increase in DNA will be considered first. Brodersen (5)

observed 1.5–4.5 per cent mitosis in the ascites tumor, and Lettré (22) calculated that each cell undergoes mitosis once daily, and that the mitotic procedure lasts for 15 minutes, the percentage of mitoses being 1.7. These observations may at least partly explain our findings of the increased DNA content of the ascites tumor cells, on the basis of a high mitotic rate, i.e. high chromosome or DNA synthesis.

Besides, the following observations are available which point into the same direction:

Caspersson and Santesson (7) observed that in the so called A-cells of solid tumors (with which the ascites cells can be most likely compared, as pointed out before) there is no diminution in the nucleic acid content of euchromatin between two divisions. Koller (19) supposed that the nucleic acid content rises to abnormally high values in the chromosomes of tumor cells. As Dittmar and Maas (13) found that mitotic abnormalities and multinucleate cells are rather common in the ascites tumor, even polyploidy may be a factor contributing to increased DNA content.

Isolation of nuclei of the ascites tumor cells caused no loss of DNA. Recently Ris and Mirsky (25) came to the same conclusion by comparing the intensity of Feulgen reaction of sectioned calf liver nuclei with smears of isolated nuclei from the same tissue.

## SUMMARY

Nucleic acid determinations were carried out on cells of Ehrlich ascites tumor of mice. Ascites fluid was withdrawn a certain period of time after the inoculation of $0.8 \times 10^6$ $39 \times 10^6$ cells, and the nucleic acid content was determined per ml fluid and per cell after counting the number of cells. The following results were obtained:

1. The content of nucleic acids in 65 animals was on an average:

$$\begin{aligned} \text{NA} &= 4.09 \times 10^{-6} \ \mu\text{g P per cell} \\ \text{PNA} &= 2.68 \times 10^{-6} \ \mu\text{g P per cell} \\ \text{DNA} &= 1.42 \times 10^{-6} \ \mu\text{g P per cell} \\ \text{PNA/NA} &= 65.6 \text{ per cent} \\ \text{PNA/DNA} &= 1.94 \end{aligned}$$

The variability between animals was low (14.1 per cent for PNA, 21.3 per cent for DNA).

2. In spite of the variation in the inoculated number of cells from $0.8 \times 10^6$ to $39 \times 10^6$, and a corresponding decrease in the median survival time from 11 to 5 days, there was no difference in cell nucleic acid content observed when sacrificing the animals on the median survival time $\pm 2$ days.

3. Starvation for 48 hrs had no effect on the PNA content of the tumor cells in spite of having a deteriorating action on the general condition of the animals.

4. The isolation of nuclei performed with 1 per cent citric acid had no influence on the DNA content, the values per nucleus were the same as per whole cell.

5. The DNA content of tumor cells was about twice and the PNA content about fivefold the value obtained on non-tumorous exudate cells, which were:

$$\text{PNA} = 0.44 \times 10^{-6} \ \mu\text{g P per cell}$$
$$\text{DNA} = 0.77 \times 10^{-6} \ \mu\text{g P per cell}$$
$$\text{PNA/DNA} = 0.59$$

6. U.V. examination at 257 mμ showed a rather uniform and high absorption in ascites tumor cells, while solid Ehrlich carcinoma cells had highly varying absorption.

## REFERENCES


1. Arnesen, K., Goldsmith, Y., and Dulaney, A. D., *Cancer Research*, **9**, 669 (1949).
2. Boivin, A., Vendrely, R., and Vendrely, C., *Compt. rend.*, **226**, 1061 (1948).
3. Bliss, C. I., *Quart. J. Pharm. Pharmacol.*, **11**, 92 (1938).
4. Bliss, C. I., and Cattell, M., *Ann. Rev. Physiol.*, **5**, 479 (1943).
5. Brodersen, H., *Strahlentherapie*, **73**, 196 (1943).
6. Caspersson, T., *Symp. Soc. Exp. Biol.*, **1**, 127 (1947).
7. Caspersson, T., and Santesson, L., *Acta Radiol. Suppl.*, **46** (1942).
8. Cochran, W. G., *Ann. Applied Biol.*, **25**, 426 (1938).
9. Davidson, J. N., *J. Physiol.*, **105**, 32 P (1946).
10. —— *Cold Spring Harbor Symposia on Quant. Biol.*, **12**, 50 (1947).
11. Davidson, J. N., Leslie, I., and White, J. C., *J. Path. Bact.*, **60**, 1 (1948).
12. Davidson, J. N., and Waymouth, Ch., *Biochem. J.*, **38**, 379 (1944).
13. Dittmar, C., and Maas, H., *Z. Krebsforsch.*, **55**, 109 (1944).
14. Dounce, A. L., *J. Biol. Chem.*, **151**, 235 (1943).
15. Fisher, R. A., Statistical Methods for Research Workers, Edinburgh and London, 1936.
16. Fiske, C. H., and Subbarow, Y., *J. Biol. Chem.*, **66**, 375 (1925).
17. Gopal-Ayengar, A. R., and Cowdry, E. V., *Cancer Research*, **7**, 1 (1947).
18. Klein, E., Kurnick, N. B., and Klein, G., *Exp. Cell Res.*, **1**, 127 (1950).
19. Koller, P. C., *Nature*, **151**, 244 (1943).
20. Kurnick, N. B., and Mirsky, A. E., Unpublished experiments (1947—48) quoted from ref. 18.
21. Lettré, H., *Z. physiol. Chem.*, **268**, 59 (1941).
22. —— *Naturwissenschaften*, **31**, 467 (1943).
23. Loewenthal, H., and Jahn, G., *Z. Krebsforsch.*, **37**, 439 (1932).

24. Mark, D. D., and Ris, H., *Proc. Soc. Exp. Biol. Med.*, **71**, 727 (1949).
25. Ris, H., and Mirsky, A. E., *J. Gen. Physiol.*, **33**, 125 (1949).
26. Schmidt, G., and Thannhauser, S. J., *J. Biol. Chem.*, **161**, 83 (1945).
27. Schneider, W. C., *Cold Spring Harbor Symposia on Quant. Biol.*, **12**, 169 (1947).
28. Stowell, R. E., *Cancer Research*, **5**, 283 (1945).
29. —— *Symp. Soc. Exp. Biol.*, **1**, 190 (1947).
30. Teorell, T., *Biochem. Z.*, **230**, 1 (1931).
31. Tippett, L. H. C., *Biometrica*, **17**, 386 (1925).
32. Vendrely, R., and Vendrely, C., *Experientia*, **5**, 327 (1949).

# THE ISOLATION OF THREADS FROM INTERPHASE NUCLEI

W. G. P. LAMB

*Biophysics Research Unit, King's College, London*

Received April 11, 1950

## INTRODUCTION

As it was the intention of the Biophysics Group at King's College London to study cells and their components in the electron microscope, it seemed that a beginning might be made by examining isolated chromosomes. Mirsky and Ris (6, 7, 8) had already isolated chromatin threads from the interphase nuclei of salmon erythrocytes and calf thymus, liver and pancreas cells by the use of either a Waring blender or a colloid mill. They had obtained the threads in sufficient quantities to enable chemical tests to be made, and stated that they were able to identify particular threads by their morphological characteristics, and thus to establish them as isolated chromosomes. Claude and Potter (2), on the other hand, had failed to obtain chromosomes by the use of the Waring blender, and had resorted to grinding tissue with sand. After centrifugation they obtained structures which they termed chromatin threads.

Hovanitz (3) and Hovanitz *et al.* (4) prepared chromatin threads from chick erythrocytes by the grinding process of Claude, and after the threads had been treated with various fixatives, he examined them in an electron microscope. Those preparations which had been fixed with osmium tetroxide showed threads which he claimed possessed a spiral or helical structure.

Calvet, Siegel and Stern (1) suspected that the threads which they obtained by the Waring blender treatment were merely nuclear fragments and, as an alternative, they exploded thymus cells in a special vacuum device. The debris was stained with lanthanum acetate and examined in an electron microscope. The authors were able to demonstrate the presence of nucleoprotein ultra-fibrils of an approximate thickness of 80–100 A.

The object of the present work was to investigate the nature of the chromatin threads isolated from interphase nuclei, and to determine something of

their structure from electron microscope observations. A brief preliminary account* of this investigation has already been published—Lamb (5).

## MATERIALS AND METHODS

Most of the experiments were performed on calf thymus tissue, but others were made on calf liver and chick erythrocytes. Fresh supplies of calf thymus and liver were obtained from the London Meat Market and transferred to the laboratory as quickly as possible. The chick erythrocytes were provided by the Strangeways Research Laboratory Cambridge and brought to London in an ice cooled container.

When the investigation was begun, a Waring blender was not available, and preliminary experiments were made with a small homogeniser. Claude's method of grinding tissue with sand was also used, and experiments were made to try the effect of ultrasonic radiation. However, no threads could be produced by this last method which broke the nuclei into small spherical fragments.

*1. The homogeniser method.* The homogeniser consisted of a glass cylinder revolving at approximately 1,000 revolutions per minute inside a glass tube. As the cylinder fitted fairly tightly within the tube a liquid suspension could be subjected to a considerable shearing force in the annulus between the two. A few grams of fresh calf thymus were minced with scissors, and, together with a few ccs. of cold physiological saline (0.14 M NaCl), placed in the homogeniser. This was then immersed in a mixture of ice and water and run at about 1,000 r.p.m. for fifteen to twenty minutes. Care was taken to ensure that the temperature of the suspension did not rise above 5° C. Samples of the suspension were removed at intervals with a small pipette and stained preparations made.

*2. Grinding with sand.* Fresh calf thymus was minced with scissors as before, and then placed in a mortar cooled to 0° C. About twice as much cold sand as tissue by weight was added, together with a small volume of cold 0.14 M sodium chloride solution. The whole was ground by hand for approximately ten minutes, further cold saline being added as required to keep the mass workable. Samples of the liquid suspension were taken with a pipette, and at the end of the process the suspension was poured from the mixture of tissue and sand. A slow speed centrifugation served to remove any remaining sand, and the threads produced by the grinding were separated from the unbroken and partially damaged cells by further centrifugation.

*3. The Waring blender method.* The Waring blender is a high speed mixer in which fairly large quantities of material may be subjected to intense mixing by a small propeller-like blade revolving at speeds up to 15,000 r.p.m. One hundred grams of thymus tissue were minced with scissors and placed in the blender (already cooled to 0° C) together with about 300 ccs. of cold 0.14 M NaCl solution. The blender was run at full speed for two minutes and then cooled in a bath of ice and methylated spirits until the temperature of the suspension had fallen to 0° C. This procedure was repeated until a total time of sixteen minutes mixing had been attained.

Samples of the suspension were taken at $^1/_2$, 1, 2, 4, 8 and 16 minutes from the be-

* In this preliminary account it was incorrectly stated that Mirsky and Ris had maintained that the isolated threads were metaphase chromosomes. In fact, they merely claimed that the threads were isolated chromosomes and not metaphase chromosomes.

ginning of the run. The suspension was filtered through muslin to remove large unbroken pieces of tissue, and centrifuged to remove small particles. These two operations were repeated several times. The final preparation contained a mass of threads. Later, the procedure was altered as follows, in accordance with an improved technique employed by Mirsky and very kindly communicated by him to the author.

The whole process was performed in a cold chamber at 0° C. One hundred grams of fresh calf thymus tissue were minced with scissors and placed in the blender, together with 350 ccs. of cold 'saline citrate' and 150 grams of crushed ice. The 'saline citrate' consisted of M/100 sodium citrate in 0.14 M NaCl solution. The Waring blender was run for six minutes, this being the time taken for the ice to melt under the frictional heat generated by the propeller blade. After the treatment the volume of the suspension was made up with saline citrate to approximately 1,000 ccs, and after filtration through muslin it was centrifuged in an International Refrigerated Centrifuge at 2,000 r.p.m. for seven minutes. The sediment was taken up in more saline citrate and thoroughly mixed in the blender run at slow speed for about one minute. The suspension was filtered through a linen teacloth and recentrifuged. This last process of filtration and centrifugation was repeated twice more. As before, samples of the suspension were taken during the process.

*4. Cytological Methods.* In order to follow the progress of the experiments immediate examination of fresh unfixed preparations was made with the aid of the phase contrast microscope, whilst other samples were stained and fixed with aceto-orcein and examined in the ordinary light microscope.

Permanent preparations for the light microscope were made by fixing material in acetic alcohol, 2 per cent osmium tetroxide or Maximow's fixative, and staining with Ehrlich's haematoxylin or by Feulgen's method.

The same three fixatives were used in the preparation of samples for the electron microscope. For this purpose a few drops of suspension were added to an excess of fixative. After one minute of fixation the threads or nuclei were sedimented by centrifugation, resuspended in glass distilled water, and then recentrifuged. This washing process was repeated several times until a drop of the suspension placed on a formvar film, used for mounting objects in the electron microscope, yielded clean specimens after evaporation.

## RESULTS

### *1. Nuclear structure of thymus cells*

Thymus tissue contains two main types of cells termed thymocytes and reticular cells. These were examined in preparations made from fresh calf thymus tissue. Both types have relatively large nuclei in proportion to their cytoplasm. The thymocytes are far more numerous than the reticular cells, but are much smaller, having a diameter of 5 or 6 μ, while the diameter of the larger reticular cells may be two or three times as great. Considerable nuclear structure may be seen in unfixed cells of both types in the phase contrast microscope, or after staining with aceto-orcein (Fig. 10) or with

Feulgen's stain. In the thymocytes this nuclear structure consists of dots of stainable material together with a network of very fine filaments, too small to be resolved clearly in the light microscope. The nuclei of the larger cells also contain lumps of stainable material which are much smaller than those in the thymocytes, and a network of fine filaments which are usually much more easily discerned than those of the thymocyte nuclei.

### 2. *The Formation of Nuclear Threads*

The homogeniser, the grinding process and the Waring blender produced similar results in that thread-like bodies were to be found in the samples taken from the suspensions produced by all three methods. In general, the threads from the homogeniser and grinding methods were longer than those from the blender (Figs. 11 and 14), but were formed in the same way. The following account of thread-formation therefore applies to material obtained by all three techniques. When stained by Feulgen's method many of the threads showed strongly Feulgen positive regions here and there along their length (Fig. 5). In spite of a careful search in both the light and electron microscopes it was not possible to recognise individual threads from their morphological characteristics. The electron micrographs showed the threads to be of arbitrary length and shape, and in some instances to possess a complex and twisted structure (Figs. 1 and 2). Often they carried filament-like projections (Fig. 4) and other material along their length and at their ends (Fig. 3).

As well as the threads, the preparations contained many nuclei in various stages of distortion and disintegration. Early samples, that is those taken $^1/_2$ and 1 min. after the start of the mixing process, exhibited nuclei which were only slightly deformed and appeared to have a slight bulge. Later samples showed many severely distorted nuclei which were drawn out into lengthy protrusions (Figs. 8 and 9).

In the Feulgen-stained preparations Feulgen positive lumps or dots of

---

Figs. 1, 3 and 4. Electron micrographs of threads produced by the Waring blender method from calf thymus tissue. The thread shown in Fig. 3 appears to have some material attached at one end, and that in Fig. 4 exhibits two or three pieces of material attached along its length.

Fig. 2. An electron micrograph of a thread produced by the homogeniser method from calf thymus tissue. This thread exhibits a marked twisted structure.

Fig. 5. Light micrograph of a thread produced from calf thymus tissue with the aid of the Waring blender. It has been stained by Feulgen's method and exhibits several Feulgen positive regions along its length.

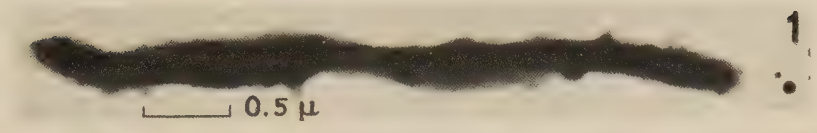


1

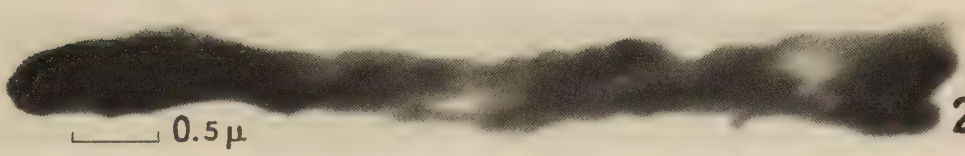


2

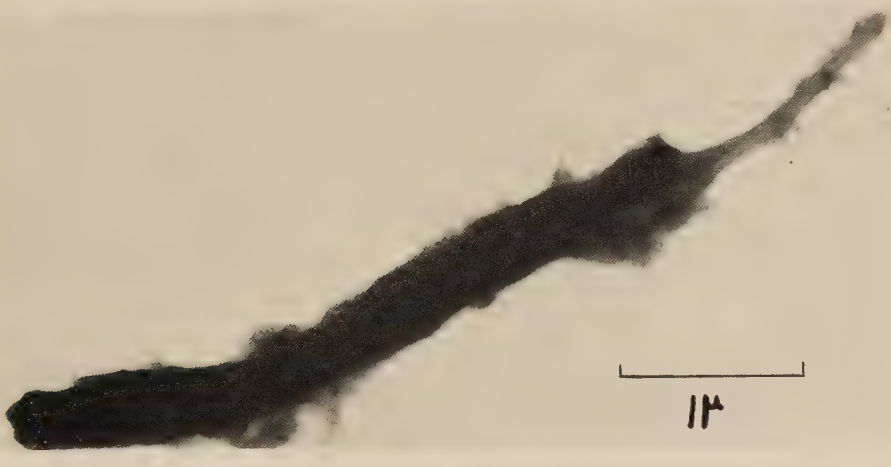


3

4

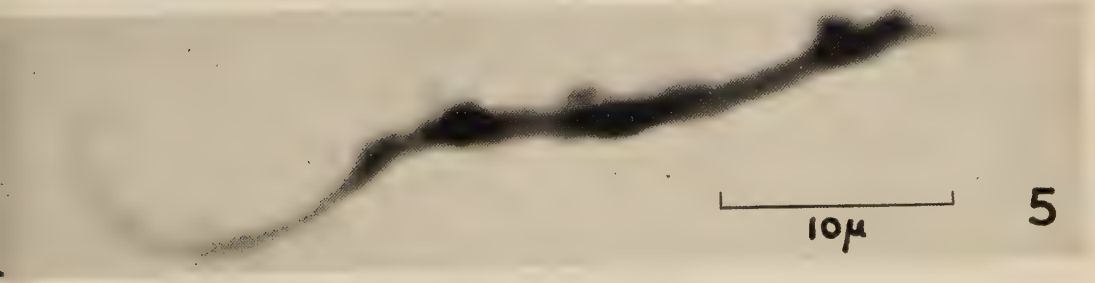


5

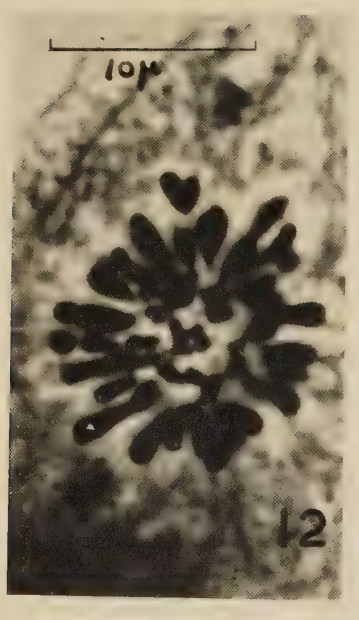


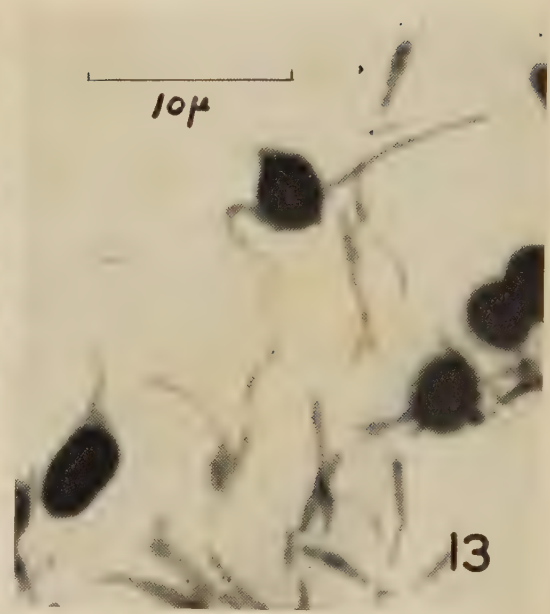


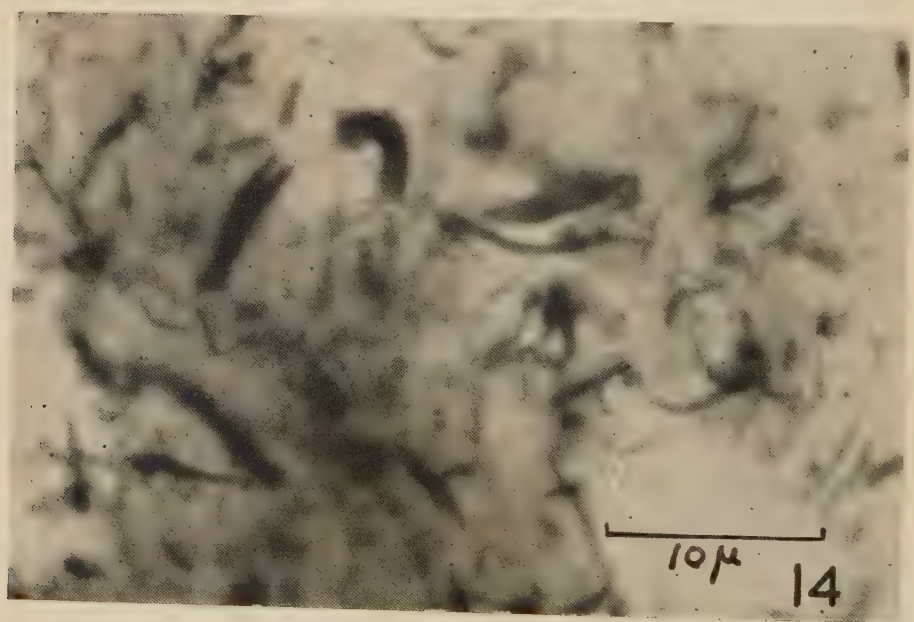


Fig. 12. Light micrograph of a thymus cell in a tissue culture. The cell is at the metaphase stage of mitosis. Stain: Ehrlich's Haematoxylin.

Fig. 13. Light micrograph of a number of threads produced from chick erythrocytes by the Waring blender treatment. Several erythrocyte nuclei are also present in the sample. Stain: Feulgen's method.

Fig. 14. Threads isolated from calf thymus nuclei by the Waring blender treatment. Stain: Feulgen's method.

material could be observed within the undamaged nuclei, and in those nuclei which had been drawn out into protrusions some of the material in an elongated and distorted form was observed within the protrusions, as well as in the main body of the nucleus (Figs. 6 and 7).

These protrusions appeared to be the first step in the formation of the chromatin threads. As stated above, they appeared originally as a slight bulge or distortion, and became longer and thinner; eventually they were broken off by the mixing process and remained in the suspension as isolated threads with discrete particles of Feulgen positive material here and there along their length. All steps in this process were seen in the preparations. In some of the nuclei from the blender suspensions, however, fine threads were to be seen apparently emerging from the surface membrane. These were very much smaller than the protrusions described above, and were suggestive of chromonemata penetrating the nuclear membrane. As they were beyond the resolving power of the light microscope, a search was made for them with the electron microscope. Of those examined in the electron microscope, however, all appeared to be threads of material attached to the nucleus rather than chromonemata emerging through the nuclear membrane.

Preparations made with liver instead of thymus were very similar to those described above, but the chick erythrocytes proved very difficult to break up and they yielded fewer threads (Fig. 13).

### *3. Further Experiments with the Waring blender*

(a) The effect of operating at low speed. Since the homogeniser produced much longer threads than did the blender, and as the latter was a much more violent process, it was decided to try the effect of operating the blender at a lower speed comparable with that of the homogeniser. As a result, it was found that the threads produced were much longer and appeared to be similar to those from the homogeniser.

(b) The effect of different salines. The use of 0.14 M NaCl solution as a physiological saline is open to the objection that it is very simple, has no buffer, and is therefore subject to changes of pH; for this reason it was decided to try other salines. The experiment with the Waring blender was repeated with Tyrode solution; there was, however, no change in the result. A buffered medium recommended by H. G. Callan (personal communication) was also used. This consisted of 2.3 per cent $KH_2PO_4$ and 1.5 per cent $K_2HPO_4$ solution in a ratio of 60/40, together with $MgHPO_4$ added to saturation. This medium had a pH of between 6.4 and 6.6. Callan has

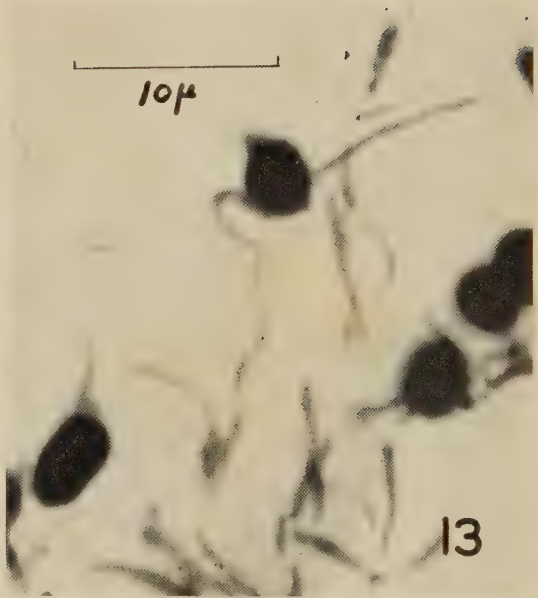


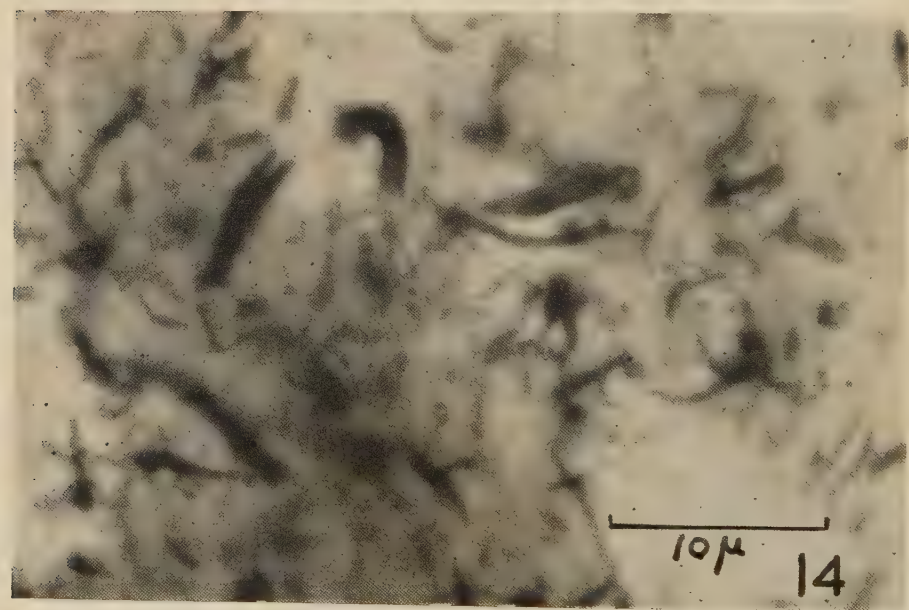


Fig. 12. Light micrograph of a thymus cell in a tissue culture. The cell is at the metaphase stage of mitosis. Stain: Ehrlich's Haematoxylin.

Fig. 13. Light micrograph of a number of threads produced from chick erythrocytes by the Waring blender treatment. Several erythrocyte nuclei are also present in the sample. Stain: Feulgen's method.

Fig. 14. Threads isolated from calf thymus nuclei by the Waring blender treatment. Stain: Feulgen's method.

material could be observed within the undamaged nuclei, and in those nuclei which had been drawn out into protrusions some of the material in an elongated and distorted form was observed within the protrusions, as well as in the main body of the nucleus (Figs. 6 and 7).

These protrusions appeared to be the first step in the formation of the chromatin threads. As stated above, they appeared originally as a slight bulge or distortion, and became longer and thinner; eventually they were broken off by the mixing process and remained in the suspension as isolated threads with discrete particles of Feulgen positive material here and there along their length. All steps in this process were seen in the preparations. In some of the nuclei from the blender suspensions, however, fine threads were to be seen apparently emerging from the surface membrane. These were very much smaller than the protrusions described above, and were suggestive of chromonemata penetrating the nuclear membrane. As they were beyond the resolving power of the light microscope, a search was made for them with the electron microscope. Of those examined in the electron microscope, however, all appeared to be threads of material attached to the nucleus rather than chromonemata emerging through the nuclear membrane.

Preparations made with liver instead of thymus were very similar to those described above, but the chick erythrocytes proved very difficult to break up and they yielded fewer threads (Fig. 13).

### *3. Further Experiments with the Waring blender*

(a) The effect of operating at low speed. Since the homogeniser produced much longer threads than did the blender, and as the latter was a much more violent process, it was decided to try the effect of operating the blender at a lower speed comparable with that of the homogeniser. As a result, it was found that the threads produced were much longer and appeared to be similar to those from the homogeniser.

(b) The effect of different salines. The use of 0.14 M NaCl solution as a physiological saline is open to the objection that it is very simple, has no buffer, and is therefore subject to changes of pH; for this reason it was decided to try other salines. The experiment with the Waring blender was repeated with Tyrode solution; there was, however, no change in the result. A buffered medium recommended by H. G. Callan (personal communication) was also used. This consisted of 2.3 per cent $KH_2PO_4$ and 1.5 per cent $K_2HPO_4$ solution in a ratio of 60/40, together with $MgHPO_4$ added to saturation. This medium had a pH of between 6.4 and 6.6. Callan has

shown that it is desirable to maintain the pH in this region because at pH 7.2 the structural proteins of the nuclear sap undergo hydration, and at 7.4 the nucleoli dissolve. On the other hand, at pH 6 the structural proteins and chromatin coagulate. The behaviour of the nuclei in the blender was not altered by the use of this medium.

*4. Observations on the mitotic chromosomes of calf thymus cells in tissue cultures*

Tissue cultures of thymus were made by Miss E. J. Hanson in order to study the chromosomes at division and compare them with the threads obtained by the mixing processes. The thymocytes did not divide in the cultures, but merely wandered out from the explant and degenerated.

On the other hand, many reticular cells were observed in the various stages of division. Chromosomes in these cells (Fig. 12) were carefully compared with the isolated threads of the suspensions, but it was not possible to identify individual chromosomes in the latter.

## DISCUSSION

It was concluded that the effect of the shearing and mixing forces in the three processes was first to remove the cytoplasm from the thymocytes and reticular cells, and then to distort and draw out the nuclei. The protrusions thus formed carried within themselves pieces of Feulgen positive material. When the protrusions became longer, they were broken off from the main body of the nucleus and existed in the suspension as isolated threads. Since not every protrusion carried Feulgen positive material, some threads were produced which contained none; others were only partly stained, while others again appeared to consist of Feulgen positive material only. When the threads were compared with chromosomes in dividing cells of tissue cultures there was found to be little resemblance between the two. Many of the threads were too long to be considered as mitotic chromosomes, whilst they were too broad to be interphase chromonemata.

Mirsky has mentioned the double nature of the threads produced by the blender treatment. It is probable that the limit of resolving power of the light microscope facilitates the conclusion that some of the threads are double. In the electron microscope, on the other hand, the threads are clearly seen to be single. In some instances threads were observed which appeared to be double when viewed at low magnification (1,000 ×) but were found to

be single at a normal magnification of 10,000 ×. This effect was due to these threads possessing a splayed end like a fish-tail which, when seen at low magnification, gave the impression of doubleness.

It is suggested that the chromatin threads produced by these three methods are not isolated chromosomes, but are nuclear fragments mechanically manufactured and consisting mainly of various tangled fragmentary chromonemata with or without Feulgen positive particles.

## SUMMARY

In an attempt to isolate chromosomes from interphase nuclei suspensions were treated by three methods: (1) in a homogeniser, (2) by grinding with sand in a mortar, and (3) in a Waring blender.

The effect of the three methods was to draw out the nuclei into threads which consisted of mixtures of nuclear material of fragmentary character.

These threads were found to bear little resemblance to interphase chromonemata or mitotic chromosomes.

## ACKNOWLEDGEMENTS

The author wishes to express his gratitude to Dr. H. B. Fell of the Strangeways Research Laboratory Cambridge, to Professor J. T. Randall, F. R. S. and Miss E. J. Hanson of King's College London, and to Mr. H. G. Callan[1] of the Institute of Animal Genetics Edinburgh for encouragement and advice during the prosecution of the work.

## REFERENCES

1. Calvet, F., Siegel, B., and Stern, K., *Nature*, **162**, 305 (1948).
2. Claude, A., and Potter, J. S., *J. Exp. Med.*, **77**, 345 (1943).
3. Hovanitz, W., *Genetics*, **32**, 500 (1947).
4. Hovanitz, W., Denues, A. R. T., *The Wasmann Collector*, **7**, 233 (1949).
5. Lamb, W. G. P., *Nature*, **164**, 109 (1949).
6. Mirsky, A. E., and Ris, H., *J. Gen. Physiol.*, **31**, 1 (1947).
7. —— *Nature*, **163**, 666 (1949).
8. —— *J. Gen. Physiol.*, **32**, 489 (1949).

[1] Now Professor of Zoology at the University of St. Andrews.

# THE QUALITATIVE DISTRIBUTION OF METACHROMATIC POLYSACCHARIDE MATERIAL DURING HAIR GROWTH[1]

BENGT SYLVÉN

*Cancer Research Division of Radiumhemmet, Karolinska Institutet, Stockholm*

Received April 27, 1950

## INTRODUCTION

Metachromatic material provisionally interpreted as a polysaccharide ester sulfate of unknown chemical composition has been demonstrated in a variety of growing mesenchymal tissues (Bensley, Holmgren, Sylvén). Only small or insignificant amounts of the same or a similar substance could previously be observed in the cytoplasm of growing epithelia treated with common fixatives (31, 35), a process which apparently involves heavy loss of water-soluble cell constituents. Unpublished reinvestigations have revealed that much larger amounts of this material are demonstrable following the freezing-vacuum dehydration of growing epithelia. The present paper deals with the distribution of metachromatic material in the hair follicles and papilli during the cyclic growth of rat coat hair. The biological implications as to keratin synthesis and the possible role of the stromal matrix in the supply of sulfurous raw material will be discussed. The occurrence of alcohol-resistant metachromatic material in the papilli and external connective tissue root sheaths of growing animal and human hair was originally briefly mentioned by Holmgren (1939, 1940) and Sylvén (1938, 1949). Mainly due to defective fixation methods as mentioned above, the cytoplasmic metachromasia of growing hair epithelia was, however, overlooked at that time.

With regard to hair growth, only one aspect of sulfur supply and metabolism will be dealt with. The qualitative distribution of -SH compounds by means of the nitroprusside test was described by Giroud and Bulliard (15–17). Chemical data on the approximate amounts and localization of

[1] Aided by grants from the Swedish Medical Association, the Anti-Cancer Society of Stockholm, and the Board of Karolinska Institutet.

organic sulfurous constituents in wool and other animal hair may be obtained from papers by Block, Rudall, Stoves, Beveridge and Lucas, Geiger, Lindley, and others. Quantitative histochemical determinations of the total sulfur content of hair by means of roentgen absorption spectrography (11) would be of considerable value. Important biophysical data on the differentiation of hair keratin was recently reported by Mercer (26).

The cyclic growth pattern of the first and second coats in the developing albino rat from birth until the age of maturity as described by Butcher (6) was corroborated also in our strain of rats. For morphological details and physiological factors influencing hair growth in rats, reference is made to papers by Butcher (6–10). The distribution of alkaline phosphatase was studied by Johnson, Butcher and Bevelander (22).

## MATERIAL AND METHODS

Altogether 29 albino rats from our laboratory stock were sacrificed at intervals from birth until the 51st day of age (Fig. 1). Records were made of the body weight and the approximate length of coat hairs from the mid-dorsal and mid-ventral skin areas, as well as of the maximum length of the whiskers. Specimens from these skin areas and the upper lips were routinely treated with (*1*) freezing-vacuum dehydration according to Altmann-Gersh, and additional specimens with the following mordants: (2) a 4 per cent aqueous solution of basic lead acetate for 24 hours (19) and subsequent neutral formaldehyde (5 per cent) fixation for a further 24 hours; and (*3*) an aqueous solution of formaldehyde (4 per cent), acetic acid (8 per cent) and corrosive mercuric chloride (4 per cent). Paraffin sections of standard thickness (4 microns) perpendicular to the skin surface were stained in alcoholic solutions of 0.04–0.08 per cent Azure A (National Aniline Co.). The alcohol concentrations ranged from 10 to 90 per cent (19, 31). Sections were preferably mounted in cedar oil. After staining, it is necessary to pass the sections through 96 per cent alcohol, thereby definitely avoiding all "false" metachromatic colour variations, mostly due to adsorption. All sections were inspected under an ordinary light microscope, and selected unstained freeze-vacuum dehydrated ones under the polarizing microscope.

Under our standardized sectioning and staining conditions the observed intensity of metachromasia and basophilia allow approximate estimations of the amounts of metachromatic and basophilic material present in the slides (31, 34). Structures devoid of metachromatic material always

present a bluish-green orthochromatic colour corresponding to the α and β bands of the dissolved dye-stuff.

The contention may be anticipated that the pertinent acid polysaccharide esters form lipo-protein complex compounds whose water solubility is partly dependent on the actual hydrogen ion concentration (23). Now, as mentioned earlier, it was found in this material that the usual fixation methods involve an almost complete loss of metachromatic material from the cytoplasm of hair epithelia. This is provisionally regarded as an effect of dissolution. The losses are minimized by applying the freezing-vacuum dehydration technique, which actually made this investigation possible. However, as long as aqueous stains have to be used some diffusion artefacts must be taken into consideration.

The results thus refer to freezing-vacuum dehydrated material from two standard skin areas (mid-dorsal and mid-ventral), and further to alcohol-resistant stable metachromatic staining reactions.

## RESULTS

As regards the synthesis and orientation of keratin in hair follicles the following epithelial levels must be distinguished. The *isotropic* part of the hair bulbs includes poorly differentiated and dividing epithelia covering the connective tissue papilli. The *anisotropic* levels, characterized by a step-wise orientation of fibrous keratin, are found above the constriction of the bulb, and may arbitrarily be divided into an unconsolidated zone and a zone of keratin hardening (26). This is called the pre-keratinous region of the hair shaft.

Present cytological and histochemical serial observations have been compiled in Fig. 1. They indicate that considerable amounts of alcohol-stable brightly red-stained metachromatic material are demonstrable in the mesenchymal papilli and in the cytoplasm of the isotropic part of the hair bulbs *only* during the first six to eight days of the first and second hair cycles (Fig. 1 & 2). Smaller amounts of this material are also found in the pre-keratinous zone of the shaft. After this time, and parallel with the tapering off of growth activity on the part of the hair epithelia, the structures mentioned above gradually lose their basophilia and metachromasia; the latter being completely lacking during the second part of both hair cycles. This corresponds to the period of quiescence terminating in follicular atrophy (Fig. 1). A remarkable conformity is seen between the distribution of metachromatic material and cytoplasmic basophilia.

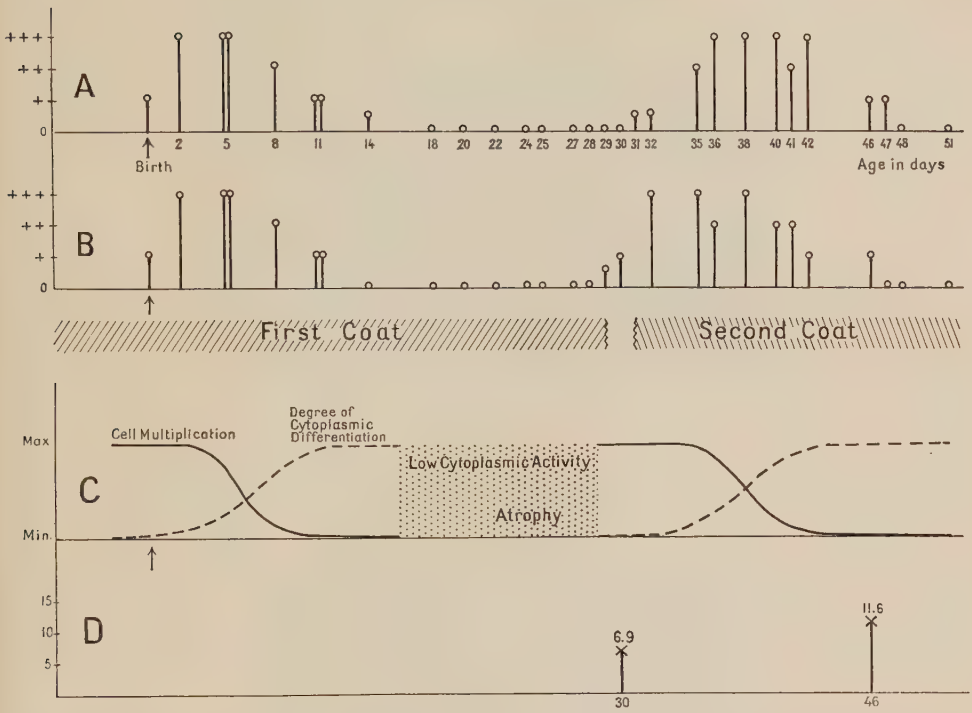


Fig. 1. Rough diagram of the observations reported on rat hair growth cycles. Degrees of papillary and cytoplasmic metachromasia during the first and second cycle in mid-dorsal (A) and mid-ventral (B) skin region. The cytology of hair bulb epithelia compiled in diagram C. Data (D) on the amounts of hair expressed in mg/g body weight (mean values) in albino rats living on a similar normal diet are added from H. D. Lightbody and H. B. Lewis (24) in order to illustrate the rapid increase during the second cycle.

At birth and during the first few days of postnatal development, gradually decreasing amounts of metachromatic material are found in the subepidermal connective tissue matrix (20, 21) and also in the cytoplasm of the epidermal cells and in the inter-epithelial spaces. The epithelia of the primitive hair buds in newborn rats present a quite similar picture with pronounced cytoplasmic basophilia and a moderate degree of cytoplasmic metachromasia. At this stage marked accumulations of metachromatic material are lacking in or around the prospective papilli.

The rapidly enlarging folliculi of 1 and 2 day old rats show an appreciable increase in metachromatic material both in the well-developed papilli and in the isotropic hair epithelia. A maximum seems to be reached between the 3rd and 8th or 10th days after birth. The condensed papilli of all wool hairs are devoid of this staining reaction between the 17th or 20th day of life until the subsequent second cycle begins. In large guard hairs, however, smallish amounts associated with signs of persisting growth may still be seen.

A similar cycle was repeated during the development of the second coat. During the first week of both cycles the isotropic hair epithelia were characterized by pronounced cytoplasmic basophilia as well as a cell picture consistent with protein synthesis (Fig. 1 & 2). Non-mitotic nuclei were always devoid of metachromasia. Commonly seen mitotic structures showed a metachromatic reaction in the cytoplasm surrounding the chromosome coils, but the chromatin itself always stained orthochromatically bluish (Fig. 2).

Smaller and decreasing amounts of metachromatic material were also discernable in the cortex epithelia of the pre-keratinous zone, until it became lost in the zone of fully oriented keratin. This means that, as far as the epithelia is concerned, the metachromatic reaction showed a similar distribution as that of the unoxidized thiol (-SH) groups previously described by Giroud and Bulliard.

Similar observations were made on the development and differentiation of the epithelial root sheaths. The external connective tissue root sheaths fully developed in the second hair generation contained a smallish amount of metachromatic material between the 30th to about the 46th day. The bulbar growth zones of all epithelial root sheaths evidenced a cytoplasmic metachromasia of low to moderate degree, diminishing at the level of bulbar constriction. The first signs of keratin orientation were seen in the hair cuticula and inner root sheaths a short distance above the bulbar constriction.

The fibroblasts of growing hair papilli (Fig. 3) showed a cytological picture differing from that of the surrounding regular fibroblasts. The first-mentioned had smaller nuclei, more marked nuclear basophilia, a small distinct and strongly basophilic nucleolus, and very small cytoplasmic volumes. This picture is indicative of a low degree of differentiation. Mast cells have not been observed in rat hair papilli, but have occasionally been noted in human ones.

On closer investigation, the observed metachromasia of papilli and matrix cells evidences a very high intensity and a pronounced alcohol stability, comparable to that seen in the microsome material of tissue mast cells (heparin-lipoprotein complex) and cartilage (chondroitin sulfate). The reaction still appears in sections stained in very low concentrations of Azure A dissolved in 70–80 per cent alcohol, provided that freezing-vacuum dehydrated material is used.

Corresponding observations were made in series of rat tactile hairs from birth until maturity which, however, present another growth cycle, and also in occasionally investigated human hairs from the scalp, face, trunk, extremities, and sexual regions. As this material is inhomogeneous it is not included here.

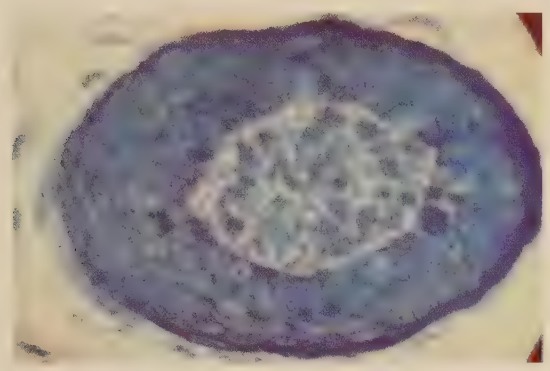

Fig. 2. Metachromatic and basophilic material in a cross-sectioned hair follicle from 3 days old albino rat. Freeze-vacuum dehydration; Stained in Azure A 0.08 per cent in 40 per cent alcoholic solution. Microphotograph in colour (ANSCO) without filters. Magnification ×600. Similar specimens fixed in formaldehyde solutions present no trace of metachromatic material in the cytoplasm of hair epithelia.

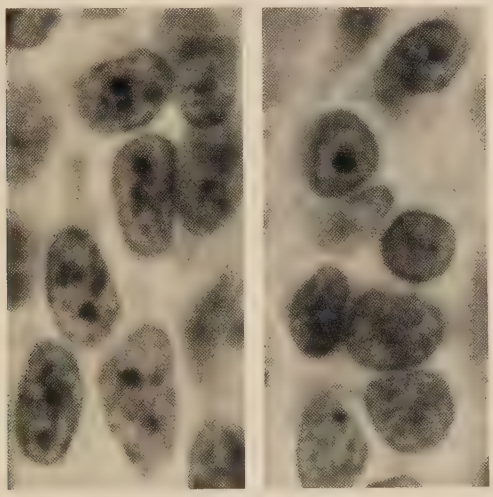

Fig. 3. Cytology of stromal fibroblasts in growing rat hair as described in text. Section 4 microns, stained in Azure A; ×2.100.

## DISCUSSION

Despite a present lack of corroborating data as to the biochemical composition of the metachromatic material in question, the claim is maintained that the alcohol-resistant metachromatic staining reaction of Lison is reason-

ably specific for polysaccharide ester sulfates (35). A number of limitations inherent in this staining method revealed by investigations to be reported elsewhere constitute no serious objection to the use of the reaction so far as mammalian tissues are concerned (35).

Available data suggest that polysaccharide ester sulfates are transferred from the papillary depot to the growing hair matrix epithelia, which contain this or derived material during the first stages of keratin synthesis. The alleged transport route illustrates the functional dependence of epithelia on their stromal matrix. The gradients in the amount of metachromatic material noted further suggest that the biological role of this substance is most probably associated with cytoplasmic growth processes (Fig. 1). Tentative speculations as to the possible significance of this substance have been advanced elsewhere (1, 12, 13, 18, 35).

With reference to the synthesis of fibrous proteins it may further be stressed that both collagen and keratin develop in a matrix rich in metachromatic material probably of polysaccharide nature (31). In both cases the substance gradually disappears parallel with an increase in molecular orientation.

The polysaccharide ester sulfates and the -SH groups present different concentration patterns in relation to hair growth. An accumulation of -SH groups was found in the pre-keratinous region, and was absent in the papillary connective matrix (15). On the other hand, some similarity in the distribution and concentration patterns has been noted for alkaline phosphatase (22) and ester sulfate, both claimed to be correlated with cell proliferation.

The ester sulfates seem to play a role for the supply of sulfurous constituents in keratin synthesis, and should accordingly be regarded as labile S-bearing compounds. Future studies by means of labelled compounds may elucidate this aspect.

## SUMMARY

The distribution of basophilic and metachromatic material during the development of the first and second coats in albino rats is reported. A comparison is made between freeze-vacuum dehydrated specimens and material treated with common fixatives. By using the first mentioned technique considerable amounts are demonstrable both in the stromal papilli and in the cytoplasm of growing and differentiating epithelia. This material is associated with periods of intense proliferation of hair epithelia, and is most

likely supplied *via* the stromal matrix. The pronounced alcohol stability of the staining reaction is regarded as indicative of polysaccharide ester sulfate, but analytical evidence is still lacking. The biological implications with reference to growth and keratin synthesis are mentioned.

## REFERENCES


1. Balazs, A., and Holmgren, Hj., *Proc. Soc. Exp. Biol. Med.*, **72**, 142 (1949).
2. Bensley, S. H., *Anat. Record*, **60**, 93 (1934).
3. Beveridge, J. M. R., and Lucas, C. C., *Biochem. J.*, **38**, 88 (1944).
4. Block, R. J., *Cold Spring Harbor Symposia Quant. Biol.*, **6**, 79 (1938).
5. —— *J. Biol. Chem.*, **128**, 181 (1939).
6. Butcher, E. O., *Anat. Record*, **61**, 5 (1934).
7. —— *Am. J. Physiol.*, **120**, 427 (1937).
8. —— *J. Nutrition*, **17**, 151 (1939).
9. —— *Am. J. Physiol.*, **129**, 553 (1940).
10. —— *Am. J. Physiol.*, **138**, 408 (1942/43).
11. Engström, A., *Acta Radiol., Suppl.* 63 (1946).
12. Fischer, A., *Protoplasma*, **26**, 344 (1936).
13. Fischer, A., and Nyström, P., *Biochem. Z.*, **262**, 364 (1933).
14. Geiger, W. B., *Am. Dyestuff Reptr*, **33**, 117 (1944).
15. Giroud, A., and Bulliard, H., *Arch. Morphol.*, **29**, 7 (1930).
16. —— *Protoplasma*, **19**, 381 (1933).
17. Hammet, F. S., and Chapman, S. S., *J. Lab. Clin. Med.*, **24**, 293 (1938–39).
18. Heilbrunn, L. V., and Wilson, W. L., *Proc. Soc. Exp. Biol. Med.*, **70**, 179 (1949).
19. Holmgren, Hj., *Z. wiss. Mikroskop.*, **55**, 419 (1938).
20. —— *Anat. Anz.*, **88**, 193 (1939).
21. —— *Jahrb. Morph. mikr. Anat.*, **47**, 489 (1940).
22. Johnson, P. L., Butcher, E. O., and Bevelander, G., *Anat. Record*, **93**, 355 (1946).
23. Julén, C., Snellman, O., and Sylvén, B., *Acta Physiol. Scand.*, **19**, 289 (1950).
24. Lightbody, H. D., and Lewis, H. B., *J. Biol. Chem.*, **82**, 485 (1929).
25. Lindley, H., *Nature*, **160**, 190 (1947).
26. Mercer, E. H., *Biochim. et Biophys. Acta*, **3**, 161 (1949).
27. Rudall, K. M., *Proc. Leeds Phil. Lit. Soc., Sci. Sect.*, **4**, 178 (1944).
28. Stoves, J. L., *Nature*, **151**, 304 (1943).
29. —— *J. Intern. Soc. Leather Trades' Chemists*, **32**, 254 (1948).
30. Sylvén, B., *Klin. Wochschr.*, **17**, 1545 (1938).
31. —— *Acta Chir. Scand.*, **86**, *Suppl.* 66 (1941).
32. —— *Acta Obstet. Gynecol. Scand.*, **25**, 189 (1945).
33. —— *Acta Obstet. Gynecol. Scand.*, **25**, 202 (1945).
34. —— *Acta Radiol., Suppl.* 59 (1945).
35. —— *Acta Radiol.*, **32**, 11 (1949).

# THE EFFECTS OF FLUOROACETATE ON BEATING EMBRYO CHICK HEART IN TISSUE CULTURE

C. B. ALLSOPP and HONOR B. FELL
*Guy's Hospital Medical School, London*, and *Strangeways Research Laboratory, Cambridge*

Received May 23, 1950

Recent work by Peters and others (9, 8, 3) has drawn attention to some unusual features of the high toxicity for mammals exhibited by fluoroacetates (5). These substances, unlike their iodine analogues which are also toxic, have no known action on any isolated enzyme system (2). Their main physiological effects are on the central nervous system and the heart, and are accompanied by an accumulation of citrate in the heart and kidneys. The experiments described in the present paper were made on cultures of embryonic chick heart growing *in vitro*, and show that while very high concentrations of methyl fluoroacetate had little or no effect on the growth of the cultures, they rapidly stopped them beating. In contrast, methyl chloroacetate at equivalent concentrations appeared to stimulate beating initially, but then killed the cultures.

## I. EFFECT OF METHYL FLUOROACETATE ON GROWTH

The methods of preparing the tissue cultures, and of investigating the effects of toxic agents on them, were the same as those already described for experiments on mustard gas (4) except that explants of chick heart were used instead of choroid or sclerotic.

After 48 hours' growth in normal medium, cultures were transferred to medium containing 125 μgm and 12.5 μgm of methyl fluoroacetate per c.c. respectively. In one experiment no difference could be detected between the experimental cultures and a control set grown in normal medium; but in another experiment, cultures grown in the medium containing the higher concentration were slightly inferior to the controls. Fragments of tissue similarly explanted in medium containing 116 μgm and 11.6 μgm per c.c. of fluoroacetic acid respectively grew almost as well as the controls in normal medium.

Massive concentrations, obtained by placing cultures in direct contact with liquid methyl fluoroacetate, were lethal, the cells being killed by coagulation of the protoplasm without much distortion of form. Much the same effect was produced by saturated methyl fluoroacetate vapour, but the coagulation took place more slowly and the cells began to round up before it was complete. These effects were probably due to change of pH rather than to any specific effect of the agent.

## II. EFFECT OF METHYL FLUOROACETATE ON THE HEART BEAT IN CULTURE

Explants of 9- or 10-day chick embryo heart muscle were grown *in vitro* by the usual hanging drop method for 48 hours and were then transferred to medium containing various concentrations of toxic material, as set out in the Table. The cultures were examined periodically on the stage of a microscope enclosed in a hot-box maintained at 37° C. Each was watched for one minute, and the number of beats per half-minute was counted as a measure of the vigour of the muscle action.

Table

| Substance | Concentration mg/c.c. | No. of Experimental Cultures | No. of Control Cultures |
|---|---|---|---|
| Methyl fluoroacetate..... | 0.12 | 23 | 21 |
| | 0.095 | 30 | 29 |
| | 0.01 | 24 | 21 |
| Methyl chloroacetate..... | 0.11 | 24 | 23 |

The results are recorded graphically in Fig. 1. Grown in normal medium, explants of 9- or 10-day embryo chick heart muscle usually began to beat within a few hours after explantation, the optimum period being from 24 to 48 hours, and continued to beat for 3 or 4 days (Fig. 1, curve a). In the presence of methyl fluoroacetate the explants also began to beat, but stopped much earlier than the untreated controls, the maximum number beating being observed not later than 24 hours after explantation. In any single experiment, some explants failed to beat, the number depending on the concentration of methyl fluoroacetate, as can be seen by comparing the heights of the maxima of the dotted curves in Fig. 1 (b) (0.12 mg/c.c.), (c) (0.095 mg/c.c.) and (d) (0.01 mg/c.c. of methyl fluoroacetate in the clot). With

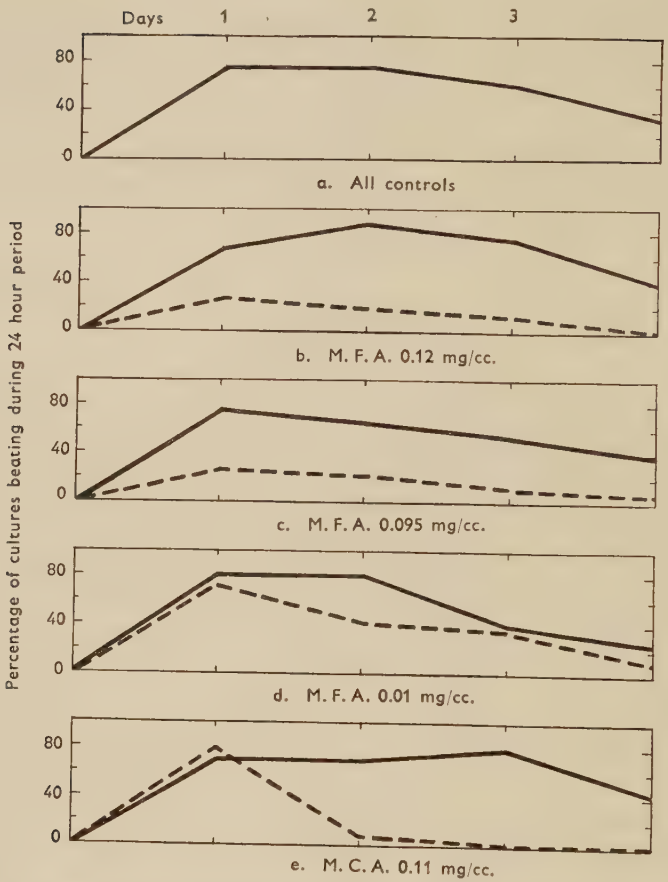
Days 1 2 3
80
40
0
a. All controls
b. M. F. A. 0.12 mg/cc.
c. M. F. A. 0.095 mg/cc.
d. M. F. A. 0.01 mg/cc.
e. M. C. A. 0.11 mg/cc.
Percentage of cultures beating during 24 hour period

Fig. 1. Effect of methyl fluoroacetate and of methyl chloroacetate on beating chick heart cultures. ———— = untreated cultures. — — — — = treated cultures.

the most dilute of these concentrations there was, after 24 hours, no significant difference between the numbers of control and experimental cultures still beating, but all the curves for cultures treated with methyl fluoroacetate returned to zero much earlier than the curves for the controls.

Rather different results were obtained with cultures grown in a medium containing methyl chloroacetate at a concentration comparable with the highest used for the fluoroacetate. The methyl chloroacetate apparently had a stimulating effect on the heart muscle, since the treated explants began to beat freely in the earlier stages (Fig. 1 e), but the cultures subsequently sickened rapidly and died. This stimulating action was particularly notice-

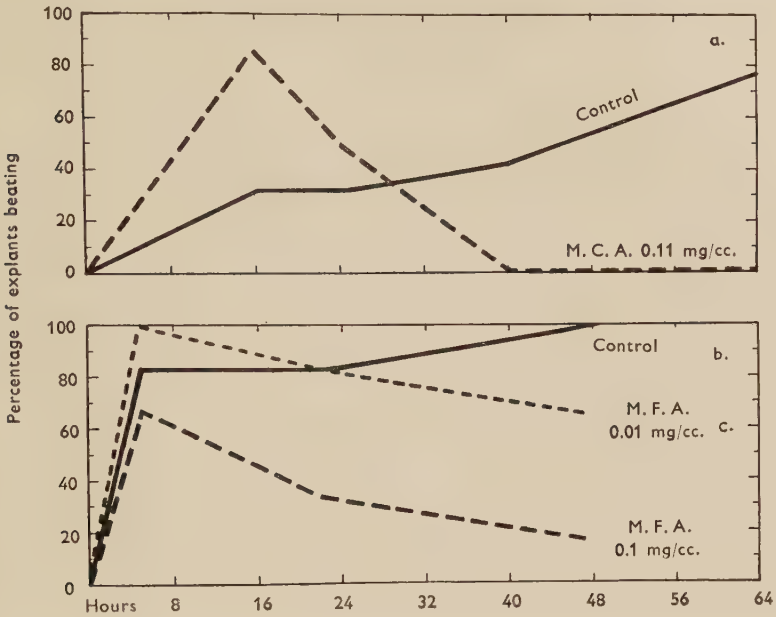


Fig. 2. Stimulatory action of methyl fluoroacetate and methyl chloroacetate on beating heart cultures.

able in two experiments in which the beating of the control explants began sluggishly, so that they were not all beating until the third day after explantation. The curve for the treated cultures in these two experiments, however, reached its maximum during the first 24 hours, and the cultures were all dead in 48 hours (Fig. 2 a).

There were some indications that methyl fluoroacetate might have a similar stimulating effect in the very early stages, but it proved difficult to establish this directly since some hours elapse before the explants recover from the effects of transplantation. Curves for an experiment in which good observations were obtained after only 5 hours, however, are drawn in Fig. 2 b.

Attempts were made to compare the *rates* of beating of the explants in the various concentrations of methyl fluoroacetate and in the controls, but the observations were unreliable, the rates depending, *inter alia*, on the size and degree of development of the embryo; in each individual experiment, however, there was evidence that the explants treated with fluoroacetate or chloroacetate tended to beat a little more rapidly than the controls, especially in the period immediately preceding the point at which they ceased to beat altogether.

## DISCUSSION

Peters (*loc. cit.*) has suggested that fluoroacetate is toxic because it enters the tricarboxylic cycle in the same way as acetate and "jams" the cycle, thus producing a gradual accumulation of the citrate formed in metabolism from carbohydrate and fat. The accumulation of citrate in the presence of fluoroacetate has also been described by Kalnitsky (6, 7). Our observation that comparatively large concentrations of fluoroacetate did not seriously affect the growth of tissue cultures is not inconsistent with this hypothesis, since sufficient energy to maintain growth of tissue is available from the subsidiary process of anaerobic glycolysis. In our experiments, however, the same concentrations affected function, and muscular contraction in the cultures was inhibited; whether this toxic effect was correlated with accumulation of citrate is not known. That chloroacetate acts differently and kills the tissue is to be expected in view of the chemical differences between the C–Cl and C–F bonds. Chloroacetate might be expected to behave similarly to iodoacetate, which vigorously attacks enzymatic -SH groups and owes its toxicity to this cause.

## SUMMARY

Methyl fluoroacetate in concentrations of up to 125 μgm per c.c. has little or no effect on the *growth* of embryo chick heart muscle cultures, but rapidly inhibits beating. At this concentration, methyl chloroacetate kills the cultures.

These experiments formed part of a programme of research carried out at the Strangeways Laboratory during 1944 for the Department of Chemical Defence, Ministry of Supply, and were described more fully in a confidential report to the Ministry (1). We are indebted to the Chief Scientist, Ministry of Supply, for permission to publish this condensed account.

## REFERENCES

1. Allsopp, C. B., and Fell, H. B., Unpublished Ministry of Supply Report, 3rd August, 1944.
2. Bartlett, G. R., and Barron, E. S. G., *J. Biol. Chem.*, **170**, 67 (1947).
3. Buffa, P., and Peters, R. A., *Nature*, **163**, 914 (1949).
4. Fell, H. B., and Allsopp, C. B., *Cancer Research*, **8**, 145 (1948).
5. Kalmbach, E. R., *Science*, **102**, 232 (1945).
6. Kalnitzky, G., *Arch Biochem.*, **17**, 403 (1948).
7. Kalnitzky, G., and Barron, E. S. G., *Arch. Biochem.*, **19**, 75 (1948).
8. Liebecq, C., and Peters, R. A., *Biochem. et Biophys. Acta*, **3**, 215 (1949).
9. Peters, R. A., *The Advancement of Science*, **6**, 257 (1949).

# BRIEF NOTES

## A UNIVERSAL ULTRAMICROSPECTROGRAPH FOR THE OPTICAL RANGE

T. CASPERSSON

*Institute for Cell Research and Genetics, Karolinska Institutet, Stockholm*

Received April 15, 1950

Ultramicrospectrographic procedures have been developed for the study of cell structure of around 1 μ size (1, 2). In order to permit the determination of amino acids at the same time as polynucleotide components –an indispensable condition for work on cellular protein metabolism—the spectrograph must fulfil a number of conditions with regard to the properties of its optical system. These have been summarized in detail earlier (for details and references see (3). Furthermore it must be possible to measure the absorption with high accuracy and in the wavelength range where the main selective amino acid absorptions are located; that is to measure in a continuous spectrum. In the routine work the demand for accuracy, knowledge of the energy of light falling on the specimen, wavelength range and mode of the measurements has continuously to be modified to suit the biological material under investigation. Furthermore some lines of work necessitate integration of measurements on larger cell areas, exact determinations of the light scattering in the preparation, detailed determination of certain optical properties in the object, as well as combination with other cytochemical methods.

Because of these factors, it has proved to be most efficient for large scale routine work with optical ultramicrospectrography to device a convenient routine instrument allowing a number of types of measurements with a minimum of modification of the instrument. The basic principles of the photoelectric microspectrophotometry have been described earlier (2), for details see (3). The new, fairly elaborate routine instrument is only presented here with a diagram and a photograph. The instrument has proved to be very time-saving and reliable in large scale work on biological problems.

For the further development of the scope of optical microspectrography, certain lines of work have been pursued in this laboratory which have led to the construction of special instruments, all of these being directly intended for use in, or to-

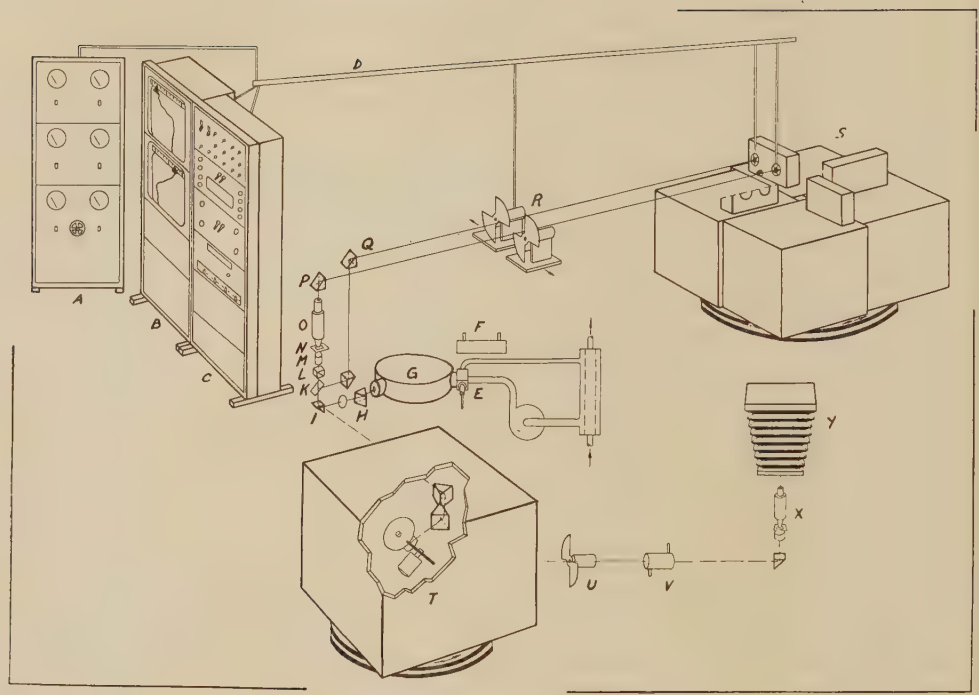


Fig. 1. A. Regulatory panel for the most important sources of light in the routine work. E, super-high pressure mercury lamp cooled by circulating distilled water, serving as source of an almost continuous optical spectrum from 2,600 Å upwards and giving individual wavelengths below 2,540 (obtained by changing running conditions in different wavelength ranges). F, hydrogen tube, giving a continuous spectrum, only suitable for the measurement of large areas because of low energy output. T, high energy rotating spark gap serving as source of light in 20 individual wavelengths, strictly monochromatic, from 2,020 to 3,600.

B, Regulatory panel containing recording instrument for continuous recording of wavelength and of light absorption in an object, scanned by the measuring beam with aid of an instrument not shown in the figure.

C, Regulatory panel for the four different photocells, amplifiers, and ratio calculator.

D, Shelf for electric and other leads from the photocells, sectors to the regulatory panels.

G, H, Monochromator.

I, K, optics between monochromator and microscope condensor and arrangement for splitting the optical beam in order to compensate intensity fluctuations in the light source.

L, Polarizing prism in a turnable holder, for control and measurement of dichroitic phenomena.

M, Interchangeable condensor, different for different wavelength ranges.

N, Object holder allowing a reproduceable movement of the object with an accuracy of 0.05 μ (described in detail in Caspersson 1950). For scanning measurements this object holder is replaced by a special arrangement which will be published later.

O, Microscope with optics suitable to the wavelength range in which measurements are to be made.

P, Totally reflecting prism in a centering device allowing a very accurate centering of the optical axis of the microscope system into the center of window of the photoelectric cells.

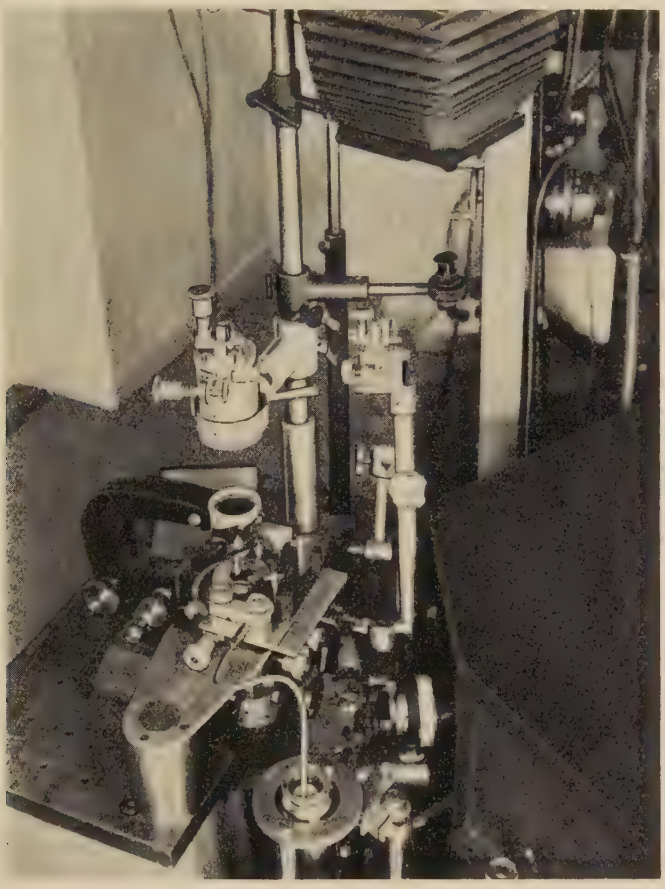

Fig. 2. The central optical system, corresponding to letters G—Q in the preceding diagram.

---

Q, Corresponding prism for the compensatory beam.
R, High precision rotating shutters, which can be regulated while running by aid of electric and pneumatic remote controls. Accuracy 1/40 degree of the incident light.
S, Four groups of photoelectric cells mounted with accessories on a turn-table, by aid of which one group after the other can be used without recentering the optical system. For work in the middle ultraviolet region and with low precision the photomultipliers (ev. cooled by dry ice) are used; for high precision work specially built sodium cells are used with high insulation resistance.
U—Y, Indicates the arrangement for photographic spectrophotometry, a necessary complement to the photoelectric device. The latter arrangement works according to the principles given in Caspersson 1936.
U, Rotating shutter.
V, Filter holder.
X, Microscope.
Y, Camera.

gether with, the universal microspectrograph to which reference is made. They comprise the following: Determination of the light scattering around the object to be measured (Larsson), determination of the degree of orientation in the object (Ruch); short wave ultraviolet work down to 2,050 Å and recording with high resolution the light transmission of individual parts of whole cells, plus automatic calculation of the total extinctions for the cell as a whole. The universal microspectrograph to be described here has been designed especially in order to enable the incorporation of all these complementary procedures in the routine work. All these specialized lines will be presented in detail in publications in the near future.

Fig. 1. presents a semidiagrammatic drawing of the universal spectrograph. The central part of the object holder and the central optical arrangement can be seen in Fig. 2.

## REFERENCES

1. Caspersson, T., *Skand. Arch. Physiol.*, **73**, Suppl. nr. 8 (1936).
2. —— *J. Roy. Microscop. Soc.*, **60**, 8 (1940).
3. —— *Cell Growth and Cell Function.* W. W. Norton, Co Inc., New York, (1950).

# THE PROTEIN METABOLISM OF SEA URCHIN EGGS DURING EARLY DEVELOPMENT STUDIED BY MEANS OF $^{15}N$-LABELED AMMONIA

TORE HULTIN

*The Wenner-Gren Institute for Experimental Biology, Stockholm*

Received July 5, 1950

Unlike most other substances, ammonia is readily taken up from the surrounding medium by sea urchin eggs (3). The present experiments show that $^{15}N$-labeled ammonia is utilized by the eggs for the syntheses of proteins (cf. 1, 6). Labeled ammonia can therefore be used as a tool in the study of protein metabolism during egg development.

## EXPERIMENTAL

Eggs from the sea urchin *Paracentrotus lividus* (LM.)[1] were used in the experiments. The egg jelly was removed by the usual acid treatment. The isotope was added in the form of $^{15}NH_4Cl$, containing 61 per cent excess $^{15}N$. For each 100 mg of eggs (dry weight) 15 μM of $^{15}NH_4Cl$ in 10 ml of sea water (20° C) were given. Two kinds of experiments were performed:

(1) Comparison between unfertilized and fertilized eggs, incubated with $^{15}NH_4Cl$ for 0–5 hours (Fig. 1):

Egg suspensions were divided in two equal parts, one of which was fertilized. The isotope was added immediately to both parts. Samples were taken after different periods (1/2–5 hours) and were washed by means of a hand centrifuge, (1) once in sea water containing 0.015 M ordinary $NH_4Cl$, (2) twice in pure sea water, and (3) once in 0.622 M NaCl. The washed eggs were frozen and dried in the frozen state. The dry material was extracted according to Schneider (5) with cold 10 per cent trichloroacetic acid (TCA), lipid solvents, and 5 per cent TCA at 90° C. The nitrogen of the remaining sediment was preliminarily considered as protein-nitrogen.

(2) Velocity of $^{15}NH_4Cl$ uptake during development (Fig. 2):

From egg suspensions equal samples were taken (1) just before fertilization, and (2) 0–45 hours after fertilization with intervals of 5 hours. All samples were treated with $^{15}NH_4Cl$ for 5 hours. They were then washed and dried as described above.

[1] The material was prepared at the Zoological Station in Naples during spring 1949 and spring 1950.

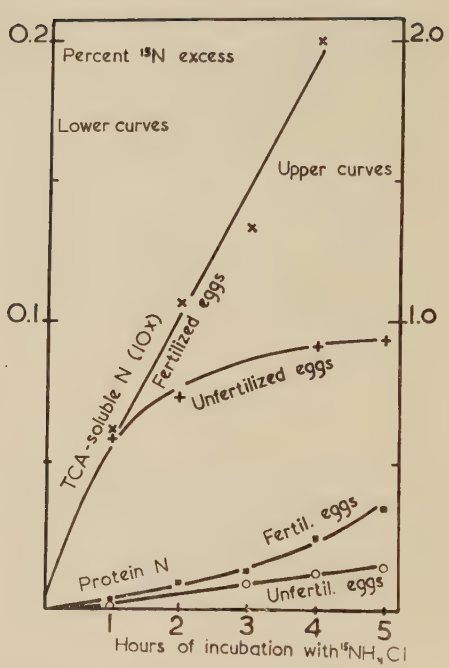


Fig. 1. Isotope distribution in unfertilized and fertilized sea urchin eggs, kept in $^{15}NH_4Cl$-containing sea water for 0–5 hours.

In some series of experiments the dried eggs were extracted with distilled water 3 times by grinding them for 30 minutes with an air-driven, rotating glass-rod (ice-bath). The water-extracts and the residues were then precipitated and purified as described above.

## RESULTS

The initial velocity of the ammonia uptake was about the same in both unfertilized and fertilized eggs (Fig. 1, TCA-soluble N). The unfertilized eggs, however, were more rapidly saturated, and the total amounts of ammonia taken up by them were therefore smaller. About 10 hours after fertilization the ammonia-accumulating capacity of the blastulae decreased rapidly, and the plutei (45–50 hours) had about the same ammonia uptake as the unfertilized eggs (Fig. 2). So far the present experiments confirmed the results of Örström (3).

The ammonia uptake peak appeared at the same time as the formation of the fertilization membrane space and the blastocoel. It decreased rapidly during hatching and disappeared entirely when the gastrulation was performed. The labeled ammonia enclosed within the named cavities could hardly have been entirely removed by the washing procedure. The peak of the "TCA-soluble N"-curve (Fig. 2) was therefore not believed to give an adequate picture of the actual amounts of $^{15}N$-

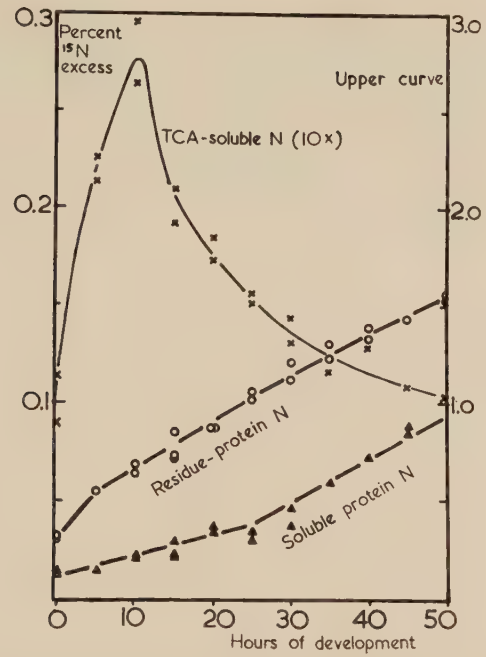


Fig. 2. Velocity of isotope uptake at different stages of development. All egg samples kept in isotope containing sea water during the final 5 hours.

labeled precursors[1] for protein synthesis present in the egg cytoplasm. No corresponding peak could be found in the protein nitrogen curves.

The incorporation of labeled nitrogen into the egg proteins proceeded at a low and fairly constant rate in the unfertilized eggs (Fig. 1). After fertilization, however, the incorporation was continously accelerated (Fig. 1, 2). In the experiment series, where the soluble and insoluble proteins had been separated, the insoluble proteins were found to have the highest isotope incorporation velocity. Probably the insoluble protein fraction included the mitochondria and microsomes of the eggs (cf. 2). On fertilization the isotope uptake of this fraction was most accelerated, probably indicating the initiation of a progressive reduplication of the small, granular cytoplasm constituents.

The isotope incorporation rate of the water-soluble protein fraction also increased during development. Most probably this fraction included cell-fluid proteins, emitted from the cytoplasmic granules (cf. 2). The experiments indicated that the increase became more rapid from about 25 hours after fertilization (gastrula stage). This is in agreement with the recent results of Perlmann and Gustafson (4), who found in serological experiments that a new antigen appeared in water extracts of sea urchin larvae between 12 and 48 hours after fertilization.

[1] A more detailed investigation of this problem is in progress.

In one egg series the plutei arms did not grow out to full length (45–50 hours). At the same time the isotope incorporation rate was successively retarded. The retardation was first noticed in the water-insoluble protein fraction.

In a preliminary experiment, $^{15}N$-labeled gsycine was added to developing eggs of *Psammechinus miliaris*. Higher concentrations of isotope than in the ammonia experiments were required for getting the same isotope uptake. The distribution of the isotope in the protein fractions, however, was essentially the same.

## REFERENCES

1. Foster, G. L., Schoenheimer, R., and Rittenberg, D., *J. biol. Chem.*, **127**, 319 (1939).
2. Hultin, T., *Exp. Cell Res.*, **1**, 376 (1950).
3. Örström, Å., *Z. Physiol. Chem.*, **271**, 1 (1941).
4. Perlmann, P., and Gustafson, T., *Experientia*, **4**, 481 (1948).
5. Schneider, W. C., *J. biol. Chem.*, **161**, 293 (1945).
6. Sprinson, D. B., and Rittenberg, D., *J. biol. Chem.*, **180**, 707 (1949).

# THE RECONSTITUTION OF COLLAGEN FIBRILS AS REVEALED BY ELECTRON MICROSCOPY

G. BAHR

*Department of Cell Research, Karolinska Institutet, Stockholm*

Received August 11, 1950

The original work of Nageotte (2) and Huzella (1) on the reconstitution of collagen fibrils from collagen tissue dissolved in dilute acids has not been extensively followed up (3, 4). It seemed therefore desirable to study this problem anew. This paper will report on preliminary electron microscope observations on the fine structure of reconstituted collagen fibrils. Tendons, mostly taken from rat tails, were dissolved in dilute acetic acid (1 : 25 000 vol per cent) following the instructions of Nageotte. The solutions were filtered through a fine glass filter and finally centrifuged. These clear viscous solutions contained 0.75–0.045 per cent dry substance. Preparations for electron microscopy were obtained by dialysis in commercial tubes, or by dialysing the collagen solutions against a number of anion—cation combinations in a special chamber, depositing the precipitated fibrils directly on the collodion supporting films of the electron microscope grids. Solutions containing 0.7–1.5 per cent salt were most effective. Univalent ions with the smallest ion diameter gave the largest fibril deposits. Trivalent ions gave negative results. The reconstitution of the fibrils seems to occur only at a pH ranging from 3.8–7.0, with the exception of KCNO which precipitated fibrils at pH 9.58. The reconstituted fibrils can be made to dissolve again by a successive dialysis against distilled water and acetic acid, which might be interpreted in this case as representing a certain antagonism between salts and acids. KCN inhibits the

Fig. 1. Density curves of fibrils. Precipitated with NaCl, I, II general type of band pattern in fibrils. III pattern of fibrils precipitated with Na-glycerine-phosphate, IV with Lioxalate, V with Ba-acetate.

precipitation, but the process is not irreversible, since subsequent dialysis against distilled water and acetic acid reestablishes its ability to react with other salt solutions, giving fibrous precipitates. In some cases solutions and fibrils were modified by standing for longer periods and certain results were not constantly reproducible.

Electron micrographs have been taken of unstained, phospho-tungstic acid stained and platinum-palladium shadowed fibrils, mostly after fragmenting the fibrous precipitates in a Waring blendor. The main period of the reconstituted collagen fibrils was of the order of 635 Å in most cases, although density curves

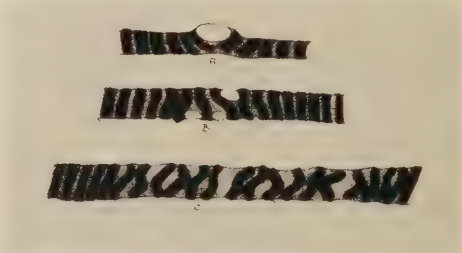

Fig. 2. The effect of stretching on fibrils, schematically. Different kind of band distortion.

taken along the fibrils show variations of the intraperiod bands, depending upon the type of salt solution used to precipitate the fibrils. Some of the curve types are shown schematically in Fig. 1. The tops correspond to the highest mass density in the main period or in the intraperiods. If two or three tops coincide the resulting top is enlarged, corresponding to a higher mass concentration in that region of the fibril. Two general types of curves are found. One with fairly evenly distributed bands (Fig. 1, I–IV), and a more block-like type (V). Prolonged exposure to the electron beam of high intensity shows a pronounced stretching effect in the fibrils. Holes are produced in the supporting film and in the fibrils (Fig. 2, A and B) which reveal interesting distortion patterns of the bands (Fig. 2, C).

The experiments are beeing continued and will be reported in detail later.

## REFERENCES

1. Huzella, Th., *Zeitschr. f. Krist.*, **83**, 89 (1932).
2. Nageotte, J., and Guyon, L., *Compt. Rend. Assoc. Anat.*, Réunion, 408 (1934).
3. Schmitt, F. O., Hall, C. E., and Jakus, M. A., *J. Cell. Comp. Physiol.*, **20**, 11 (1942).
4. Wyckoff, R. W. G., Corey., *Proc. Soc. Exp. Biol. Med.*, **34**, 285 (1936).

---

Explanation of micrographs:

I. Unstained fibrils precipitated by dialysing against Ba-acetate. Pt/Pd shadowed. A typical triangular juncture is shown. The periods of adjacent fibrils are in register. 52,000 ×.
II. Unstained, unshadowed preparation. Na-glycerine-phosphate precipitated. Single and double fibril. 47,000 ×.

0.1 μ

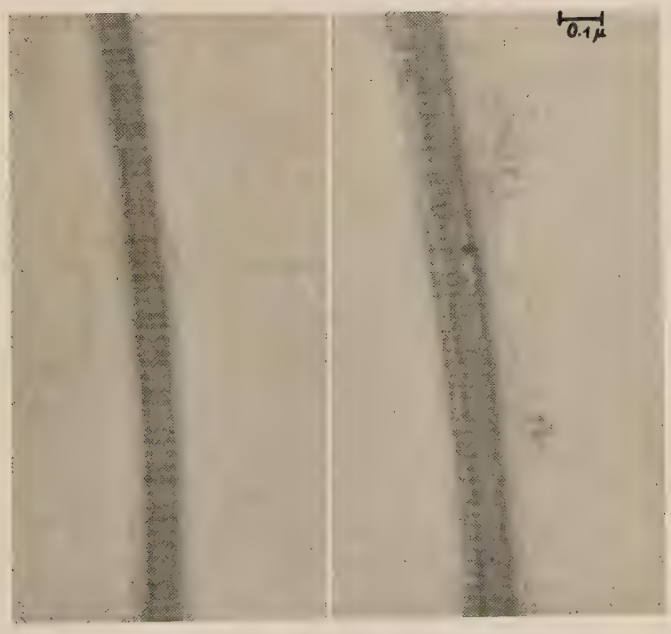
0.1 μ

III. Fibrils precipitated by KCl, PTA stained, Pt/Pd shadowed. Notice characteristic spindle-shaped ends of the fragmented fibrils. 24,000 ×.

# AUTHOR INDEX


A

Allsopp, C. B. and Fell, Honor B. The effects of fluoroacetate on beating embryo-chick heart in tissue culture, 590

Andresen, N., Chapman-Andresen, C., Holter, H., Jensen, P. K., and Levi, H. The distribution of food in amoeba cytoplasm studied by means of autoradiography, 139

B

Bahr, G. The reconstitution of collagen fibrils as revealed by electron microscopy, 603

Balazs, A., and Holmgren, Hj. The basic dye-uptake and the presence of a growth-inhibiting substance in the healing tissue of skin wounds, 206

Bisset, K. A. Observations upon the resting nucleus of the typhoid bacterium, 473

Bohus Jensen, Aa. Action of ficin on sea urchin eggs, 351

Bullough, W. S. Mitotic activity in the tissues of dead mice, and in tissues kept in physiological salt solutions, 410

C

Caspersson, T. A universal ultramicrospectrograph for the optical range, 595

Chapman-Andresen, C. See Andresen, 139

Courtines, H. See Fauré-Fremiet, 253

Crick, F. H. C. The physical properties of cytoplasm. A study by means of the magnetic particle method. Part II. Theoretical treatment, 505

and Hughes, A. F. W. The physical properties of cytoplasm. A study by means of the magnetic particle method. Part I, 37

D

Danielli, J. F. See Hörstadius, 188

E

Engström, A., and Lüthy, J. The distribution of mass and lipids in the single nerve fiber, 81

Ernster, L., Zetterström, R., and Lindberg, O. Vitamin A as a co-enzyme component in the mechanism of aerobic energy transport, 494

F

Faure-Fremiet, E., Courtines, H., and Mugard, H. Double origine des ribonucléoprotéines cytoplasmiques dans l'oocyte de Glomeris marginata, 253

Fell, Honor B. See Allsopp, 590

Fernández-Morán, H. Electron microscope observations on the structure of the myelinated nerve fiber sheath, 143

Sheath and axon structures in the internode portion of vertebrate myelinated nerve fibres, 309

Friedlaender, M. H. G. See Randall, 1

G

Gelotte, B. See Snellman, 234

Goldberg, L., Klein, E., and Klein, G. The nucleic acid content of mouse ascites tumor cells, 543

Gomori, G. The quantitative determination of histochemical reactions for enzymes, 33

Gustafson, T., and Hasselberg, I. Alkaline phosphatase activity in developing sea urchin eggs, 371

H

Harman, J. W. Studies on mitochondria: I. The association of cyclophorase with mitochondria, 382

Studies on mitochondria: II. The structure of mitochondria in relation to enzymatic activity, 394

Hasselberg, I. See Gustafson, 371

Holmgren, Hj. See Balasz, 206

Holter, H. See Andresen, 139

Holtfreter, J., Koszalka, T. R., and Miller, L. L. Chromatographic studies of amino-acids in the eggs and embryos of various species, 453

Hughes, A. F. W. See Crick, 37

Hultin, T. On the oxygen uptake of Paracentrotus lividus egg homogenates after the addition of calcium, 159

On the acid formation, breakdown of cytoplasmic inclusions and increased viscosity in Paracentrotus egg homogenates after the addition of calcium, 272

Incorporation in vivo of $^{15}N$-labeled glycine into liver fractions of newly hatched chicks, 376

The protein metabolism of sea urchin eggs during early development studied by means of $^{15}N$-labeled ammonia, 599
Hörstadius, S., Lorch, I. J., and Danielli, J. F. Differentiation of sea urchin eggs following reduction of the interior cytoplasm in relation to the cortex, 188

**J**

Jensen, P. K. See Andresen, 139

**K**

Kaplan, E. H. See Still, 403
Kihlman, B. 8-ethoxycaffeine, an ideal inducer of structural chromosome changes in the root tips of Allium Cepa, 135
Klein, E., Kurnick, N. B., and Klein, G. The effect of storage on the nucleic acid content and virulence of mouse ascites tumor 127
Klein, E. See Goldberg, 543
Klein, G. See Goldberg, 543
See Klein, E., 127
Koszalka, T. R. See Holtfreter, 453
Kriszat, G. See Runnström, 284, 355, 497
Kurnick, N. B. The quantitative estimation of desoxyribosenucleic acid based on methyl green staining, 151
See Klein, E., 127

**L**

Labaw, L. W., Mosley, V. M., and Wyckoff, R. W. G. Phosphorus uptake by bacteriophage and ultraviolet irradiated bacteria, 353
Lamb, W. G. P. The isolation of threads from interphase nuclei, 571
Levi, H. See Andresen, 139
L'Heritier, Ph. Appendice mathématique, 230
Lindberg, O. On surface reactions in the sea urchin egg, 105
See Ernster, 494
Lindegren, C. C., and Rafalko, M. M. The structure of the nucleus of Saccharomyces bayanus, 169
Lorch, I. J. See Hörstadius, 188
Lundblad, G. Proteolytic activity in sea urchin gametes, 264
Lüthy, H. See Engström, 81

**M**

Medem, F. See Rötheli, 115
Miller, L. L. See Holtfreter, 453
Miyao, G. See Yasuzumi, 501
Monné, L., and Slautterback, D. B. Differential staining of various polysaccharides in sea urchin eggs, 477
Monroy, A. A preliminary electrophoretic analysis of proteins and protein fractions in sea urchin eggs and their changes on fertilization, 92
Mosley, V. M. See Labaw, 353
Mugard, H. See Fauré-Fremiet, 253
Mühlethaler, K. The structure of plant slimes, 341

**P**

Plus, N. L'invasion d'un organisme par un virus héréditaire, 217
Polli, E. E. The behavior of chromatin in normal and pathological human blood cells, 460

**R**

Rafalko, M. M. See Lindegren, 169
Randall, J. T., and Friedlaender, M. H. G. The microstructure of ram spermatozoa, 1
Rosza, G., Szent-Györgyi, A., and Wyckoff, R. W. G. The fine structure of myofibrils, 194
Roth, H. See Rötheli, 115
Runnström, J. Analysis of the modifying effect of dissolved jelly coat substance on the formation of the fertilization membrane in eggs of Echinocardium cordatum, 304
Runnström, J., and Kriszat, G. On the effect of adenosine triphosphoric acid and of Ca on the cytoplasm of the egg of the sea urchin, Psammechinus miliaris, 284
Action of periodate on the surface reactions attending the activation of the egg of the sea urchin, Psammechinus miliaris, 355
On the influence of ATP on the fertilization and segmentation of the sea urchin egg, Strongylocentrotus lividus, 497
Rötheli, A., Roth, H., and Medem, F. Elektronenoptische Untersuchungen der Strukturveränderung agglutinierter Fischspermien, 115

**S**

Schrader, F., and Leuchtenberger, C. A cytochemical analysis of the functional interrelations of various cell structures in Arvelius albopunctatus (De Geer), 421
Slautterback, D. See Monné, 477
Snellman, O., and Gelotte, B. An investigation of the physical chemistry of the contractile proteins, 234
Still, J. L., and Kaplan, E. H. Localization of oxidases, 403
Sylvén, B. The cytoplasm of living tissue mast cells in visual phase-contrast, 492
The qualitative distribution of metachroma-

tic polysaccharide material during hair growth, 582
Szent-Györgyi, A. See Rosza, 194

V

Vilkomerson, H. The unusual meiotic behavior of Elymus Wiegandii, 534

W

Wyckoff, R. See Labaw, 353
See Rosza, 194

Y

Yasuzumi, G., and Miyao, G. Amino acid constituents of chromatin threads from erythrocyte nuclei, 501

Z

Zetterström, R. See Ernster, 494

on fertilization and segmentation, Runnström and Kriszat, 497; protein metabolism during early development, Hultin, 599; proteolytic activity of gametes, Lundblad, 264; surface reactions, Lindberg, 105
Skin wounds — dye uptake and growth-inhibiting substance in the healing of, Balasz and Holmgren, 206
Spermatozoa — proteolytic activity in sea urchin gametes, Lundblad, 264; ram — microstructure of, Randall and Friedlaender, 1; structure changes on agglutination, Rötheli *et al.*, 115
Strongylocentrotus — influence of ATP on fertilization and segmentation, Runnström and Kriszat, 497

T

Tumor — effect of storage on nucleic acid content and virulence, Klein *et al.*, 127 Goldberg *et al.*, 543

V

Virus — invasion of Drosophila by an inheritable virus, Plus, 217
Vitamin A — as co-enzyme in aerobic energy transport, Ernster *et al.*, 494

on fertilization and segmentation, Runnström and Kriszat, 497; protein metabolism during early development, Hultin, 599; proteolytic activity of gametes, Lundblad, 264; surface reactions, Lindberg, 105
Skin wounds — dye uptake and growth-inhibiting substance in the healing of, Balasz and Holmgren, 206
Spermatozoa — proteolytic activity in sea urchin gametes, Lundblad, 264; ram — microstructure of, Randall and Friedlaender, 1; structure changes on agglutination, Rötheli *et al.*, 115
Strongylocentrotus — influence of ATP on fertilization and segmentation, Runnström and Kriszat, 497

T

Tumor — effect of storage on nucleic acid content and virulence, Klein *et al.*, 127 Goldberg *et al.*, 543

V

Virus — invasion of Drosophila by an inheritable virus, Plus, 217
Vitamin A — as co-enzyme in aerobic energy transport, Ernster *et al.*, 494

PERIODICAL